

1 **Muscle systems and motility of early animals highlighted by cnidarians from the basal Cambrian**

2

3 Xing Wang^{1,2,&}, Jean Vannier^{3,&}, Xiaoguang Yang^{4,&}, Lucas Leclère⁵, Qiang Ou⁶, Xikun Song⁷ Tsuyoshi
4 Komiya⁸ and Jian Han^{4,*}

5

6 ¹Qingdao Institute of Marine Geology, China Geological Survey, Qingdao 266071, China

7 ²Function Laboratory of Marine Mineral Resources, Qingdao National Laboratory for Marine Science
8 & Technology, Qingdao 266237, China

9 ³Université de Lyon, Université Claude Bernard Lyon 1, CNRS UMR 5276, Laboratoire de géologie de
10 Lyon: Terre, Planètes, Environnement, Bâtiment GEODE, 2, rue Raphaël Dubois, Villeurbanne 69622,
11 France

12 ⁴State Key Laboratory of Continental Dynamics, Shaanxi Key laboratory of Early Life & Environment,
13 Department of Geology, Northwest University, Xi'an 710069, China

14 ⁵Sorbonne Universités, UPMC Univ Paris 06, CNRS, Laboratoire de Biologie du Développement de
15 Villefranche-sur-mer (LBDV), Villefranche-sur-mer, France

16 ⁶Early Life Evolution Laboratory, School of Earth Sciences & Resources, China University of
17 Geosciences, Beijing 100083, China

18 ⁷State Key Laboratory of Marine Environmental Science, College of Ocean and Earth Sciences, Xiamen
19 University, Xiamen 361102, China

20 ⁸Department of Earth Science & Astronomy, Graduate School of Arts & Sciences, The University of
21 Tokyo, Tokyo 153-8902, Japan

22 [&]These authors contributed equally to this work and should be considered co-first authors

23 ^{*}Corresponding author (Han J, elihanj@nwu.edu.cn)

24

25 **Abstract**

26 Although fossil evidence suggest that various animal groups were able to move actively through their
27 environment in the early stages of their evolution, virtually no direct information is available on the
28 nature of their muscle systems. The origin of jellyfish swimming, for example, is of great concern to
29 biologists. Exceptionally preserved muscles are described here in benthic peridermal olivoid
30 medusozoans from the basal Cambrian of China (Kuanchuanpu Formation, ca. 535 Ma) that have
31 direct equivalent in modern medusozoans. They consist of circular fibers distributed over the bell
32 surface (subumbrella) and most probably have a myoepithelial origin. This is the oldest record of a
33 muscle system in cnidarians and more generally in animals. This basic system was probably co-opted
34 by younger early Cambrian jellyfish to develop capacities for the jet-propelled swimming within the
35 water column. Additional lines of fossil evidence obtained from ecdysozoans (worms and
36 panarthropods) show that the muscle systems of early animals underwent a rapid diversification
37 through the early Cambrian and increased their capacity to colonize a wide range of habitats both
38 within the water column and sediment at a critical time of their evolutionary radiation.

39

40 **Introduction**

41

42 Cnidarians are generally seen as the sister group to bilaterians (Brusca et al., 2016; Erwin et al., 2011;

43 Leclère and Röttinger, 2017; Zapata et al., 2015) and are represented by a huge variety of jellyfish, sea
44 anemones, corals, sea fans, hydrozoans (including the colonial siphonophores) and less familiar
45 parasitic groups (Raikova, 1988). Although often sessile (polyps) or parasitic, many of them are motile
46 animals and a large proportion of them (such as jellyfish) use their muscles to move very actively
47 through the water column. In contrast with bilaterians, cnidarians owe most of their contractile
48 power to epitheliomuscular or myoepithelial cells that line both epithelial body layers (Brusca et al.,
49 2016; Schmidt-Rhaesa, 2007). These specialized cells contain interconnected contractile basal
50 extensions (myonemes or myofilaments) that altogether form longitudinal or circular sheets and play
51 virtually the same role as the muscle layers of other animals. Epitheliomuscular cells are connected to
52 nerve cells via chemical synapses (Westfall et al. 1971). Cnidarian muscles are characterized by
53 multifunctional capacities and plasticity and perform key functions in locomotion, defense from
54 predators, feeding and digestion at all stages (planula, polyp and medusa stages; see ref Leclère and
55 Röttinger, 2017). In medusae, locomotion is performed by the rhythmic pulsation of circular sheets of
56 epithelial striated muscles located around the bell margins and over the subumbrellar surface. These
57 contractions are counteracted by the elastic properties and antagonistic force of the mesoglea and
58 result in expelling water from beneath the bell and thus moving the medusa via jet propulsion (Brusca
59 et al., 2016).

60 The Precambrian fossil record of cnidarians remain patchy and controversial although molecular
61 models often predict a very ancient (e.g. pre-Ediacaran) origin of the group (Erwin et al., 2011). For
62 example, *Haootia quadriformis* from the Ediacaran (Fermeuse Formation; ca. 560 Ma; Newfoundland,
63 eastern Canada) roughly resembles modern stalked jellyfish, such as staurozoans, and bears very fine
64 wrinkles interpreted as putative coronal muscles (Liu et al., 2014; 2015). Whether this external
65 network corresponds to underlying muscles is uncertain and seems at odd with the assumed sessile
66 lifestyle of the animal. Numerous circular forms with a radial pattern have been described in the
67 Ediacaran (e.g. *Cyclomedusa*; Ukraine, Russia; see refs. Zaika-Novatskii et al., 1968; Fedonkin, 1981).
68 Although some of them may potentially represent bell imprints of jellyfish, others probably have a
69 different origin (e.g. circular holdfasts of non-cnidarian sessile organisms or possible gas-escape
70 sedimentary structures; see ref. Sun, 1986). In contrast, convincing evidence for ancestral
71 medusozoans comes from the early Cambrian Chengjiang Lagerstätte (ca. 521 Ma; Yunnan Province
72 China) and is best exemplified by *Yunnanoascus haikouensis* that shares a set of morphological
73 features with modern jellyfish such as a tetramerous symmetry, rhopalia, long tentacles around the
74 bell margin, and a possible manubrium in the central part of the bell (Han et al., 2016a). Although
75 Chengjiang fossils usually show extremely fine details of soft animal tissues and organs (including
76 digestive, nervous and reproductive systems), muscles remain elusive, and no trace of possible
77 coronal muscles can be seen in *Yunnanoascus*. Other jellyfish from the mid-Cambrian Marjum
78 Formation (ca. 505 Ma, Utah, USA; see ref. Cartwright et al., 2007) display fine recognizable
79 anatomical details such as the exumbrella and subumbrella, tentacles and relatively well-preserved
80 coronal muscles that suggest swimming capacities.

81 The Kuanchuanpu Formation (ca. 535 Ma, lowermost Cambrian Fortunian Stage; Shaanxi Province,
82 south China) yields a great variety of three-dimensionally preserved microfossils including cnidarians
83 such as Olivoidae (Dong et al. 2013, 2016; Han et al. 2013, 2016b; Liu et al. 2014; 2017; Steiner et al.,
84 2014). The developmental sequence of *Olivoides* starts with a spherical embryo that, after hatching,

85 gives rise to conical juveniles (Bengtson and Yue, 1997), suggesting a direct development (Han et al.,
86 2013; Steiner et al., 2014; Wang et al., 2020) with no counterpart among modern cnidarians that all
87 grow via planula larval stage. However, microtomography clearly show that post-embryonic
88 *Olivoooides* do have anatomical features typical of modern cnidarians, a radial symmetry, single body
89 opening, exumbrella and subumbrella, interradial septa (internal ridges), gonads, manubrium, oral
90 lips, apertural lobes, tentacles, frenula and velaria (Dong et al. 2013, 2016; Han et al. 2013, 2016b;
91 Wang et al., 2020), which collectively support a placement of *Olivoooides* and its related forms within
92 Medusozoa (Dong et al. 2013, 2016; Han et al. 2013, 2016b; Liu et al. 2014; 2017; Wang et al., 2020).
93 Wang et al. (2017) reported possible coronal muscles around the aperture of *Sinaster* (Olivoooidae) but
94 did not investigate their organization and possible function. We describe here secondarily
95 phosphatized muscle fibers preserved in three dimensions, in post-embryonic stages of olivoids from
96 the early Cambrian (Fortunian) Kuanchuanpu Formation. They represent the oldest occurrence of
97 muscle tissue in cnidarians and more generally in animals. We also address the nature (e.g.
98 myoepithelial) and function of this muscle system through detailed comparisons with modern
99 jellyfish.

100 These new findings prompted us to re-examine and integrate fossil data obtained from other early
101 Cambrian groups such as ecdysozoans (e.g. worms, lobopodians; see Budd, 1998; Vannier and Martin
102 2017; Young and Vinther, 2017; Zhang et al., 2016) that altogether shed light on the diversity and
103 functions of muscle systems in early animals.

104

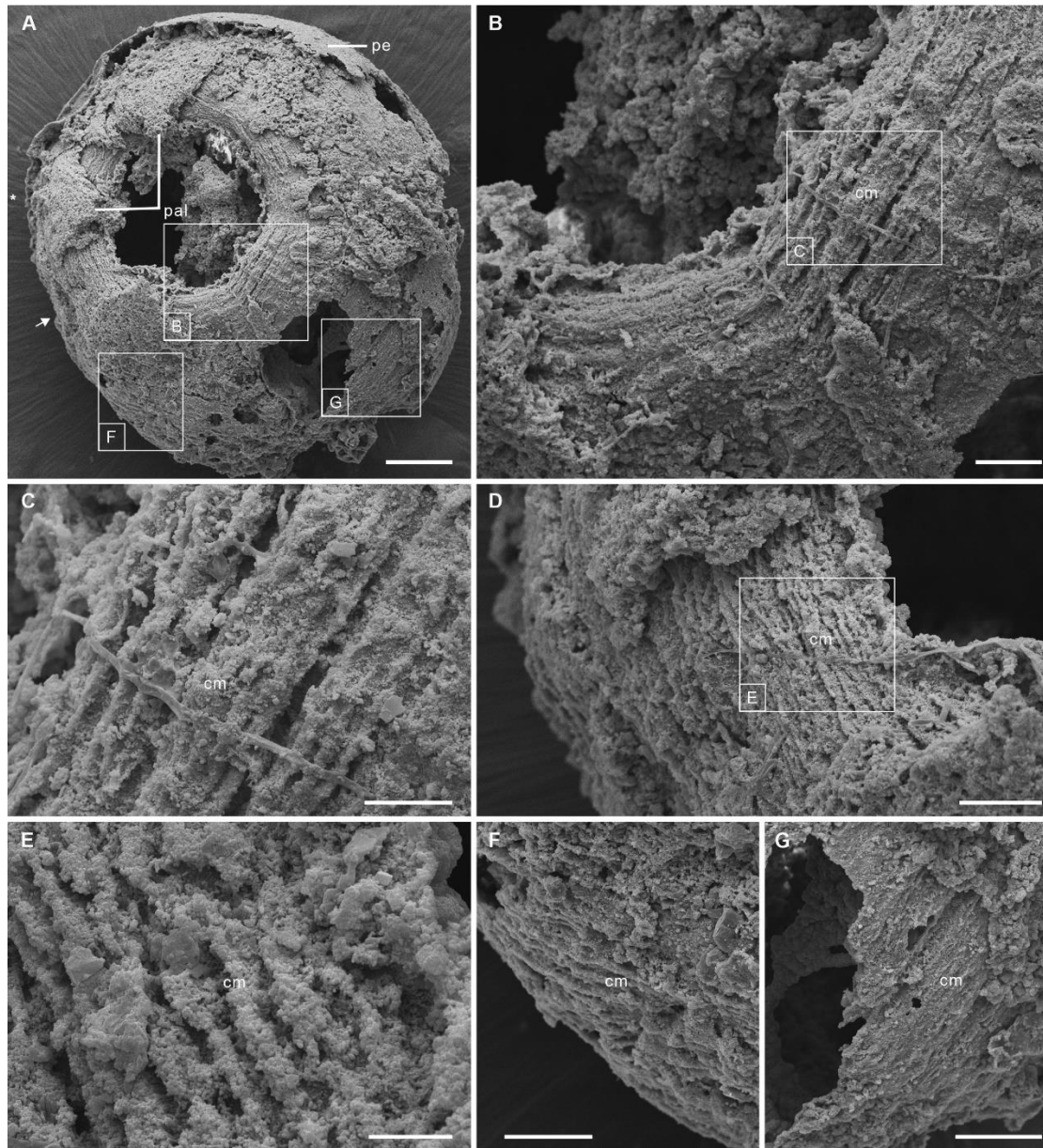
105 **Results**

106

107 The twelve fossil specimens studied here have the diagnostic features of post-embryonic olivoids
108 (Dong et al., 2013; 2016; Han et al., 2013; 2016b; Wang et al., 2017; 2020), such as an ovoid shape
109 with a pentaradial symmetry and the presence of a periderm, apertural lobes, exumbrella, perradial
110 ridges and interradial furrows (Figures. 1 and 2A-E—figure supplements 1-3). They also display a
111 well-preserved network of circular fibers (Figures. 1 and 2A-E), tentatively interpreted as coronal
112 muscles by Wang et al. (2017) in a pilot study.

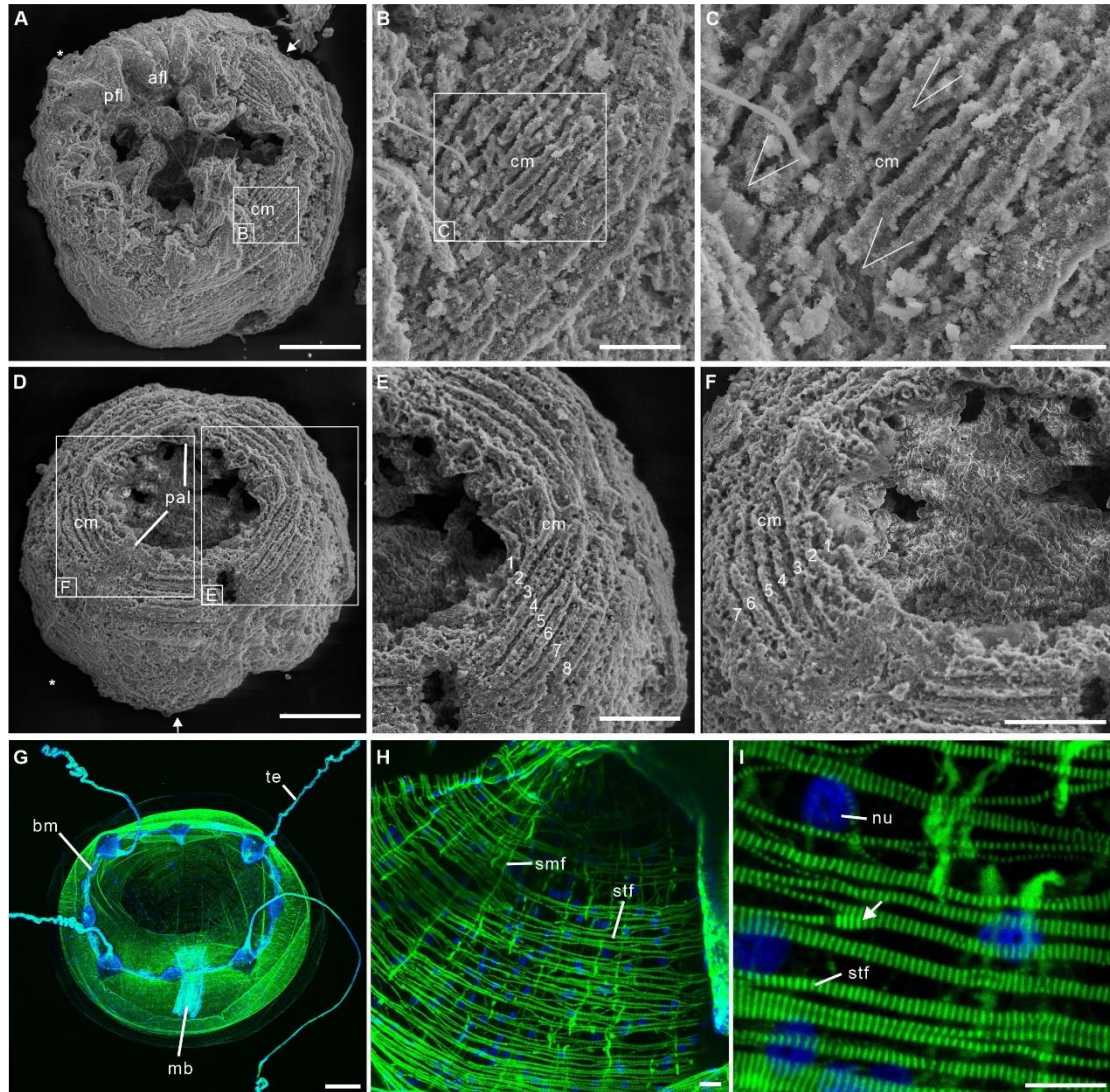
113 The body has a consistent ovoid shape and size (diameter between 560 and 580 μm) and is enclosed
114 by a smooth periderm (5-10 μm in thickness) (Figure 1A—figure supplements 2A and 3C, E-H).
115 Centripetal, triangular projections, termed perradial apertural lobes (see refs. Han et al., 2013; Wang
116 et al., 2020) can be seen around the oral aperture of most specimens. They correspond to perradial
117 and display a pentaradial symmetry (Figures 1A and 2A, D—figure supplements 1-3). The partial loss
118 of the periderm and perradial apertural lobes in numerous specimens reveals a fine network of
119 underlying closely packed, circular fibers, that are best developed around the oral aperture where
120 they form four or five separate concentric bundles (individual thickness between 9 and 15 μm), each
121 consisting of numerous (possibly up to eight) individual fibers (Figures 1B, C and 2B, C, E, F). These
122 fiber rings run around the oral aperture, have a consistent thickness and do not seem to be
123 interrupted (Figures 1A and 2A, D—figure supplements 1 and 2A, B). Comparable fibers occur all over
124 the body, but seem to be sparser towards the aboral pole (figure supplements 1B, C and 3A-F) and
125 not organized in well-defined bundles (Figures 1D-G and 2A—figure supplements 1 and 3). Individual
126 fibers are cylindrical (diameter ca. 2 μm), lying mostly parallel to each other although oblique

127 V-shaped interconnections (angle ca. 20-30°) may occur locally (Figure 2C). Fibers are finely and
128 evenly coated with microcrystalline (ca 0.4 μm) calcium phosphate (Figure 1B, C, E). Circular fibers
129 clearly extend into the triangular perradial apertural lobes (figure supplement 1A, E, F). The circular
130 fiber network seems to be overprinted by faint longitudinal depressions in the aboral half (figure
131 supplement 1D) that may correspond to interradial furrows.



132

133 **Figure 1. Post-embryonic stage of *Olivooides* sp. from the early Cambrian Kuanchuanpu Formation**
134 **(ca. 535 Ma; South China), showing exposed muscle fibers. ELISN150-278. (A) General view of oral**
135 **side. (B) Details of fiber bundles around aperture (see close-up location in A). (C) Close-up showing**
136 **individual fibers within each bundle. (D) Dense network of fibers (see location in A). (E) Close-up of**
137 **individual fibers coated with fine grains of calcium phosphate. (F), (G) Circular fibers approximately**
138 **half way between the oral and aboral poles. All Scanning electron micrographs. Abbreviations: cm,**
139 **circular muscle; pal, perradial apertural lobe; pe, periderm; *, perradii; →, interradial furrows. Scale bars: 100**
140 **μm in (A); 20 μm in (B); 10 μm in (C), (E); 20 μm in (D), (F) and (G).**



141

142 **Figure 2. Post-embryonic stage of *Olivooides* sp. from the early Cambrian Kuanchuanpu Formation**
 143 **(ca. 535 Ma; South China), showing exposed muscle fibers (A-F) and myoepithelial muscle network**
 144 **in extant hydrozoan jellyfish (G-I). (A-C) ELISN052-33. General view of oral side and details of**
 145 **apertural circular muscle fibers and the V-shaped interconnection between the fibers in (C). (D-F)**
 146 **ELISN061-19. General view of oral side and details of apertural, circular muscles fibers. (G-I) *Eirene* sp.**
 147 **(Hydrozoa) young medusa, general oral view, circular muscles along subumbrella and details of**
 148 **striated fibers; white arrow (I) indicates bifurcating fibers. Green and blue colours in (G-I) correspond**
 149 **to actin (phalloidin) and DNA (Hoechst) staining. (A-F) Scanning electron micrographs. Abbreviations:**
 150 **afl, adradial fold lappet; bm, bell margin; cm, circular muscle; mb, manubrium; nu, nucleus; pal,**
 151 **perradial apertural lobe; pfl, perradial fold lappet; smf, smooth (radial) muscle fiber; stf, striated**
 152 **(circular) muscle fiber; te, tentacle *, perradii; →, interradii. Scale bars: 200 μm in (A), (D); 100 μm in**
 153 **(G); 20 μm in (B), (E) and (F); 10 μm in (C), (H) and (I).**

154

155 **Discussion**

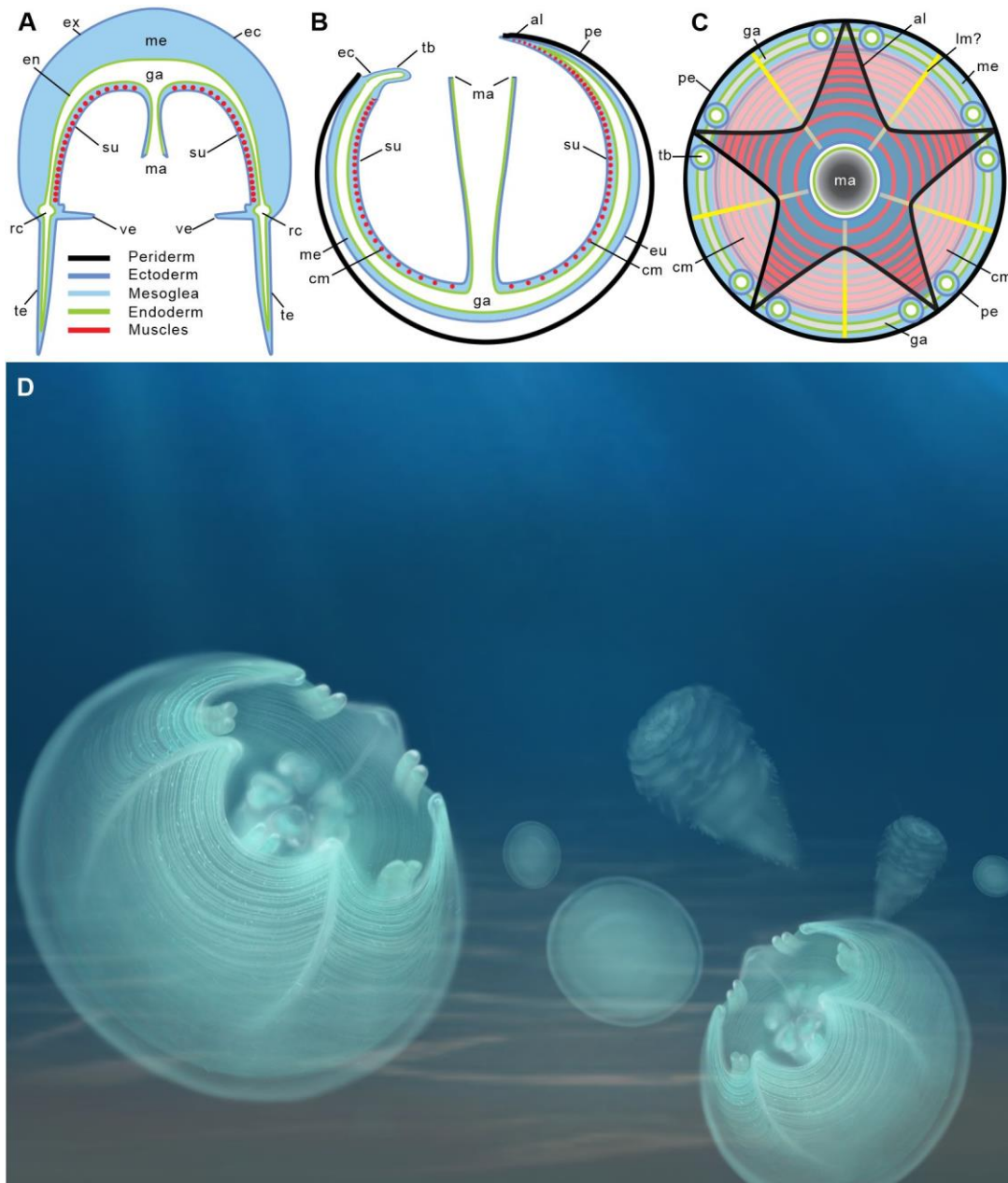
156

157 **Myoepithelial muscles in cnidarians from the basal Cambrian**

158 The close-knit circular fibers found in the bell of Olivooidea sp. can be confidently interpreted as
159 epithelial muscle fibers based on their individual cylindrical shape, size range (ca. 2 μm in diameter),
160 regular arrangement in bundles (e.g. possibly five more around bell margin), and closely-packed
161 distribution over a single anatomical surface represented by the subumbrella (Figures 1 and 2—figure
162 supplement 4). Our interpretation is also strongly supported by close similarities with the muscular
163 system of modern cnidarians (myoepithelial cells; MEC). For example, the medusae of hydrozoans
164 (Figure 2G-I) display a continuous network of circular striated and radial smooth muscles over the
165 inner layer of their bell (subumbrella). These ca. 1-to-4- μm -thick individual fibers show oblique
166 interconnections (Figure 2G-I—figure supplement 4), and sparser radial smooth fibers run
167 perpendicular to them (Leclère and Röttinger, 2017). A very similar configuration can be seen in early
168 Cambrian olivoids that display both continuous circular fibers (transverse markings imprinted on
169 circular bundles; see Figures 1, 2 and 3A-C). Microscopic series of functional units (sarcomeres) that
170 characterize striated muscles and give them a typical striated appearance (Figure 2G-I—figure
171 supplement 4) are not discernible in the muscle network of Cambrian olivoids, making it impossible
172 to distinguish their original nature, either striated or smooth (Schmidt-Rhaesa, 2007). The muscles of
173 olivoids seem to be more developed and concentrated around the bell margin, as seen in modern
174 jellyfish, such as *Clytia*, *Pelagia* and *Chrysaora* (Figure 2G-I—figure supplement 4). Other olivoids
175 from the Kuanchuanpu Formation such as *Sinaster* have a comparable concentration of strong
176 muscles around the oral aperture (possibly five bundles; see Wang et al., 2017) but, unlike those of
177 the present specimens, seem to be interrupted by interradian structures. The muscle fibers of
178 olivoids distribute over a surface interpreted as the inner layer of the bell (subumbrella), as in
179 modern medusae. In contrast with bilaterians, modern cnidarians are characterized by myoepithelial
180 cells that are fully integrated into the ectodermal and endodermal epithelial tissues. Although the
181 cellular organization cannot be seen in Cambrian olivoids we hypothesize that their muscular system
182 was similarly composed of myoepithelial cells that emitted myofilaments from their basal part. The
183 circular network of olivoids seems to have been supplemented by possibly longitudinal muscles
184 accommodated within adradial furrows (figure supplement 2B). However, no clear individual fiber can
185 be seen in these adradial areas. Paired features interpreted as tentacular buds occur around the oral
186 rim of some olivoids (Han et al., 2013; Wang et al., 2020). Their external annulations may represent
187 underlying muscle fibers (Wang et al., 2020), or, more likely, anchoring features of nematocysts. The
188 tentacles of modern cnidarians have longitudinal muscles but lack circular fibers (Hyman, 1940).

189 The current well-accepted hypothesis is that olivoids developed from an ovoid post-embryonic form
190 (present material) into a conical corrugated polyp-like structure (Bengtson and Yue, 1997; Dong et al.,
191 2016; Han et al., 2013; Liu et al., 2014; Steiner et al., 2014; Wang et al., 2020). The transition to polyps
192 is characterized by the gradual increase of external ornamented ridges that most probably resulted in
193 a complete anatomical reorganization, as commonly seen in the development cycle of modern
194 cnidarians. Unfortunately, very little is known of the internal anatomy of these polyps, except that
195 they secreted a tubular feature (periderm) comparable with that of some extant scyphozoans (figure
196 supplement 6) and had possible oral lobes. Although rare, clear traces of circular fibers do occur in the
197 polyps of *Olivooidea mirabilis* (see ref. Steiner et al., 2014; fig. 12), suggesting that key features of the
198 muscle system were conserved through the lifecycle.

199 In summary, the close-knit fibrous network described here in post-embryonic olivoids is the oldest
200 record of a muscular system in cnidarians and more generally in animals.



201

202 **Figure 3. Location of epithelial muscles in extant hydromedusae (A) and early Cambrian Olivoidae**
203 **medusozoans (B, C).** (A), (B) are simplified radial sections through body. (C) is seen in oral view. (D)
204 Artistic reconstruction of 535-million-year-old olivoid cnidarians showing eggs (no opening,
205 background), post-embryonic (foreground) and polyp (background) stages. The circular muscle system
206 is visible through the translucent periderm. Abbreviations: al, apertural lobe; cm, circular (coronal)
207 muscle; ec, ectoderm; en, endoderm; ga, gastrovascular cavity; lm?, possible longitudinal muscle; ma,
208 manubrium; me, mesoglea; pe, periderm; rc, radial canal; su, subumbrella; tb, tentacular bud; te,
209 tentacle; ve, velum. Not to scale.

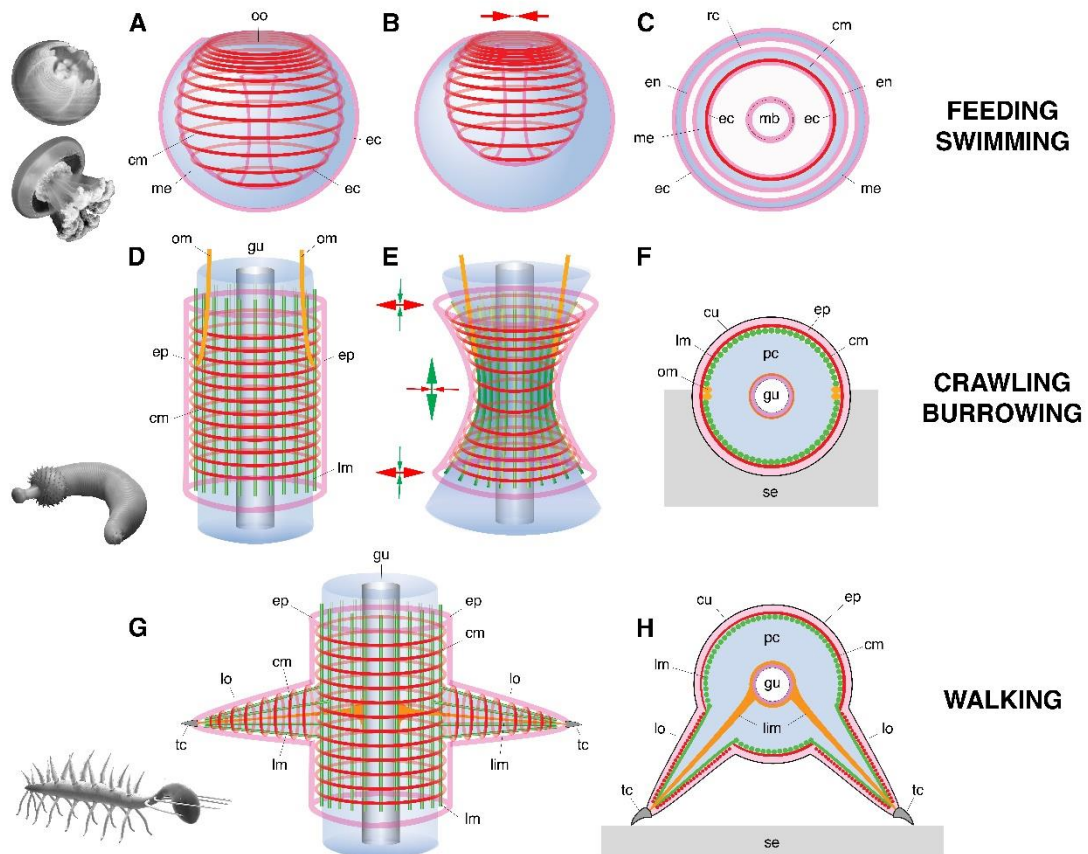
210

211 **Functions of muscles in post-embryonic olivoids**

212

213 The occurrence of strong muscles around the bell aperture and inside the periradial apertural lappets
214 suggests that olivoids could contract their bell as do modern medusae (Figures 3A-C and 4A-C). In
215 extant jellyfish, these contractions are counteracted by the elastic properties and antagonistic force
216 of the adjacent mesoglea. As a result, water is rhythmically expelled from beneath the bell and drives
217 the medusa through the water column via jet propulsion (Brusca et al., 2016). Although olivoids
218 share important external and internal morphological features with medusozoans (Dong et al., 2013;
219 Han et al., 2013; 2016b; Wang et al., 2017; 2020), they are distinguished by an unusual pentaradial
220 symmetry and life cycle (ovoid post-embryonic stage to sessile polyp crest-bearing conical polyp). This
221 life cycle has no direct counterpart in modern medusozoans (e.g. ref. Brusca et al., 2016) that develop
222 from a motile planula larva into a polyp and eventually a juvenile medusa through various processes
223 (e.g. strobilation generating ephyrae in scyphozoans; see ref. Gershwin, 1999). It has been suggested
224 (Wang et al., 2020) that the post-embryonic stage of olivoids combined the characters of a medusa
225 with those of a polyp and thus would resemble a juvenile sessile jellyfish almost encased within a
226 periderm, with its bell aperture facing upwards. At first sight, these circular muscles may suggest a
227 role in locomotion, as in modern medusae. However major structural differences separate modern
228 jellyfish from Cambrian olivoids (see above). Whereas the movement of modern medusae is
229 unconstrained, that of olivoids was most probably strongly hindered by its periderm (Bengtson and
230 Yue, 1997; Steiner et al., 2014). The assumed mesoglea layer of olivoids seems to have been very
231 thin (narrow gap between ex- and subumbrella; see Han et al., 2013, 2016b; Dong et al., 2016; Wang
232 et al., 2017, 2020) thus limiting its dynamic capacity. Swimming efficiency of modern medusae
233 depends on the power and distribution of muscles but also largely on the flexibility of the bell margin,
234 a condition that is not found in olivoids. Powerful muscle contractions may have been able to propel
235 the animal over a very short distance but are unlikely to have sustained dynamic locomotion through
236 the water column. This hypothetical “clumsy” locomotion would have probably created more
237 disadvantages (e.g. energy cost) than advantages to the animal. Moreover, it is unlikely to have
238 generated any adequate escape reaction (e.g. from predators) or effective feeding technique. We
239 favour an alternative option. One of the most vital requirements for post-embryonic olivoids was
240 probably to obtain sufficient food. Modern medusae feed on small soft-bodied prey by using
241 nematocyst-laden tentacles and oral arms that convey food to the mouth (Brusca et al., 2016).
242 Post-embryonic olivoids had tentacular buds that were not enough developed to capture food.
243 Feeding may have been achieved by a different method, such as the rhythmic contractions of their
244 circular muscles, especially those bordering the bell aperture (Figure 4A-C). Such contractions may
245 have resulted in pumping and engulfing sea water containing potential food particles. Extant jellyfish
246 such as *Aurelia* feed by using a comparable mechanism (Costello and Colin, 1994). The aperture
247 lappets of olivoids may have played the key roles in closing the aperture after contraction in locking
248 away food particles within the bell cavity before being transferred to the mouth and preventing
249 foreign matters from entering the bell. Besides, the remarkable plasticity of modern cnidarians to
250 transformation and rearrange their muscle system (e.g. transition from polyp to medusa stages;
251 Brusca et al., 2016) may have played in this evolution and diversification. Interestingly, muscle fibers
252 primarily assigned to feeding (olivoids) may have been used for other functions such as active
253 propulsion, escape reaction during evolution while maintaining an important role in prey capture. In

254 this context, we could make a bold speculation that the origin of the medusae swimming, associated
 255 by the subsequent loss of periderm, is an evolutionary inheritance of rhythmic feeding and respiration
 256 among benthic periderm-dwelling medusozoans, probably during Ediacarian-Cambrian period (Figure
 257 3D).



258
 259 **Figure 4. Basic muscle systems in early Cambrian animals and their main functions.** (A-C) Contractile
 260 epithelial muscles (MEC, myoepithelial, predominantly circular) and antagonistic mesoglea
 261 exemplified by olivoooids and free-swimming jellyfish; idealized relaxed (A) and contracted (B)
 262 states and simplified transverse section (C). (D-F) Grid-like network of circular and longitudinal subepidermal
 263 muscle fibers (HMS) around cylindrical body filled with antagonistic internal fluid (hydroskeleton)
 264 exemplified by scalidophoran worms; idealized relaxed state (D), peristaltic contractions along body
 265 (E) and transverse section (F). (G-H) Longitudinal and circular muscles and extrinsic retractor muscles
 266 in limbs; idealized relaxed state (G); transverse section (H). Images (from top to bottom) represent an
 267 olivoid cnidarian, an extant jellyfish, the scalidophoran worm *Ottoia* (see ref. Vannier, 2012) and the
 268 lobopodian *Hallucigenia* (see refs. Smith and Caron, 2015; Smith and Ortega-Hernández, 2014).
 269 Drawings and images not to scale. Abbreviations: cm, circular muscle; cu, cuticle; ec, ectoderm; en,
 270 endoderm; ep, epidermal layer; gu, gut; lc, lobopod claw; lim, limb muscle; lm, longitudinal muscle; lo,

271 lobopod (soft leg); mb, manubrium; me, mesoglea; om, oblique muscle; oo, oral opening (bell
272 margin); pc, primary cavity filled with fluid; rc, radial canal; se, sediment; tc, terminal claw.

273 **Early evolution of muscle systems**

274 The shift of the actin-myosin system from strictly intracellular to intercellular functions seems to have
275 occurred in the early stages of metazoan evolution (Schmidt-Rhaesa, 2007). Although the most basal
276 metazoans lack true muscles they do have the capacity to contract their body or part of it. For
277 example, sponges have myocytes around the osculum that play a role in expelling wastes (Bagby,
278 1966). The fiber cells of placozoans such as *Trichoplax adherens* have contractile extensions packed
279 with actin filaments that link the ventral and dorsal epithelia (Armon et al., 2018). Although the
280 gliding motility of placozoans is mainly performed by ciliated epithelial cells, fiber cells seem to be
281 involved in active body deformation and invagination possibly related to feeding (Smith and
282 Mayorova, 2019). The integration of the actin-myosin system within a dense network of myoepithelial
283 cells as seen in Cambrian and modern cnidarian is likely to have been a major innovation that
284 provided animals with new capacities for powerful movements (e.g. swimming, feeding, respiration,
285 etc.). We suggest that the myoepithelial fiber network seen in post-embryonic olivoids may
286 represent one of the oldest and basic types of animal muscle systems that probably finds its origin in
287 the late Precambrian. Larger jellyfish from the early (e.g. Chengjiang, Han et al., 2016a) and
288 mid-Cambrian (Marjum Lagerstätte; coronal muscles, Cartwright et al., 2007) are likely to have
289 co-opted this basic system for more diverse functions such as swimming within the water column (e.g.
290 active jet propulsion) and prey capture as seen in modern jellyfish such as *Aurelia*.

291

292 **Diversity of muscle systems and locomotion modes in early Cambrian animals**

293

294 Ecdysozoans (worms and panarthropods) provide additional evidence on the diversity of muscle
295 systems in early Cambrian animals.

296 Scalidophoran worms were diverse and numerically abundant in the Cambrian (e.g.
297 Burgess-shale-type Lagerstätten). Modern representatives of the group such as *Priapulid* have a
298 close-knit network of circular and longitudinal muscle lining the inner surface of the body wall, that
299 is surrounded by ECM (Figure 4D-F—figure supplement 7) and often termed “Hautmuskelschlauch”
300 (HMS; see Schmidt-Rhaesa, 2007). The enclosed mass of incompressible fluid (hydroskeleton) that fills
301 the primary cavity of such worms is the principal antagonist for muscular action (Figure 4). Dynamic
302 interactions between HMS and hydroskeleton allow them to perform repeated body contraction and
303 extension for burrowing (Figure 4D-F) (e.g. ref. Vannier et al., 2010) and feeding. The eversion of the
304 introvert is a process of pumping body fluids into the anterior body region whereas its invagination is
305 performed by extrinsic oblique retractor muscles. Based on remarkable anatomical and functional
306 similarities with modern priapulids (Figure 4D-F—figure supplement 7), we posit that Cambrian
307 scalidophorans also had a HMS-type musculature and possible retractors. This hypothesis is
308 supported by abundant crawling and burrowing traces found in the basal Cambrian (e.g. treptichnid
309 burrow systems; see refs. Kesidis et al., 2019; Vannier et al., 2010) and the late Precambrian (e.g. refs.
310 Evans et al., 2020; Gehling et al., 2001) that could not have been made without the action of HMS on

311 a hydrostatic skeleton (Figure 4D-F—figure supplement 7). HMS clearly differs from the musculature
312 of olivoid cnidarians in at least two key features: 1) it does not consist of myoepithelial cells and 2)
313 the antagonist onto which muscular force is transferred is not the primary cavity filled with fluid but
314 the mesoglea (Leclère and Röttinger, 2017).

315 Lobopodians (e.g. Ortega-Hernandez, 2015) is an informal group of ecdysozoans with an annulated
316 cuticle and paired soft legs (lobopods), that is crucial for understanding the remote ancestry of
317 euarthropods. They are best exemplified by iconic Cambrian forms such as *Hallucigenia* (Smith and
318 Caron, 2015; Smith and Ortega-Hernández, 2014) and *Microdictyon* (Pan et al. 2018). Most recent
319 phylogenetic trees (Aria et al., 2021; Giribet and Edgecombe, 2019) have resolved Cambrian
320 lobopodians as an “intermediate” group between scalidophoran worms and arthropods with an
321 arthrodized exoskeleton. The inner surface of their body wall was lined with closely packed circular
322 and longitudinal muscle fibers that seem to have extended into the limbs (see *Tritonychus* in Zhang et
323 al., 2016; Figure 4G, H—figure supplement 5A, B). This configuration strongly recalls that of
324 ecdysozoan worms (see above). In *Paucipodia* from the Chengjiang Lagerstätte (see Vannier and
325 Martin 2017; see supplement figure 5C-E) a connecting strand runs between the terminal claw of the
326 limbs and the area surrounding the gut, and is interpreted here as a possible retractor muscle (see
327 analogues in extant onychophorans (De Sena Oliveira and Mayer, 2013). Although unsegmented as in
328 smaller lobopodians, larger Cambrian lobopodians such as *Pamdelurion* from the Sirius Passet
329 Lagerstätte (ca. 520 Ma) are characterized by a more complex musculature with paired, lateral,
330 ventral and dorsal longitudinal muscles. Well-developed bundles of extrinsic and intrinsic limb
331 muscles presumably controlled leg motion as in modern onychophorans (Budd, 1998; Hoyle and
332 Williams, 1980; Young and Vinther, 2017; see Figure 4G, H).

333 Early euarthropods that co-existed with lobopodians and scalidophoran worms (e.g.
334 Burgess-shale-type Lagerstätten) had already acquired rigid exoskeletal elements (sclerotized
335 cuticular elements jointed by an arthrodial membrane, such as body sclerites and appendage
336 podomeres) that were operated by a lever-like system of segmentally arranged antagonistic muscles
337 as seen in *Kiisortoqia* and *Camparamuta* from the Sirius Passet Lagerstätte (Young and Vinther, 2017).
338 This suggests that the rise of euarthropods was associated with a profound rearrangement of the
339 muscle system inherited from lobopodian ancestors, such as the reduction of the circular HMS
340 musculature that lost its primary hydrostatic function and peristaltic capabilities because of
341 exoskeletal rigidity (Young and Vinther, 2017).

342 In summary, both fossil and indirect evidence presented here indicate that different types of
343 musculature co-existed among early Cambrian animals: (1) myoepithelial circular (MEC) muscles in
344 cnidarians, (2) grid-like and subepidermal (HMS) muscles in scalidophoran worms, (3) HMS and
345 extrinsic muscles to control leg motion in lobopodians and (4) segmentally arranged muscles tightly
346 integrated to exoskeletal elements in early euarthropods.

347 Whereas the myoepithelial system appears as the most basic one, that of ecdysozoans seems to have
348 undergone considerable changes and diversification over a relatively short time interval during the
349 early Cambrian. This remarkable diversity and plasticity of muscle systems allowed a great variety of
350 animals to explore and colonize new environments and can be seen as one of the driving forces of the
351 animal radiation.

352 **Geological setting, materials and methods**

353

354 All studied fossils come from phosphatic limestones collected from the Kuanchuanpu Formation at
355 the Shizhonggou section, (Ningqiang County, Shaanxi Province, China; see figure supplement 8).
356 Biostratigraphy (*Anabarites* – *Protohertzina* – *Arthrochities* zone, the *Siphogonuchites* – *Paragloborilus*
357 zone and *Lapworthella* – *Tannuolina* – *Sinosachites* zone; refs. Qian, 1977; 1999) indicates that these
358 rocks correspond to the Meishucunian Stage that is the equivalent of the lowermost Cambrian
359 Terreneuvian Stage. Radiochronology (U-Pb method; refs. Sawaki et al., 2008; Peng et al., 2012)
360 confirms that the Kuanchuanpu Formation is approximately 535 Ma. Secondly phosphatized fossils
361 were extracted from rocks via a standard acid digestion in 7% acetic acid. Dried residues with a
362 grain-size >60 µm were sorted and picked under a binocular microscope. Twelve specimens of
363 Olivoidae (Cnidaria) bearing well-preserved muscle fibers were selected for the present study and
364 mounted for SEM (FEI Quanta 400 FEG scanning electron microscope at Northwest University, China;
365 Au-coating, high-vacuum). They belong to *Sinaster petalon* Wang et al. (2017) (ELISN115-39),
366 *Hanagyroia orientalis* Wang et al. (2020) (ELISN107-470) and Olivoidae sp. (ELISN150-278,
367 ELISN111-54, ELISN052-33, ELISN045-143, ELISN012-16, ELISN061-19, ELISN087-64, ELISN088-48,
368 ELISN087-33 and ELISN098-19). All specimens are deposited in the collections of the Shaanxi Key
369 Laboratory of Early Life & Environments and the Department of Geology, Northwest University, China.
370 Data concerning these specimens are available on request from JH and XW.

371 Two-week-old *Clytia hemisphaerica* medusae, newly released *Eirene* sp. medusae, one-month-old
372 *Chrysaora colorata* and *Pelagia noctiluca* metaephyrae were raised in the laboratory
373 (Villeranche-sur-mer) following Lechable et al. (2020) and Ramondenc et al. (2017) culture protocols.
374 Fixation followed by Phalloidin (actin) and Hoechst (nuclei) staining were performed on the four
375 species as described for *Clytia hemisphaerica* in Sinigaglia et al. (2020). Samples were mounted in 50%
376 citifluor AF1 antifadent mountant and imaged using Leica SP8 confocal and Zeiss Axio-Observer
377 microscopes.

378 Extant priapulid worms (*Priapulid caudatus*) (see figure supplement 7) were collected (JV) from near
379 the Kristineberg Marine Station (Sweden), fixed with glutaraldehyde and dried (Critical Point) for SEM
380 observations (Univ. Lyon).

381

382 **Acknowledgements**

383

384 We thank the China Postdoctoral Science Foundation (No. 2020M672013), the Natural Science
385 Foundation of China (Nos. 41902012, 41720104002), the Strategic Priority Research Program of the
386 Chinese Academy of Sciences (No. XDB26000000), 111 Project of the Ministry of Education of China
387 (Nos. D17013, D163107), the Most Special Fund from the State Key Laboratory of Continental
388 Dynamics, Northwest University, China (BJ11060), the Région Auvergne-Rhône-Alpes and the Univ. of
389 Lyon (PAI grant to JV), for financial support, J. Sun and J. Luo for the preparation of microfossils and
390 SEM technical assistance, and the CTµ (University of Lyon) for access to electron microscopy. We
391 thank X.-G. Zhang for kindly providing images of Cambrian lobopodians. We thank Kentaro Uesugi
392 analyzing the specimens using the computed x-ray microtomography (XTM) at Tohoku University,
393 Japan, and the synchrotron of Spring-8 in Hyogo, Japan. This work was also supported by the Agence
394 Nationale de la Recherche (ANR-19-CE13-0003 to LL). We thank Alexandre Jan for raising the medusae

395 and the Paris Aquarium for providing the *Eirene* polyp stains. We thank the Marine Resources Centre
396 (CRBM and PIV imaging platform) of Institut de la Mer de Villefranche (IMEV), supported by
397 EMBRC-France. The CRBM is supported by EMBRC-France, whose French state funds are managed by
398 the ANR within the Investments of the Future program under reference ANR-10-INBS-02.

399

400 Author contributions

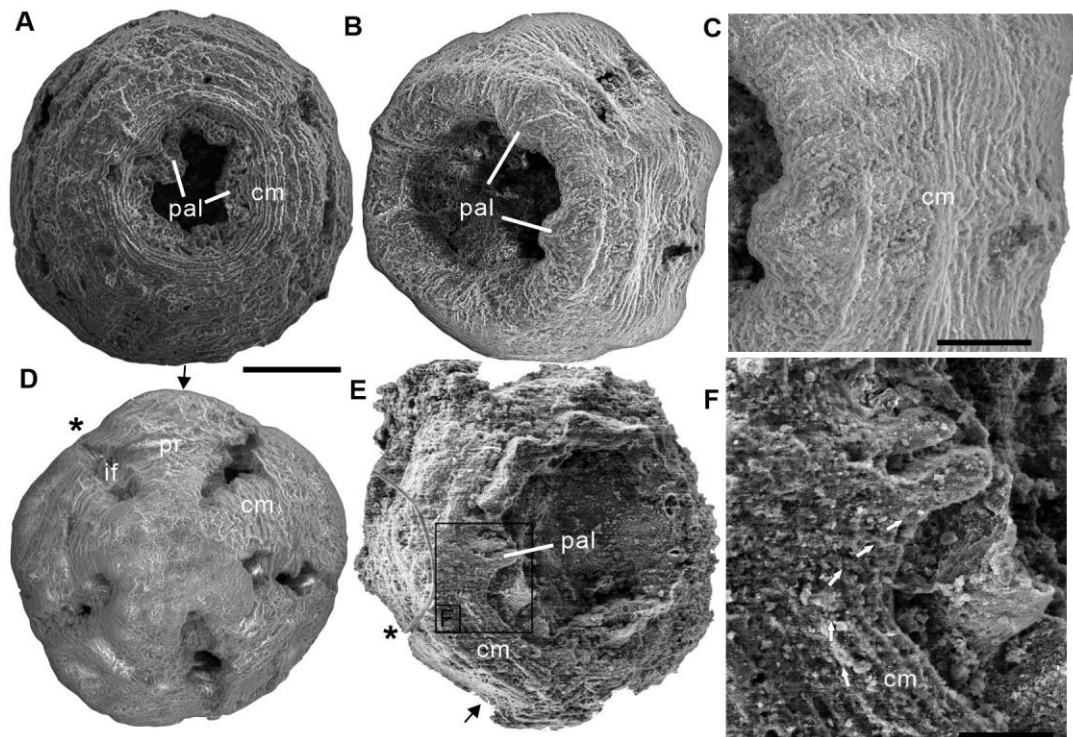
401

402 X. W., J. V. and J. H. designed the research. X. W., X.-G. Y and J. H. collected rocks (Shizhonggou
403 section, Shaanxi Province, China) and analyzed fossils. X. W. wrote the manuscript with input from all
404 other co-authors. L. L. provided comparative data and images of modern cnidarians and Q. O. made
405 insightful remarks on the MS.

406

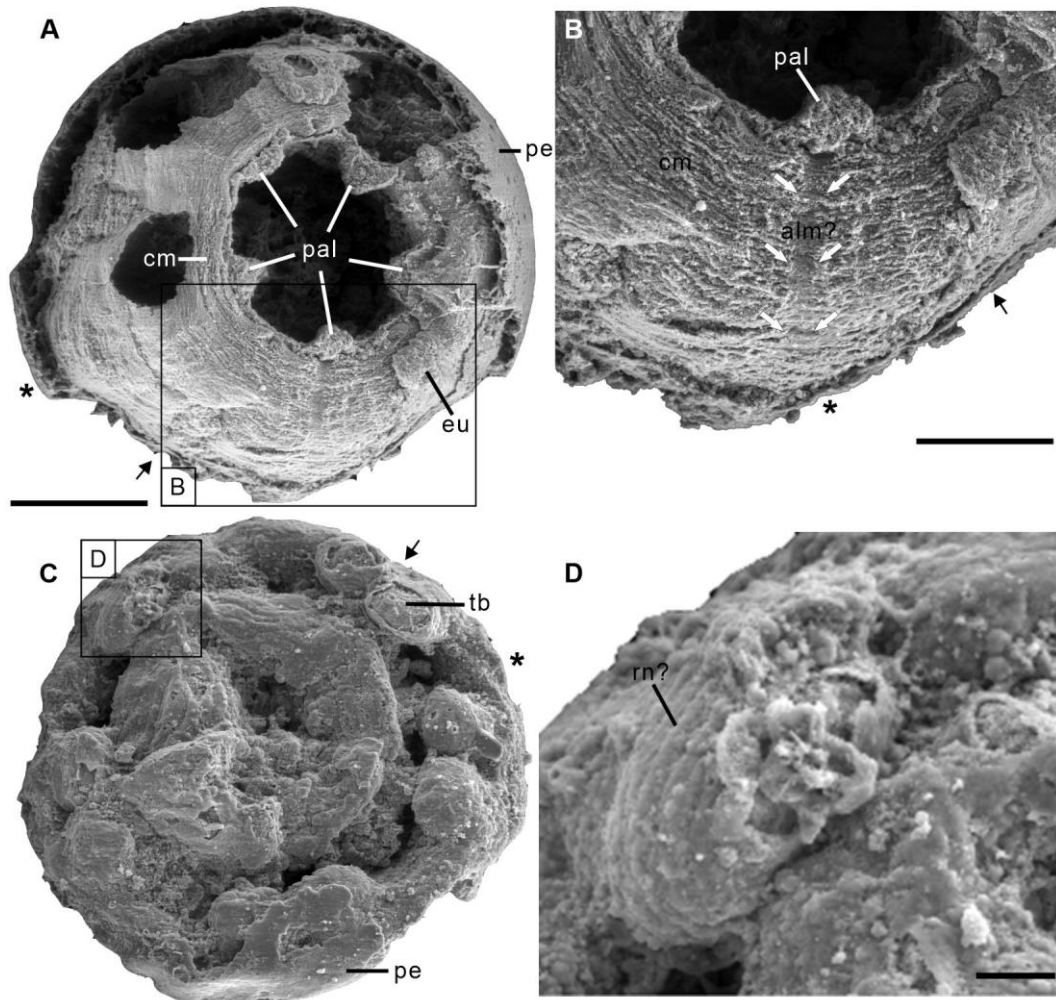
407

Supplements



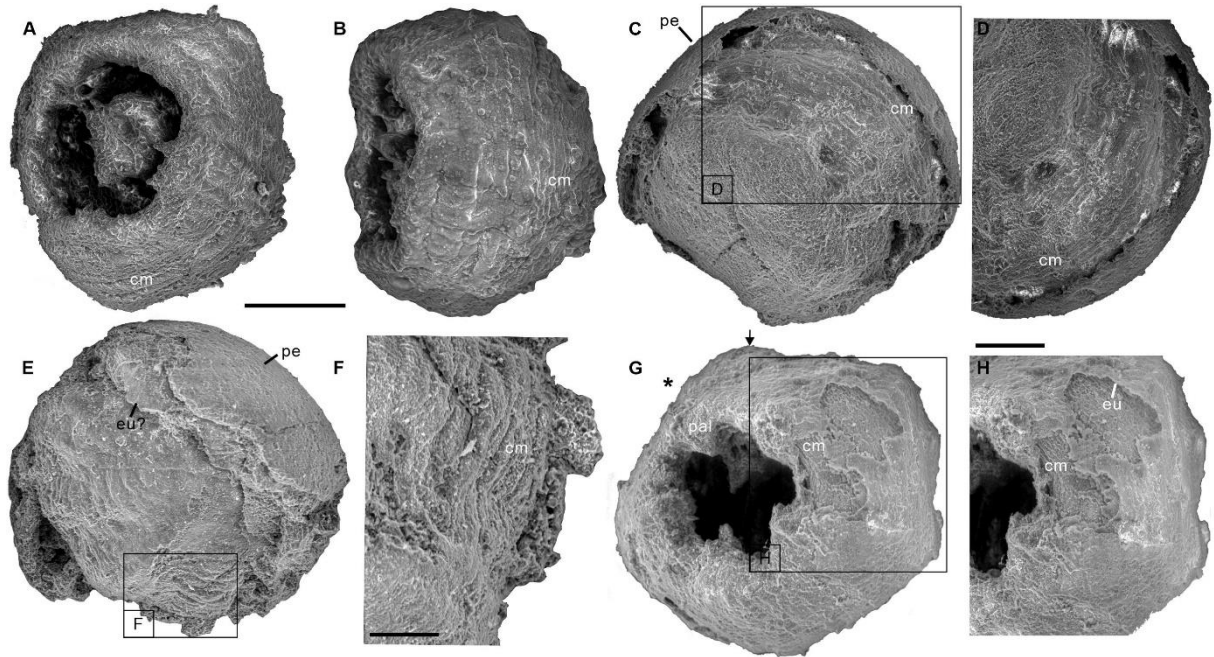
408

409 **figure supplement 1. The three scanning electron micrographs of the *Olivoides* specimens**
410 **ELISN012-16, ELISN045-143 and ELISN111-54 from the Kuanchuanpu Formation, south China. (A)** Oral
411 **view showing the external morphology of ELISN045-143 without periderm. (A), (D)** ELISN012-16.
412 **General view of oral side (A), details of muscles fibers in perradial apertural lobes and general view of**
413 **aboral side (D). (B)** Oral view showing the external morphology of ELISN045-143 without periderm. (C)
414 **Close-up view of a showing the circular muscles. (E)** Oral view showing the external morphology of
415 **ELISN111-54. (F)** The enlarged view of c showing that the circular muscles extending into the
416 **triangular perradial apertural lobes marked by the giant white arrows. Abbreviations: cm, circular**
417 **muscle; pal, perradial apertural lobe; *, perradii; →, interradii. Scale bars represent: 200 μ m in (A),**
418 **(B), (D) and (E); 50 μ m in (C); 25 μ m in (F).**



419

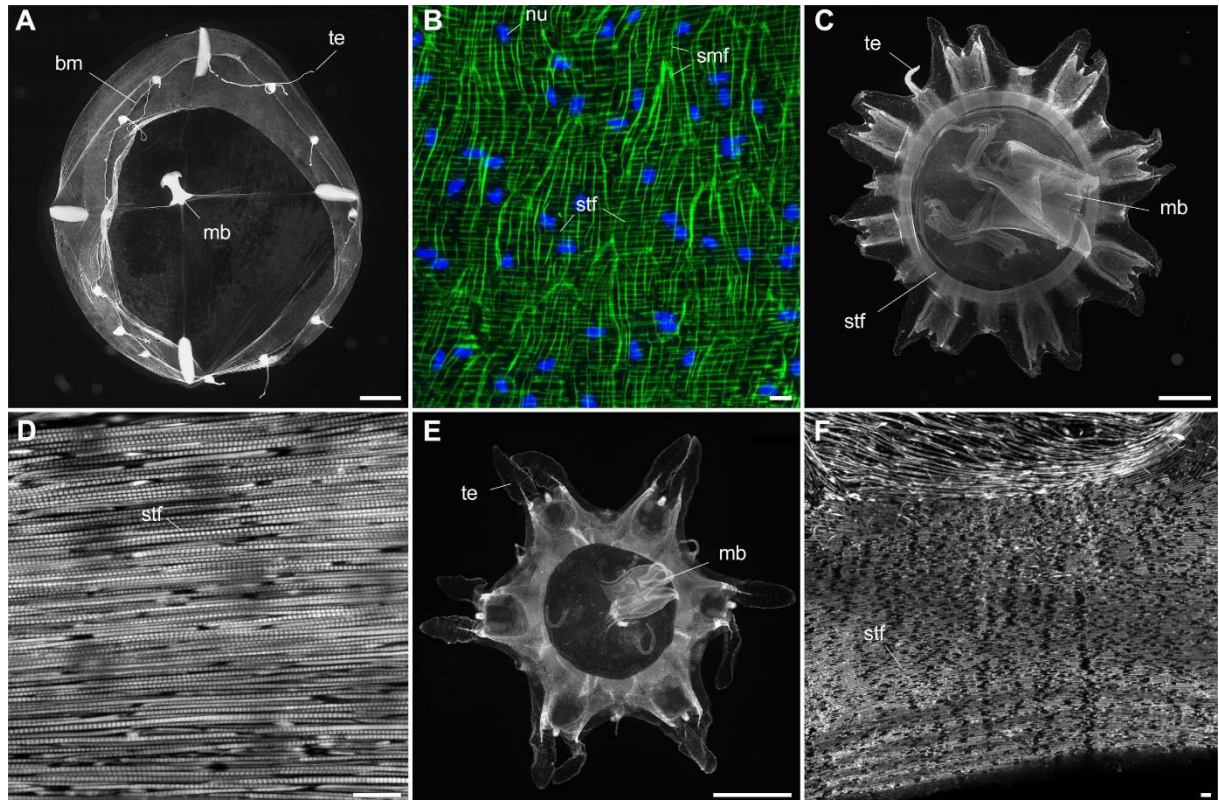
420 **figure supplement 2. The two scanning electron micrographs of the *Olivooides* specimens**
421 **ELISN115-39 (*Sinaster petalon*; Wang et al. 2017) and ELISN107-470 (*Hanagyroia orientalis*; Wang et**
422 **al. 2020) from the Kuanchuanpu Formation, south China. (A) Oral view showing the external**
423 **morphology of ELISN115-39. (B) Close-up view of (A) showing the possible longitudinal muscle bands**
424 **marked by the two rows of giant white arrows. (C) Oral view showing the external morphology of**
425 **ELISN107-470. (D) The enlarged view of (C) showing the possible rings of nematocysts on the**
426 **tentacles. Abbreviations: alm?, the possible longitudinal muscle bands at adradii; cm, circular muscle;**
427 **eu, exumbrella; pal, perradial apertural lobe; pe, periderm; *, perradii; →, interradii. Scale bars**
428 **represent: 200 μ m in (A), (C); 50 μ m in (B); 25 μ m in (D).**



429

430 **figure supplement 3. The four scanning electron micrographs of the *Olivoides* specimens**
431 **ELISN087-64 (A, B), ELISN088-48 (C, D), ELISN087-33 (E, F) and ELISN98-19 (G, H) from the**
432 **Kuanchuanpu Formation, south China. (A) General view of oral side. (B) Lateral view. (C) General view**
433 **of aboral side. (D) The enlarged view of (C) showing the circular muscles. (E) Lateral view. (F) The**
434 **enlarged view of (E) showing that the circular muscles. (G) General view of oral side. (H) The enlarged**
435 **view of (G) showing the circular muscles. Abbreviations: cm, circular muscle; eu, exumbrella; pal,**
436 **perradial apertural lobe; *, perradii; →, interradii. Scale bars represent: 200 μ m in (A-C), (E) and (G);**
437 **50 μ m in (F), (H); 25 μ m in (D).**

438



439

440 **figure supplement 4. Myoepithelial muscle network shown in extant medusozoan cnidarians. (A),**

441 **(B) *Clytia hemisphaerica* (Hydrozoa) mature medusa, general oral view and details of fiber network**

442 **(subumbrella). (C), (D) *Pelagia noctiluca* (Scyphozoa) metaephyra, general oral view and details of**

443 **closely-packed circular striated muscle fibers (subumbrella). (E), (F) *Chrysaora colorata* (Scyphozoa)**

444 **metaephyra, general oral view and details of circular striated muscle fibers. Green and blue colours**

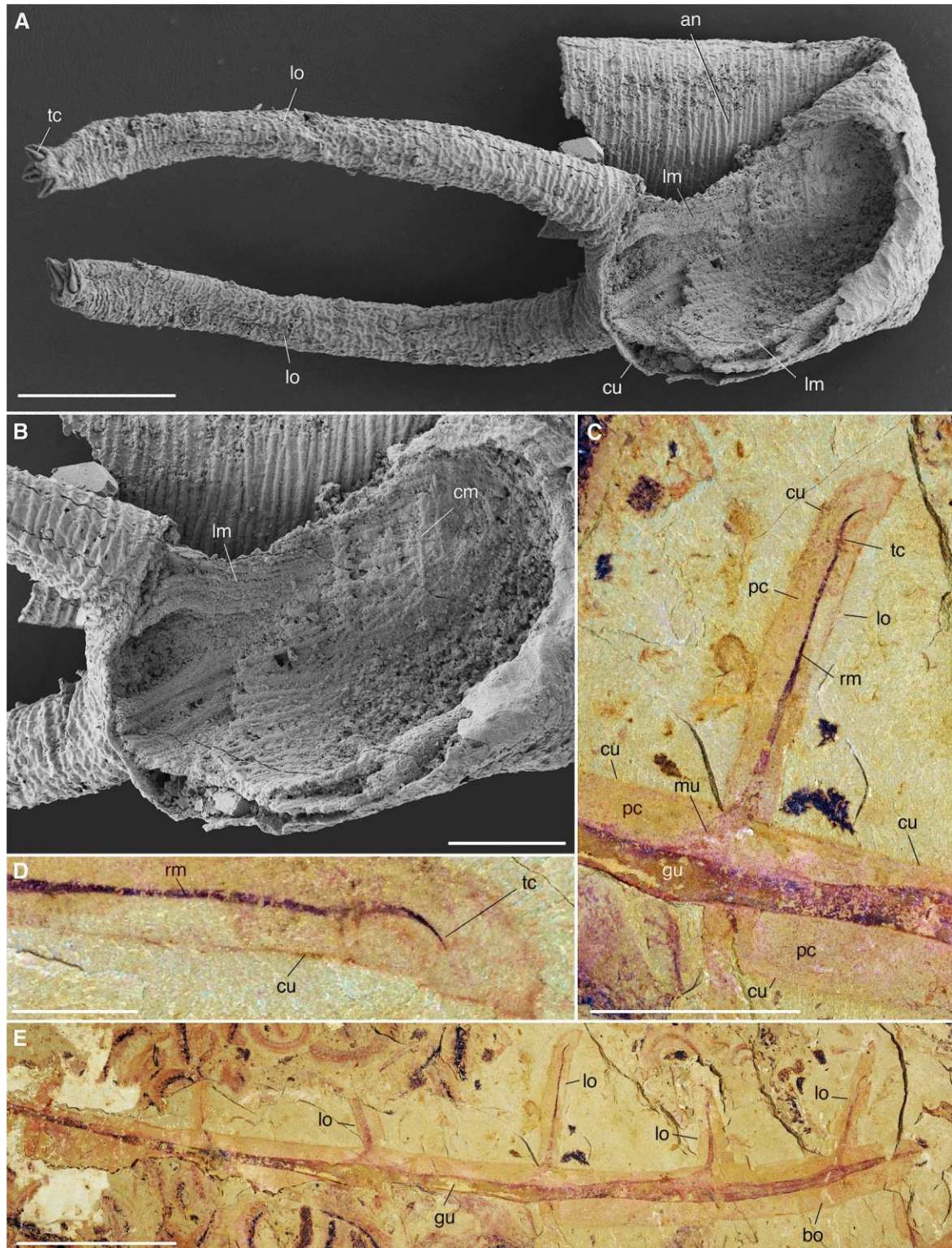
445 **(B) correspond to actin (phalloidin) and DNA (Hoechst) staining. Specimens represented by black and**

446 **white images (A) and (C-F) were stained for actin (phalloidin). Abbreviations are as follows: bm, bell**

447 **margin; mb, manubrium; nu, nucleus; smf, smooth (radial) muscle fiber; stf, striated (circular) muscle**

448 **fiber; te, tentacle. Scale bars: 1000 μ m in (A), (C) and (E); 10 μ m in (B), (D) and (F).**

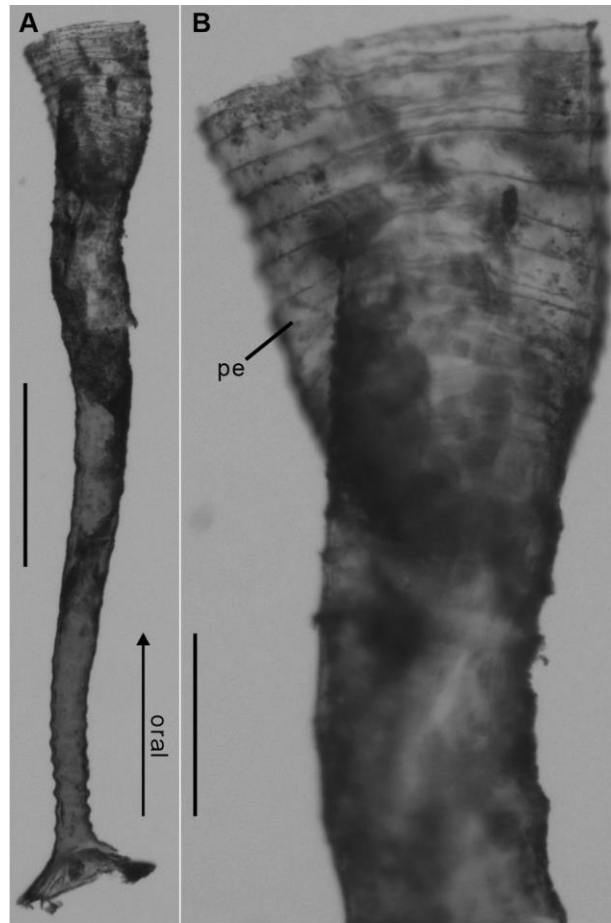
449



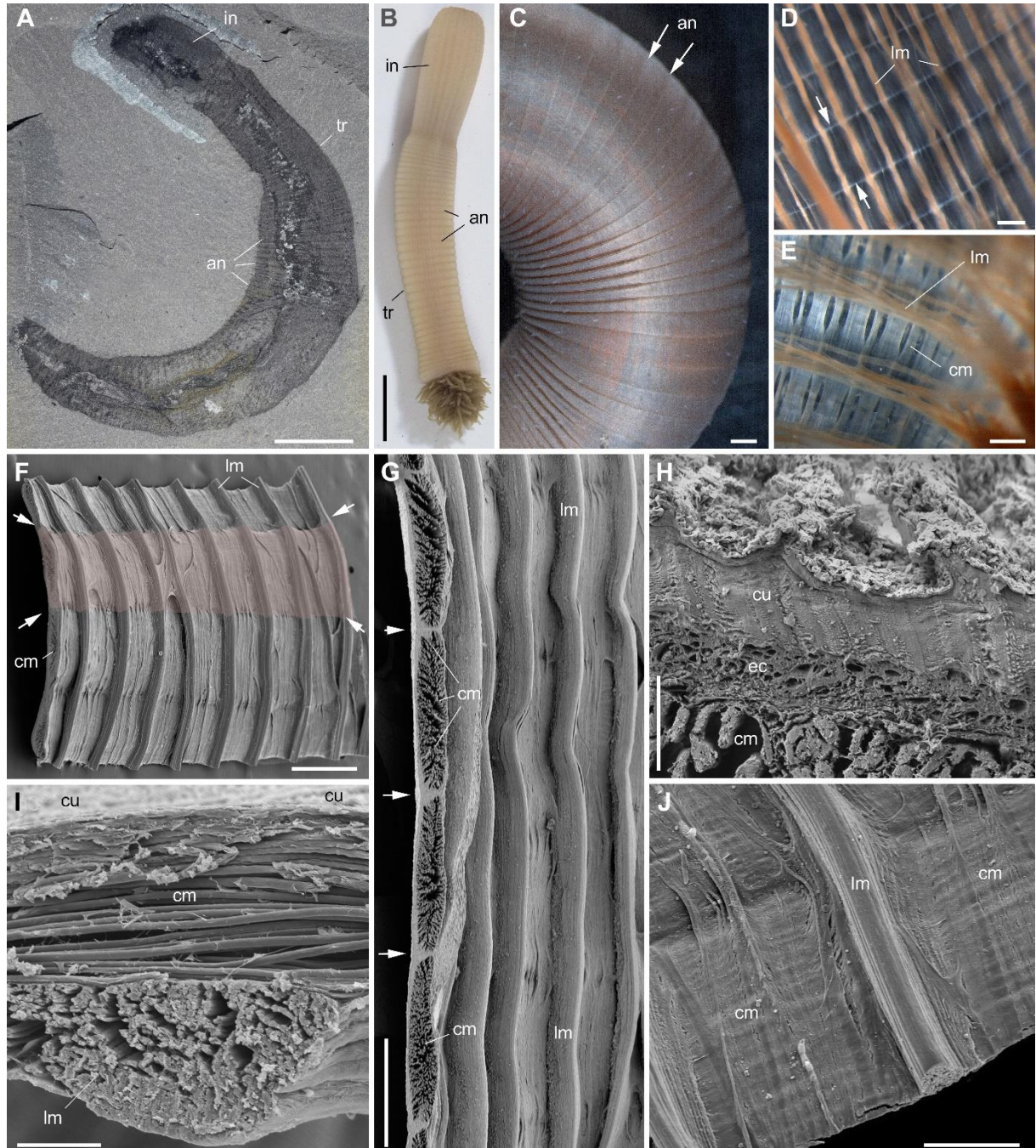
450

451 **figure supplement 5. Muscle system in Cambrian lobopodians (Ecdysozoa, Panarthropoda).** (A), (B)
452 *Tritonychus phanerosarkus* from the Yu'anshan Formation (Xiaotan section, Cambrian Series 2, Stage
453 3), Yongshan, Yunnan Province, China; general view and details of a secondarily phosphatized
454 specimen showing a pair of walking appendages (lobopods) and the inner body wall lined with muscle
455 fibers (see Zhang et al., 2016). (C-E) *Paucipodia haikouensis* from the Chengjiang Lagerstätte,
456 ELI-JS0001a (see Vannier and Martin, 2017); close-up of lobopod and terminal claw, and general view;

457 note muscle bridging claw to gut area. (A), (B) are SEM images (Courtesy Prof. Xiguang Zhang; see
458 Zhang et al., 2016). Abbreviations: an, annuli; cm, circular muscle; cu, cuticle; gu, gut; lm, longitudinal
459 muscle; lo, lobopod; mf, muscle fiber; mu, muscle; pc, primary cavity; rm, retractor muscle; tc,
460 terminal claw. Scale bars: 10 mm in (E), 5 mm in (C), 1 mm in (D), 200 μ m in (A) and 100 μ m in (B).
461



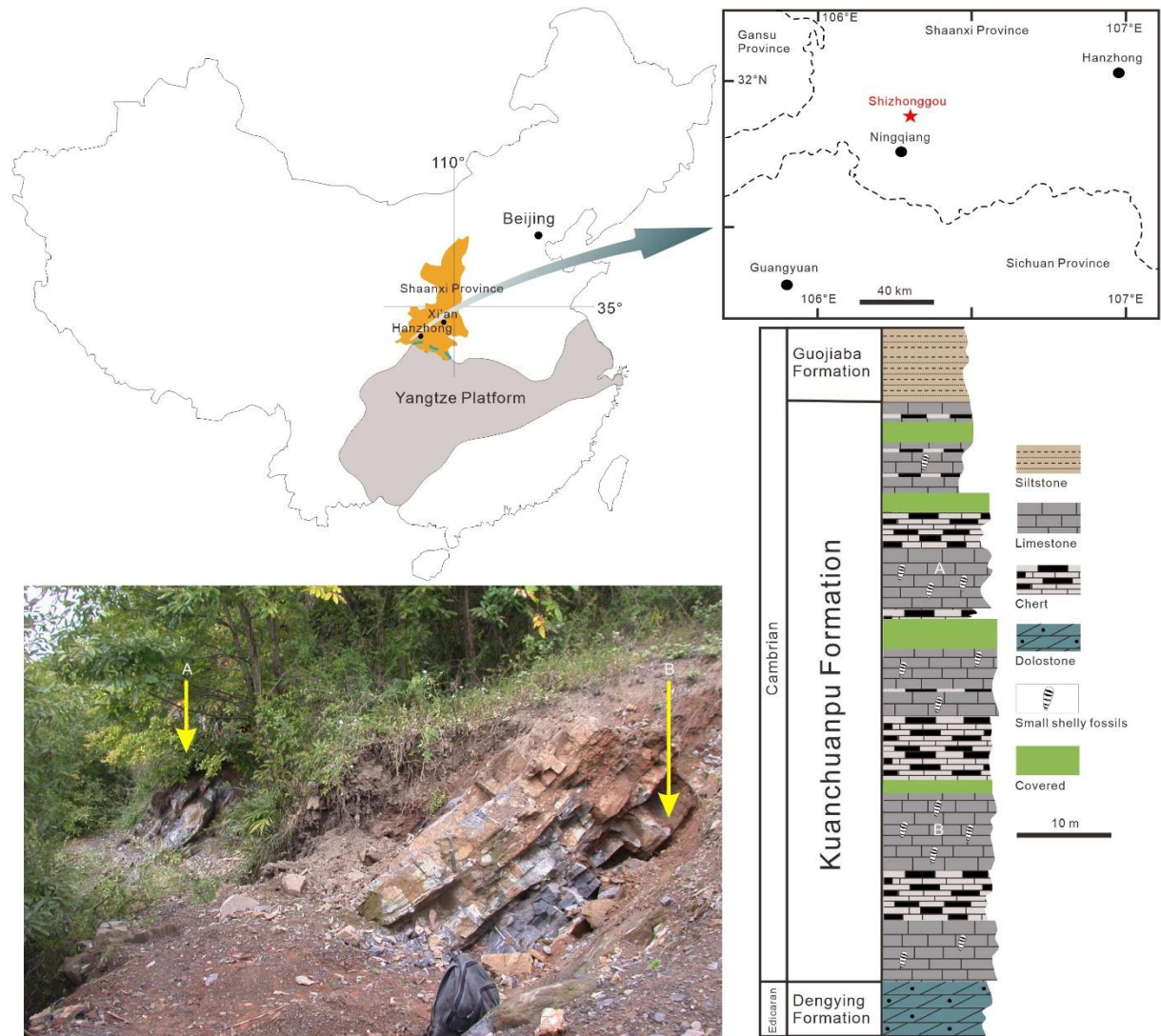
462
463 **figure supplement 6. Polyp of Coronatae sp. from South China Sea showing the periderm. (A), (B)**
464 **Lateral view and details showing corrugations. (Courtesy Dr. Xikun Song). Abbreviations are as**
465 **follows: pe, periderm. Scale bars: 400 μ m in (A); 100 μ m in (B).**
466



467

468 **figure supplement 7. Muscle system in priapulid worms (Ecdysozoa).** (A) *Ottoia prolifica* from the
469 mid-Cambrian Burgess Shale, general view showing annulated body. (B-J) *Priapulus caudatus* from
470 Sweden. (B) general view of live specimen in sea water. (C) annulated trunk. (D) muscles (trunk). (E)
471 muscles (introvert). (F) fragment of trunk showing the internal body wall with strong longitudinal
472 muscles (pink area corresponds to one annulation). (G) transverse section through circular muscles
473 (one bundle per annulation). (H) transverse section through body wall across cuticle, epithelial cells
474 and circular muscles. (I) transverse section through body wall showing circular muscles overlying
475 longitudinal ones. (J) inner wall of body showing both circular and longitudinal muscles. Small white
476 arrows indicate annulation boundaries. (A-E) are light photographs. (F-J) are SEM images.
477 Abbreviations are as follows: an, annulation; cm, circular muscle; cu, cuticle; ec, epithelial cells;

478 introvert; lm, longitudinal muscle; tr, trunk. Scale bars: 1 cm in (A), (B); 1 mm in (C); 500 μm in (D-G);
479 200 μm in (J); 50 μm in (I) and 10 μm in (H).



480
481 **figure supplement 8. Origin of the fossil material.** Location map (Ningqiang area, Southern Shaanxi
482 Province, China), photograph of outcrop (Shizhonggou Section; see red star) and stratigraphic position
483 of fossil-bearing rock samples (A), (B) within the Kuanchuanpu Formation. Modified from Steiner et al.,
484 2014.

485 **References**

486

487 Aria C, Zhao F-C, Zhu M-Y (2021) **Fuxianhuiids are mandibulates and share affinities with total-group**

488 **Myriapoda** *Journal of the Geological Society* **178**:jgs2020–246. <https://doi.org/10.1144/jgs2020-246>

489 Armon S, Bull MS, Aranda-Diaz A, Prakash M (2018) **Ultrafast epithelial contractions provide insights**
490 **into contraction speed limits and tissue integrity** *PNAS* **115**:E10333–E10341.

491 <https://doi.org/10.1073/pnas.1802934115>

492 Bagby RM (1966) **The fine structure of myocytes in the sponges *Microciona prolifera* (Ellis and**
493 **Solander) and *Tedania ignis* (Duchassaing and Michelotti)** *Journal of Morphology* **118**:167–181.

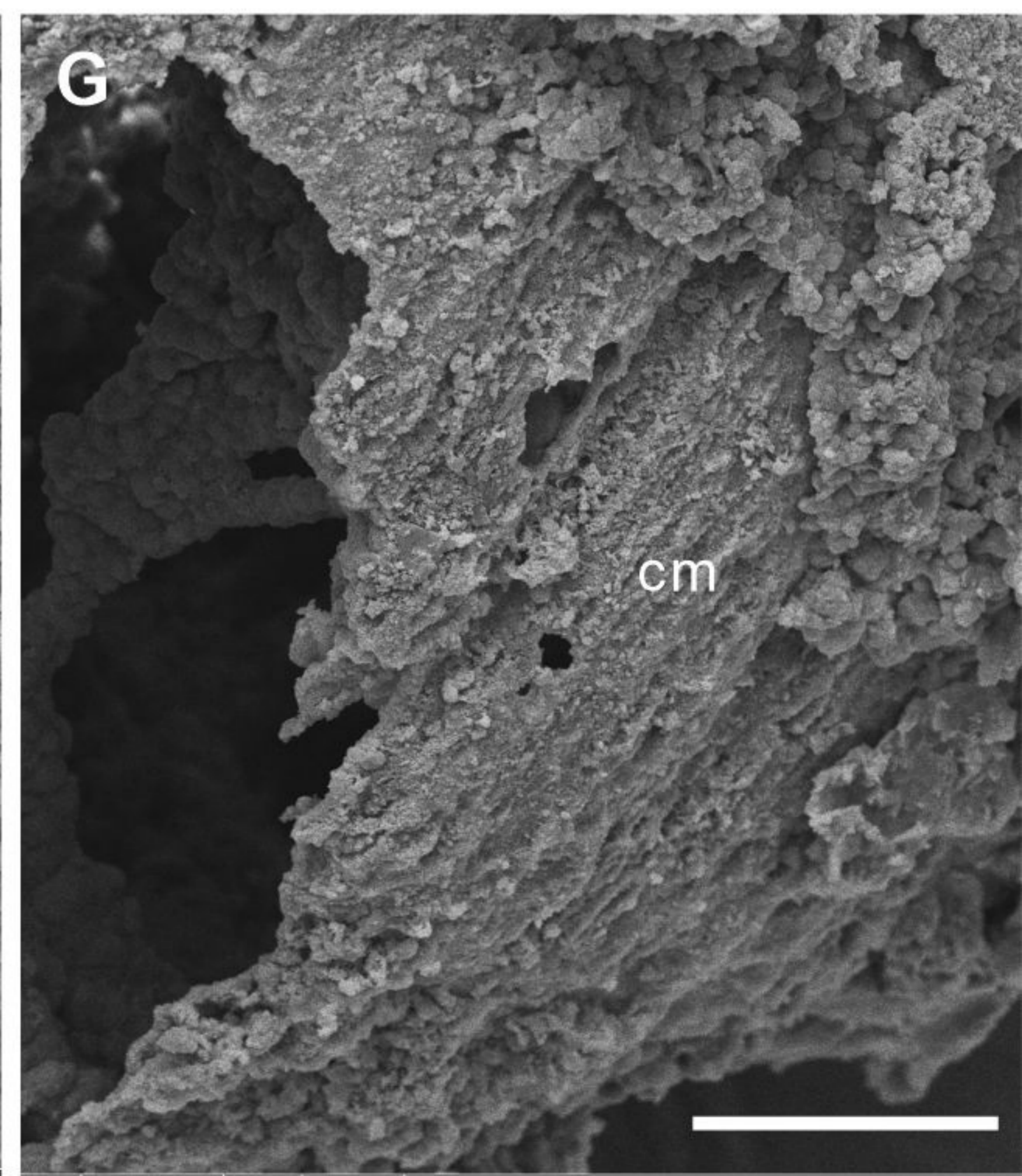
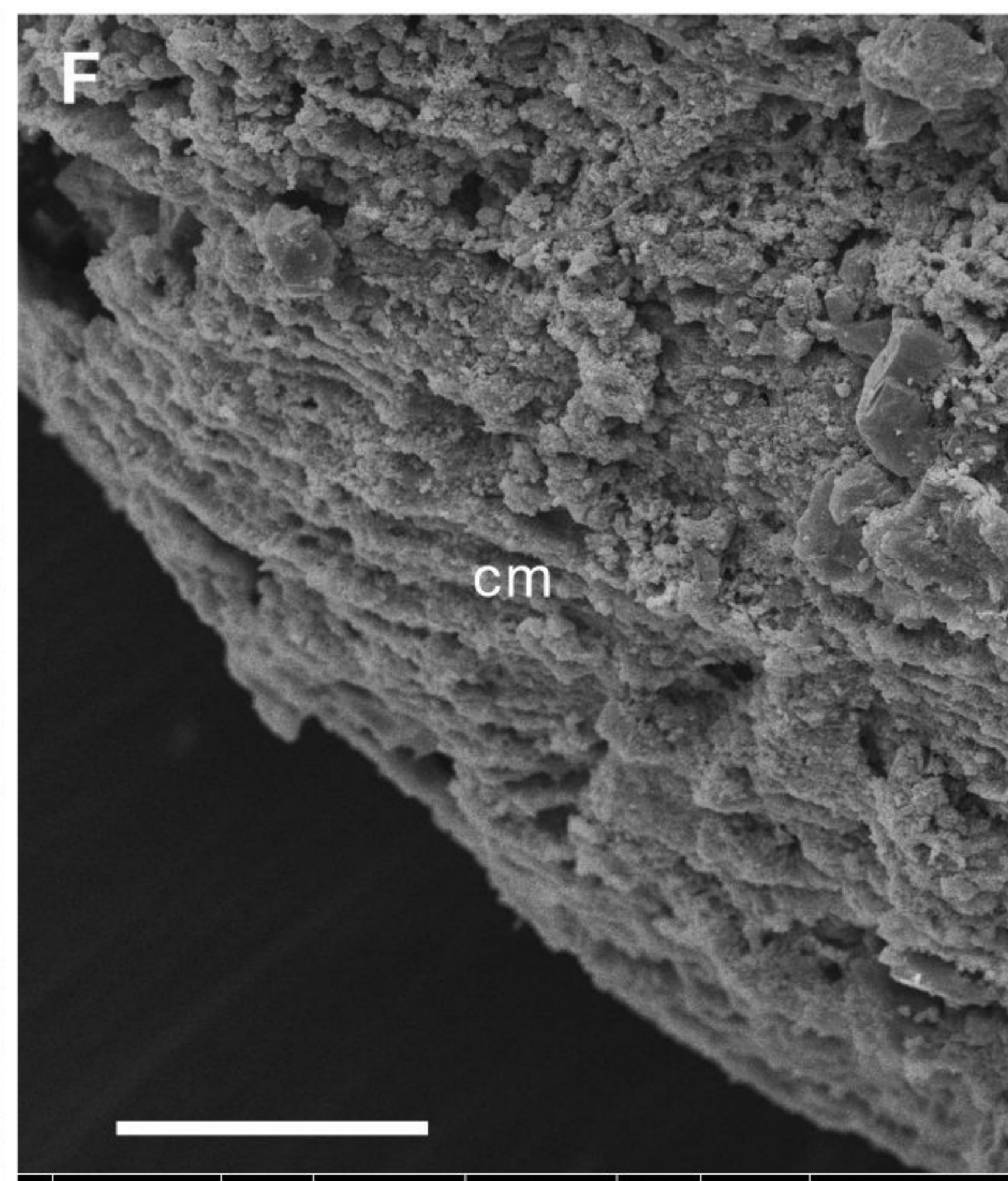
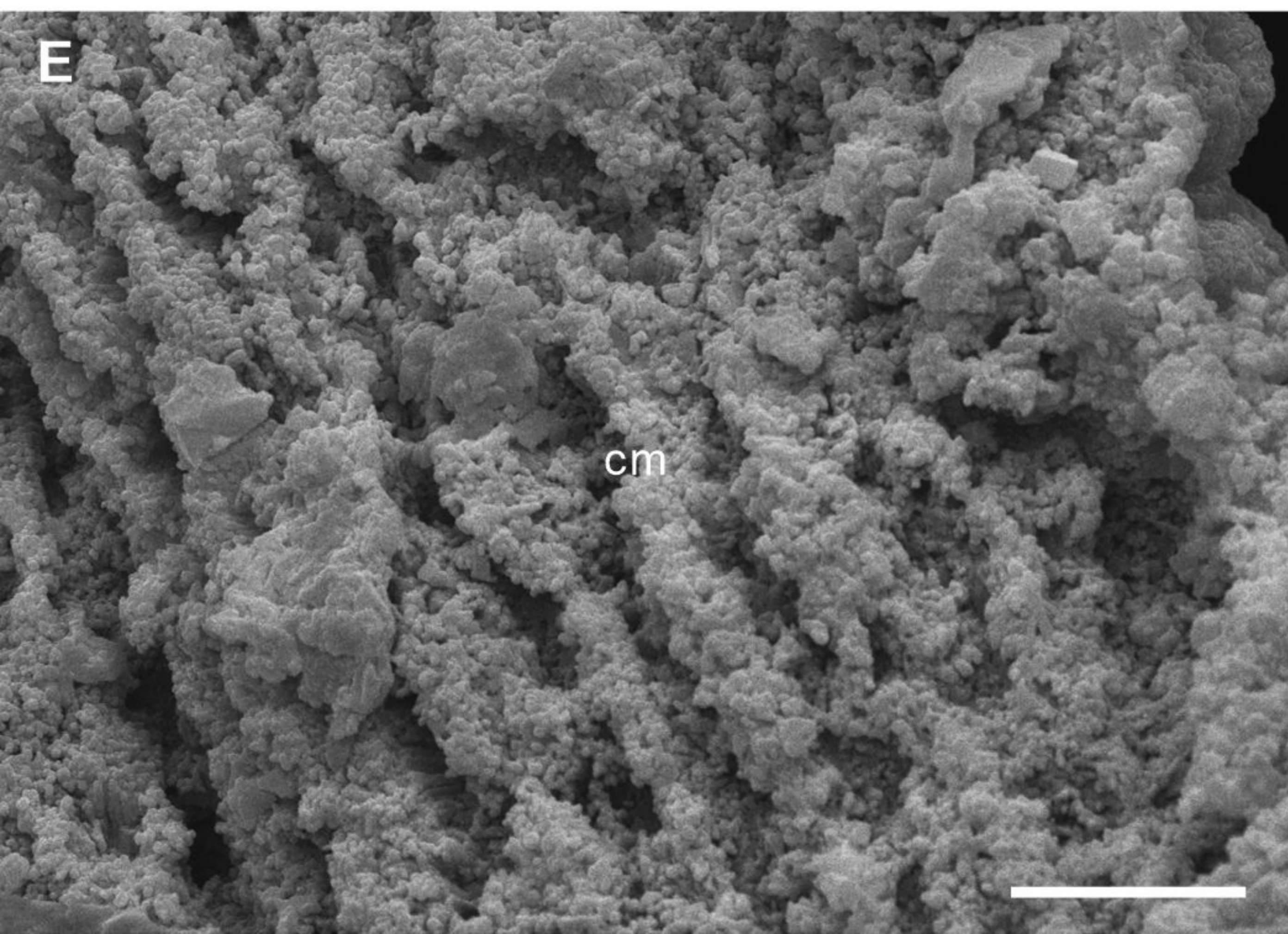
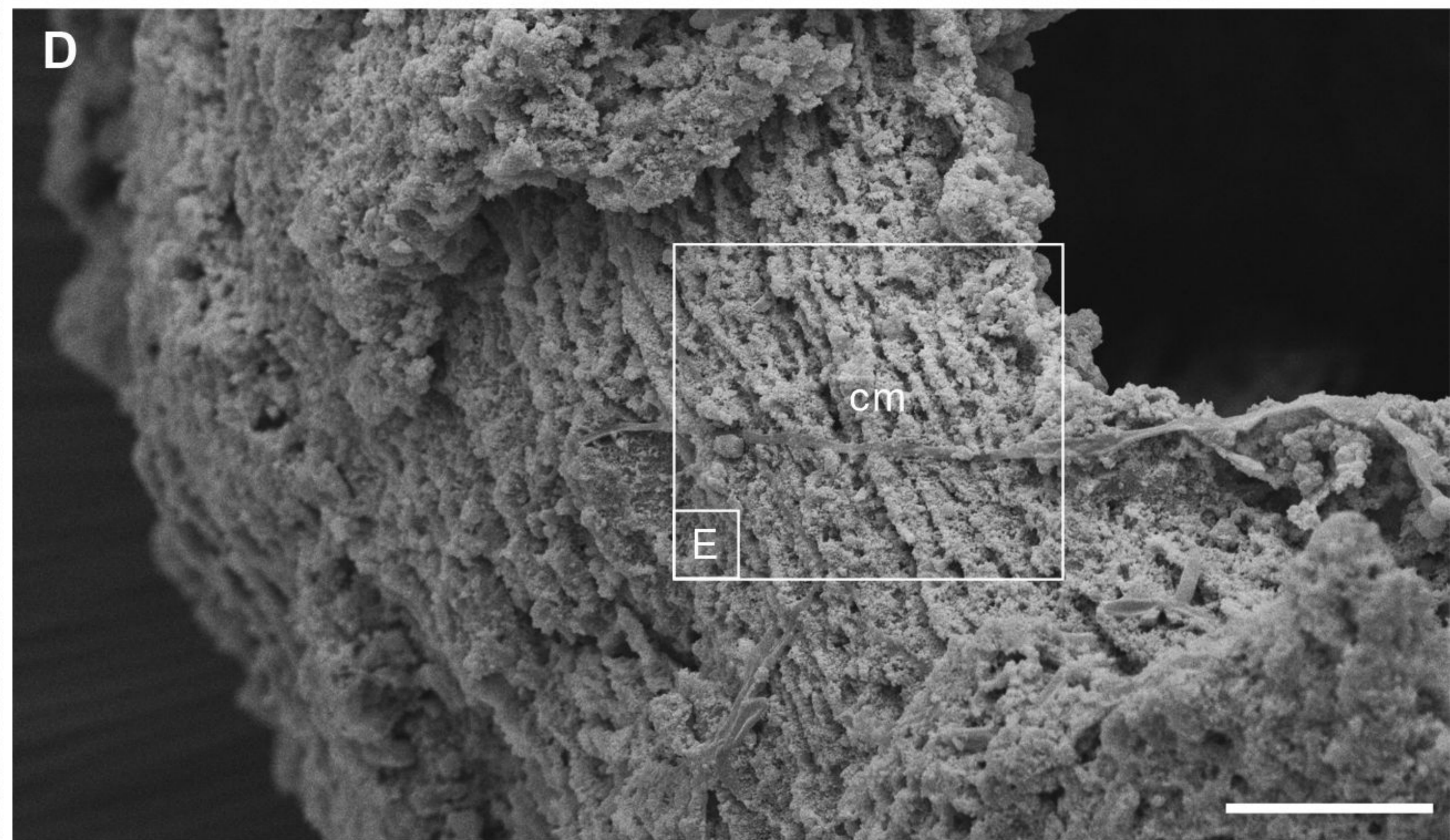
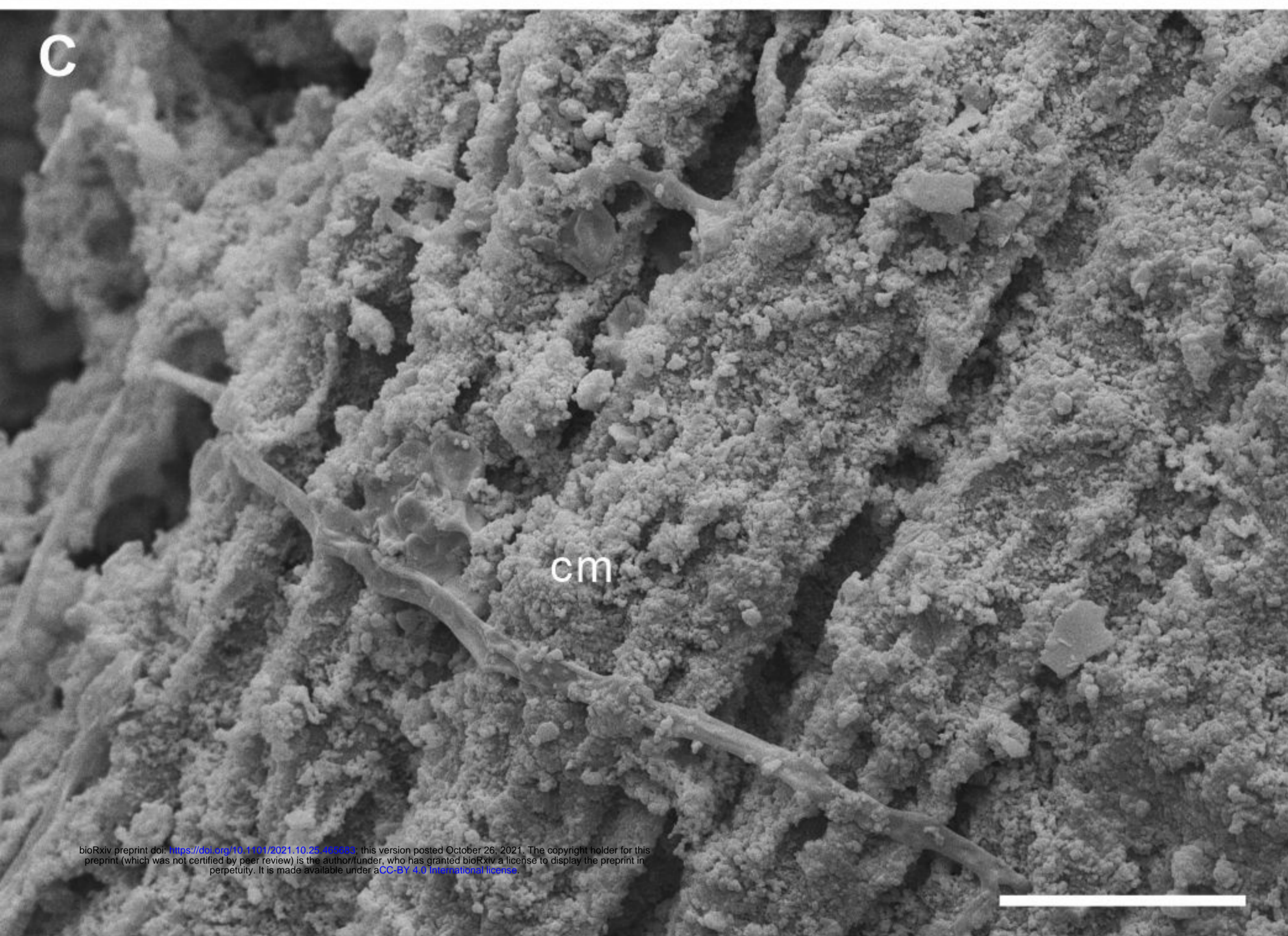
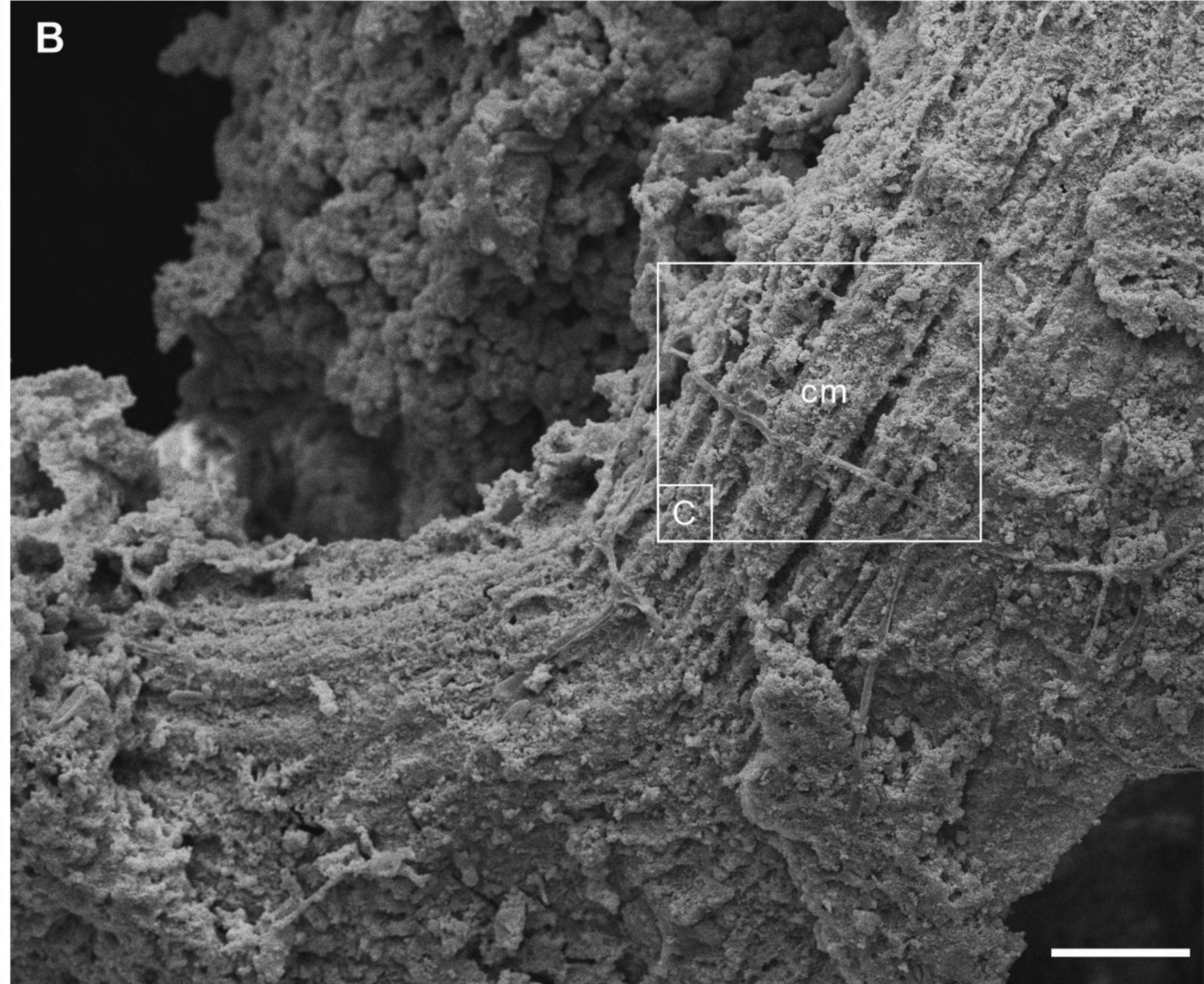
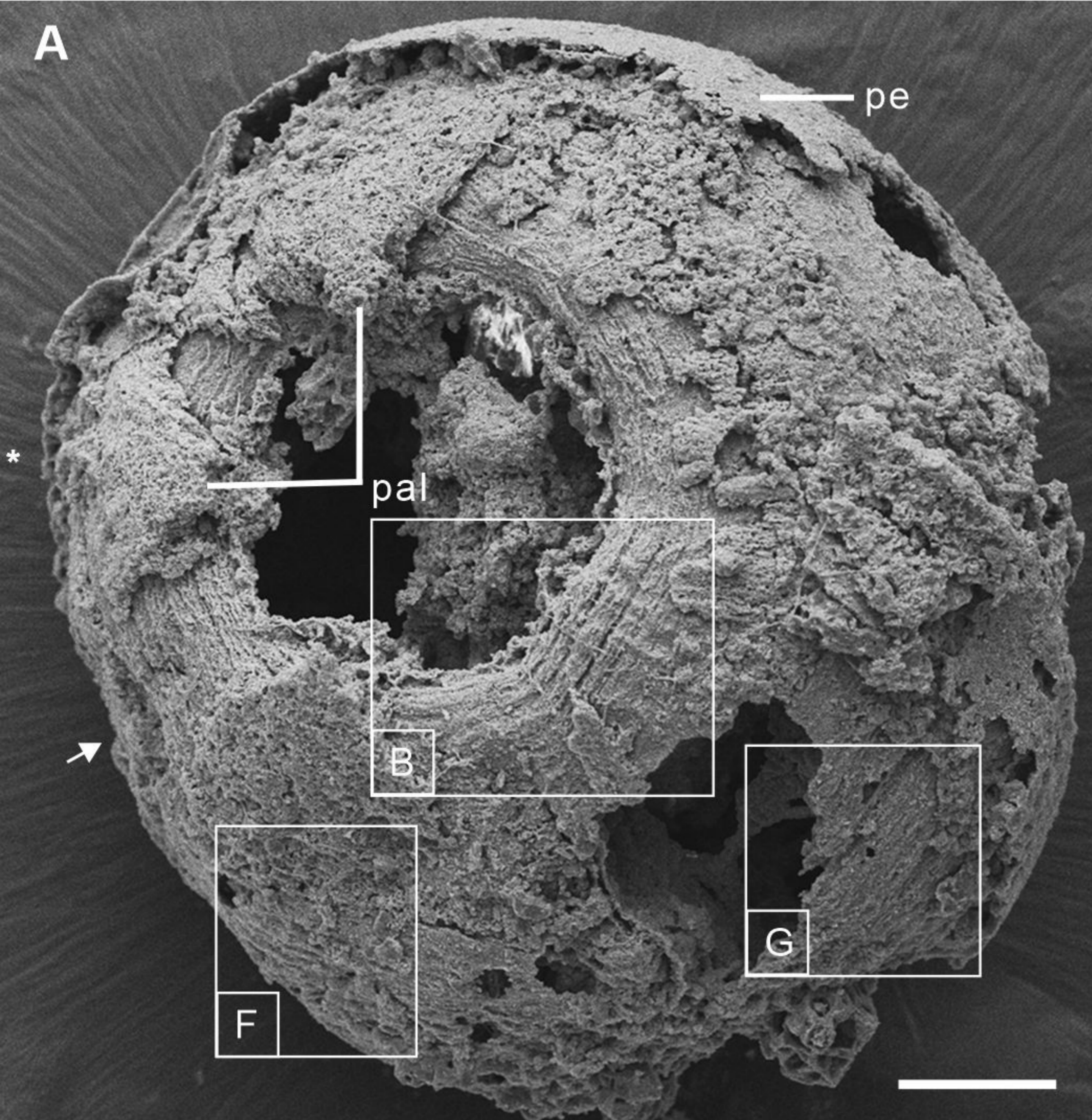
494 <https://doi.org/10.1002/jmor.1051180203>

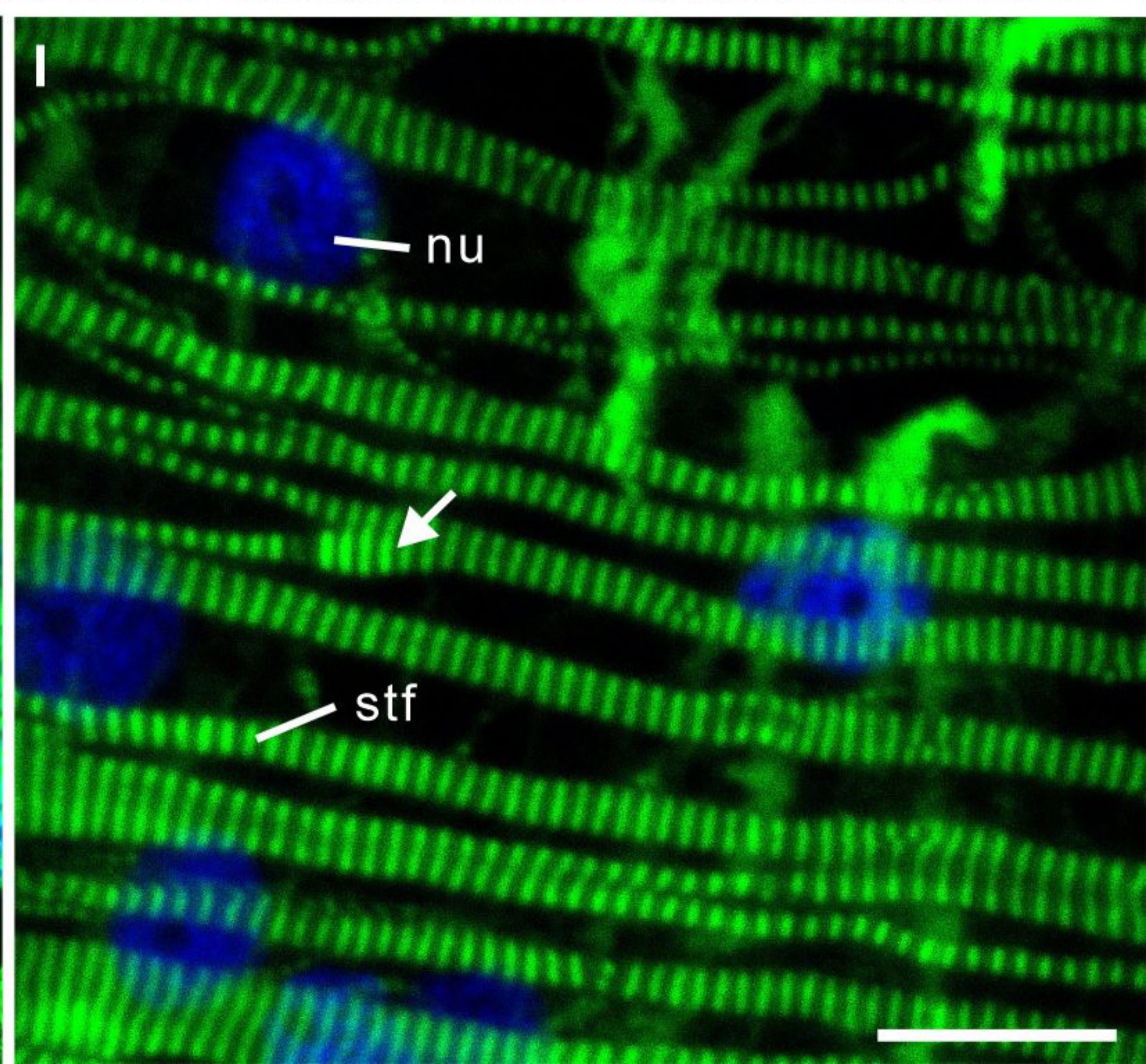
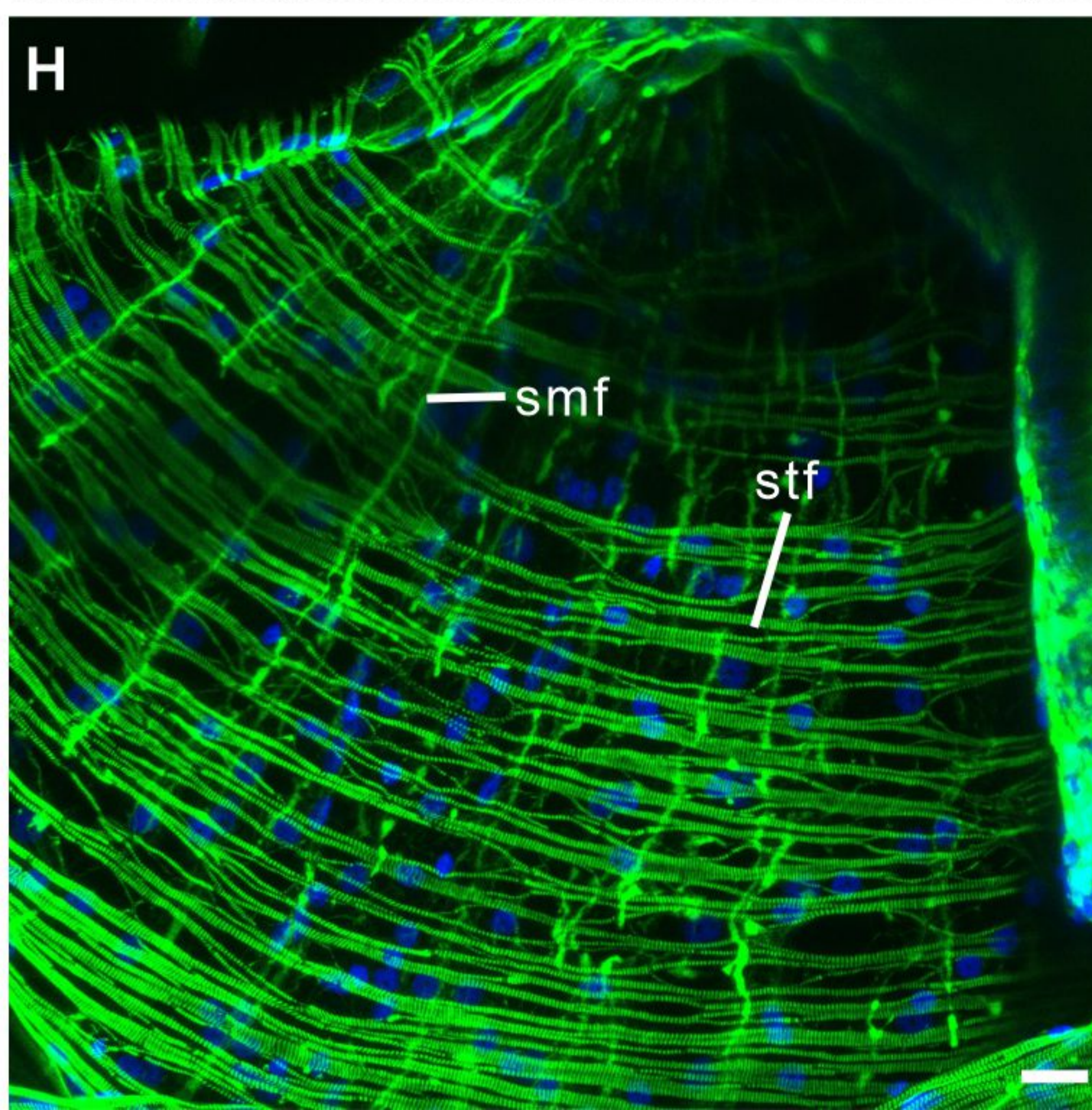
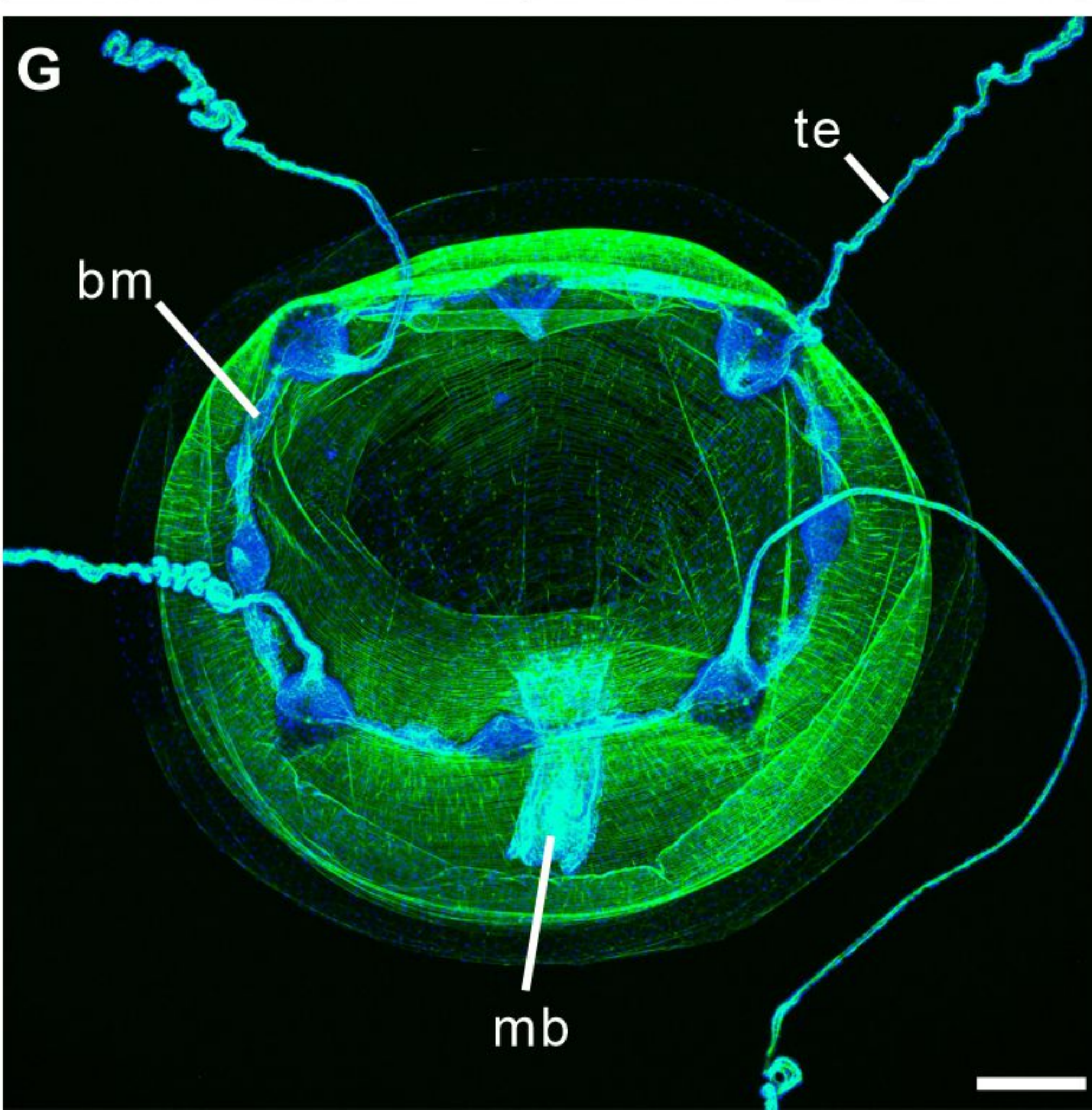
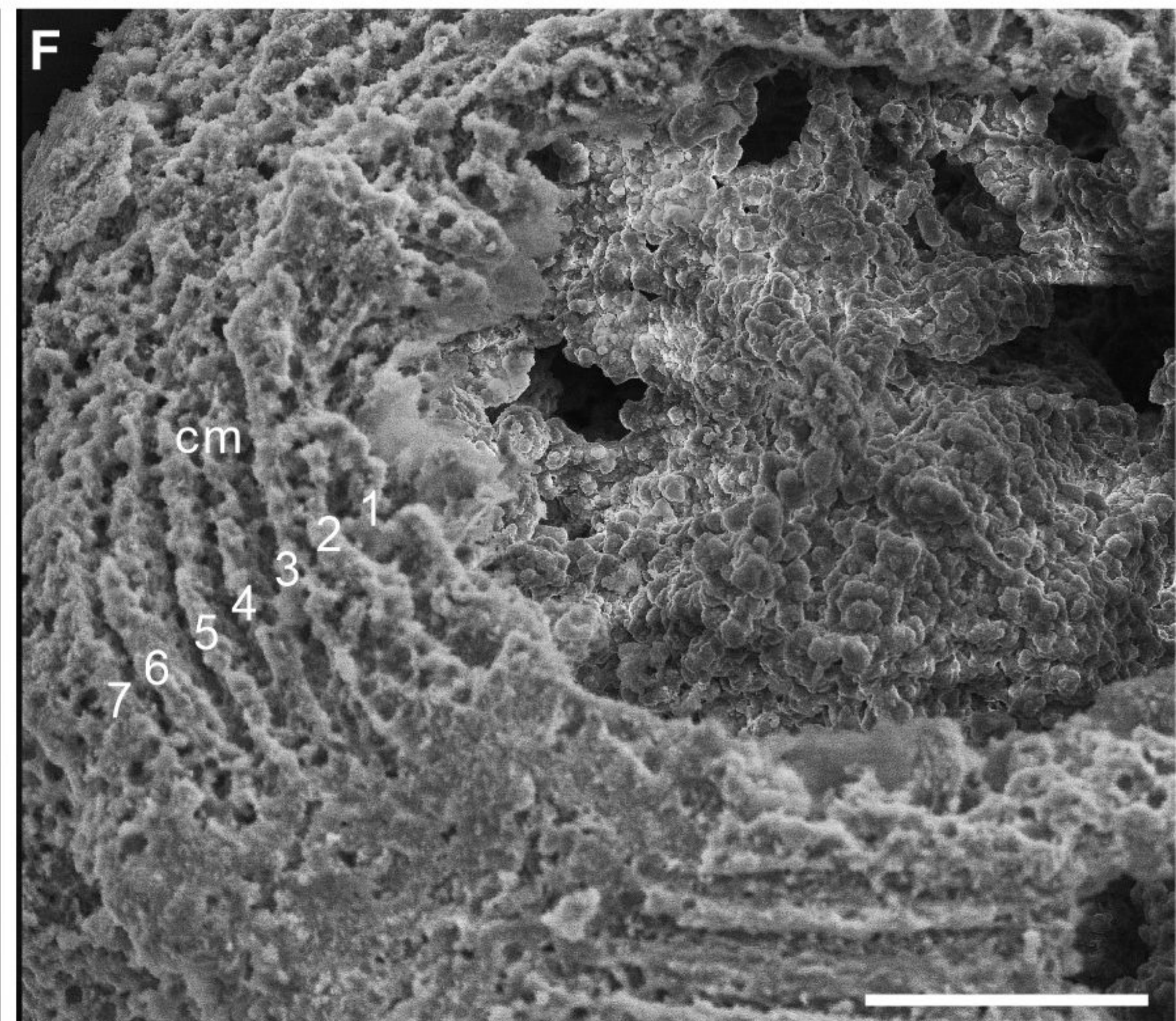
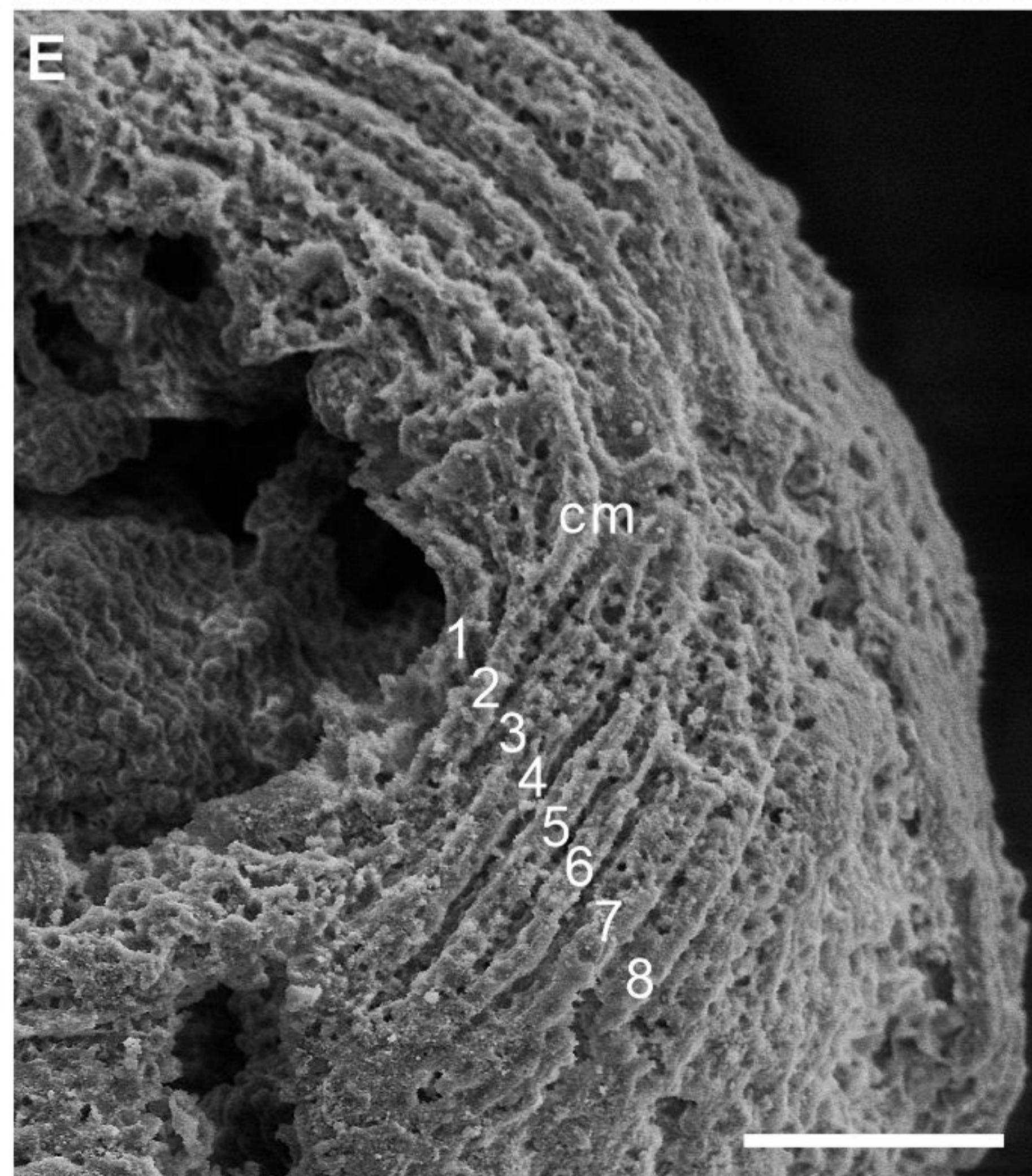
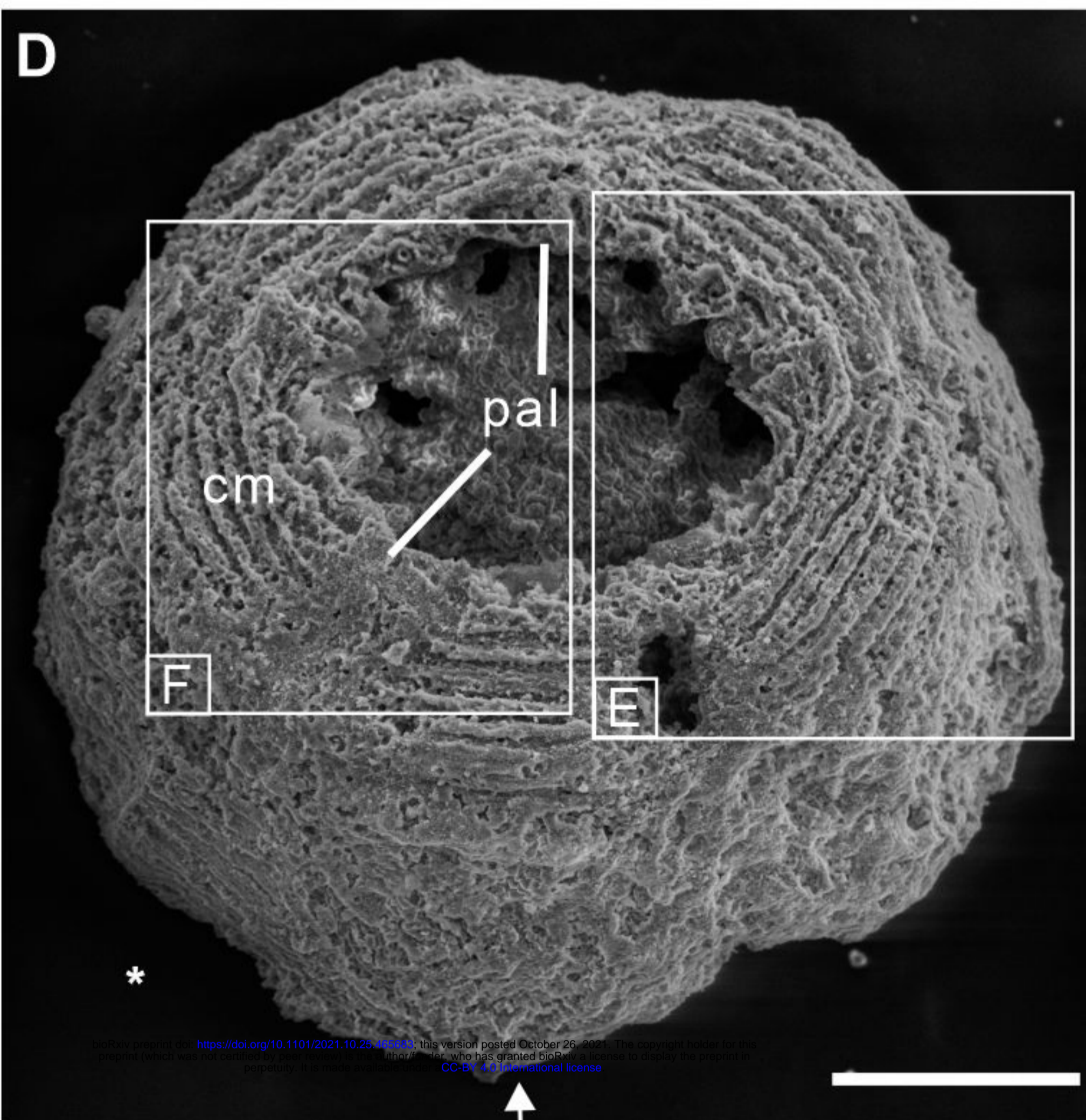
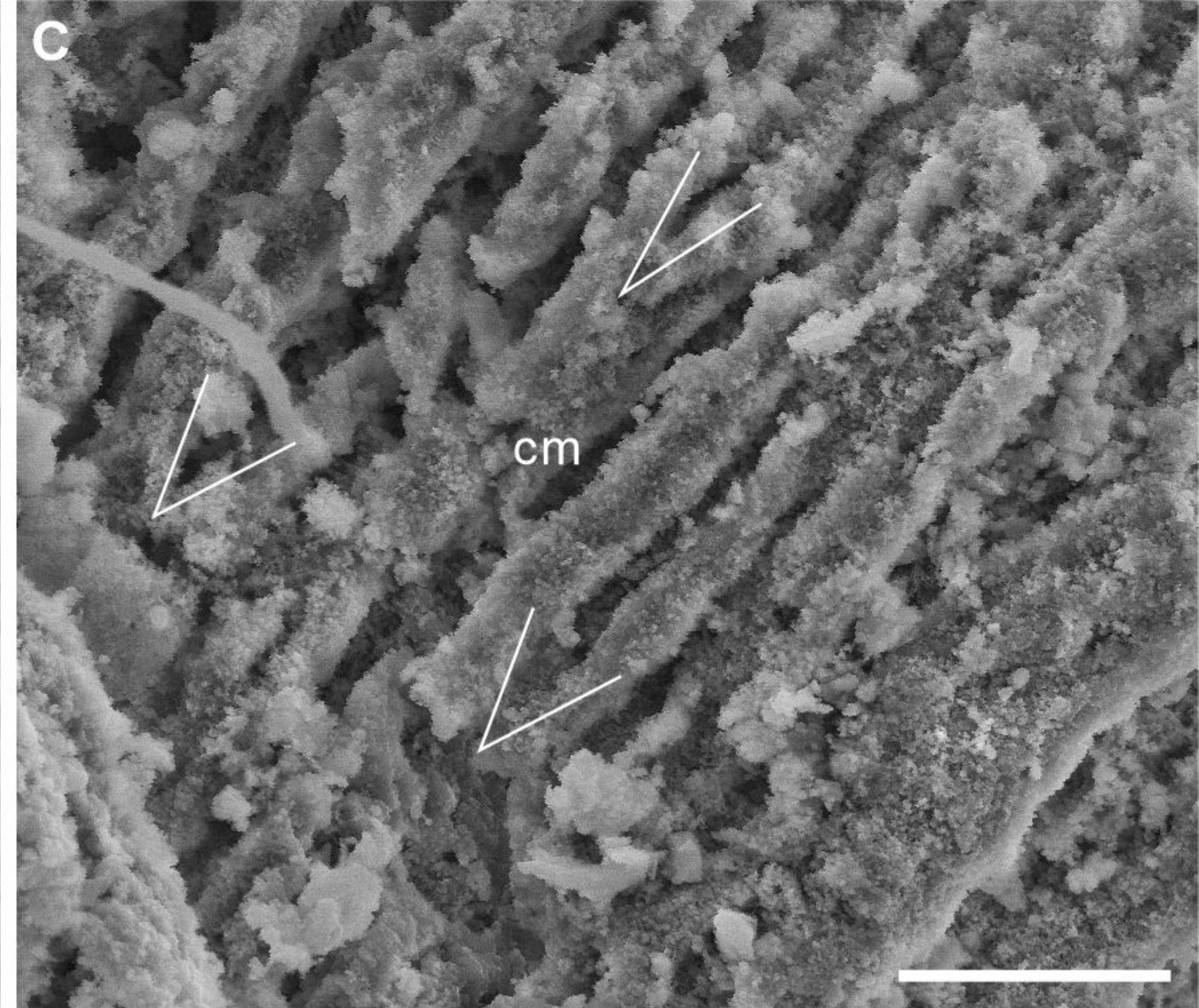
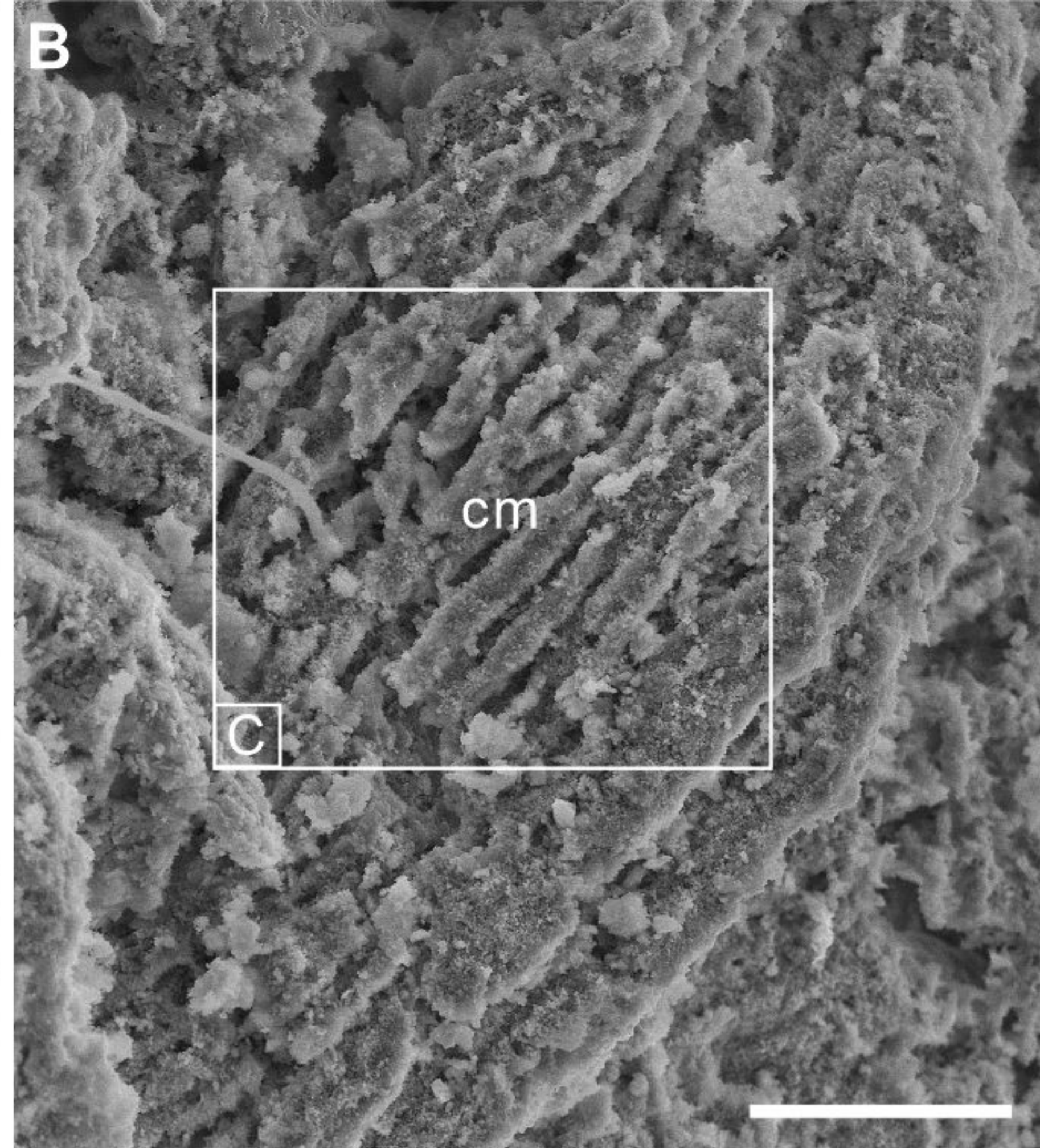
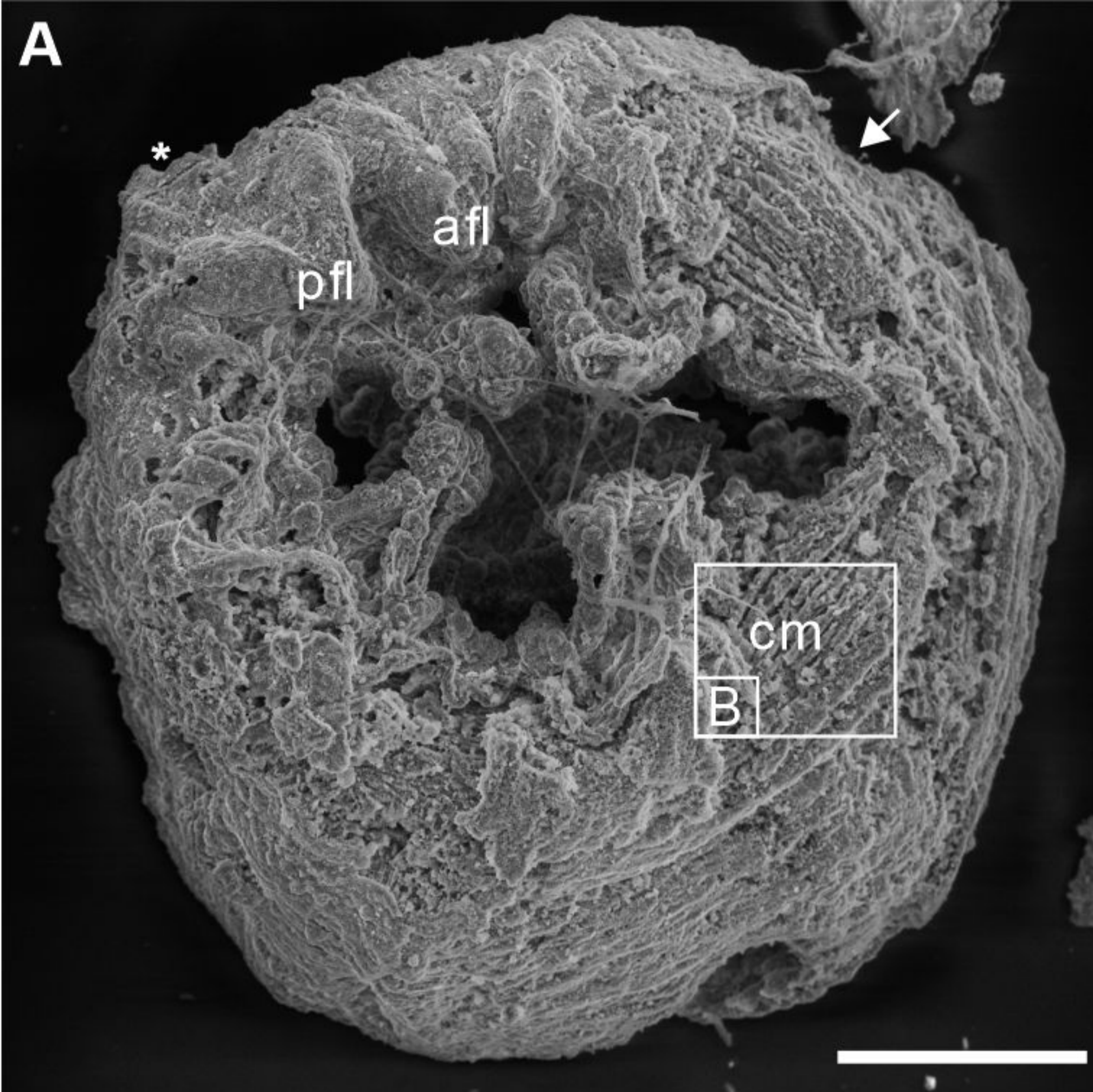
- 495 Bengtson S, Yue Z (1997) **Fossilized Metazoan Embryos from the Earliest Cambrian** Science
496 **277**:1645–1648. doi: 10.1126/science.277.5332.1645
- 497 Brusca RC, Moore W, Shuster SM (2016) **Invertebrates** 265–362 Sinauer Associates, Inc., Sunderland
498 Massachusetts USA.
- 499 Budd G (1998) **The morphology and phylogenetic significance of *Kerygmachela kierkegaardi* Budd**
500 **(Buen Formation, Lower Cambrian, N Greenland)** Transactions of the Royal Society of Edinburgh:
501 Earth Sciences **89**(4):249–290. doi:10.1017/S0263593300002418
- 502 Cartwright P, Halgedahl SL, Hendricks JR, Jarrard RD, Marques AC, Collins AG, Lieberman BS (2007)
503 **Exceptionally preserved jellyfishes from the Middle Cambrian** PLoS ONE **2**:e1121.
504 <https://doi.org/10.1371/journal.pone.0001121>
- 505 Costello JH, Colin SP (1994) **Morphology, fluid motion and predation by the scyphomedusa *Aurelia***
506 ***aurita*** Marine Biology **121**:327–334. <https://doi.org/10.1007/BF00346741>
- 507 De Sena Oliveira I, Mayer G (2013) **Apodemes associated with limbs support serial homology of**
508 **claws and jaws in Onychophora (velvet worms)** Journal of Morphology **274**:1180–1190.
509 doi:10.1002/jmor.20206
- 510 Dong X-P, Cunningham JA, Bengtson S, Thomas CW, Liu J, Stampanoni M, Donoghue PCJ (2013)
511 **Embryos, polyps and medusae of the Early Cambrian scyphozoan *Olivooides*** Proceedings of the
512 Royal Society B: Biological Sciences **280**:20130071. doi: 10.1098/rspb.2013.0071
- 513 Dong X-P, Vargas K, Cunningham JA, Zhang H-Q, Liu T, Chen F, Liu J, Bengtson S, Donoghue PCJ (2016)
514 **Developmental biology of the early Cambrian cnidarian *Olivooides*** Palaeontology **59**:387–407.
515 doi:10.1111/pla.12231
- 516 Erwin DH, Laflamme M, Tweedt SM, Sperling EA, Pisani D, Peterson KJ (2011) **The Cambrian**
517 **Conundrum: Early Divergence and Later Ecological Success in the Early History of Animals** Science
518 **334**:1091–1097. doi:10.1126/science.1206375
- 519 Evans SD, Hughes IV, Gehling JG, Droser ML (2020) **Discovery of the oldest bilaterian from the**
520 **Ediacaran of South Australia** PNAS **117**:7845–7850. doi: 10.1073/pnas.2001045117
- 521 Fedonkin MA (1981) **White Sea Biota of Vendian: Precambrian Non-Skeletal Fauna in the Russian**
522 **Platform North** Trans. Geol. Inst. Acad. Sci. U.S.S.R. **342**:100.
- 523 Gehling JG, Jensen S, Droser ML, Myrow PM, Narbonne GM (2001) **Burrowing below the basal**
524 **Cambrian GSSP, Fortune Head, Newfoundland** Geological Magazine **138**:213–218.
525 <https://doi.org/10.1017/S001675680100509X>
- 526 Gershwin L-a (1999) **Clonal and population variation in jellyfish symmetry** Journal of the Marine
527 Biological Association of the United Kingdom **79**:993–1000.
528 <https://doi.org/10.1017/S0025315499001228>
- 529 Giribet G, Edgecombe GD (2019) **The Phylogeny and Evolutionary History of Arthropods** Current
530 Biology **29**:R592–R602. <https://doi.org/10.1016/j.cub.2019.04.057>
- 531 Han J, Hu S-X, Cartwright P, Zhao F-C, Ou Q, Kubota S, Wang X, Yang X-G (2016a) **The earliest pelagic**
532 **jellyfish with rhopalia from Cambrian Chengjiang Lagerstätte** Palaeogeography Palaeoclimatology
533 Palaeoecology **449**:166–173. <https://doi.org/10.1016/j.palaeo.2016.02.025>
- 534 Han J, Kubota S, Li G-X, Yao X-Y, Yang X-G, Shu D-G, Li Y, Kinoshita S, Sasaki O, Komiya T, Yan G (2013)
535 **Early Cambrian pentamerous cubozoan embryos from South China** PLoS one **8**:e70741. doi:
536 10.1371/journal.pone.0070741

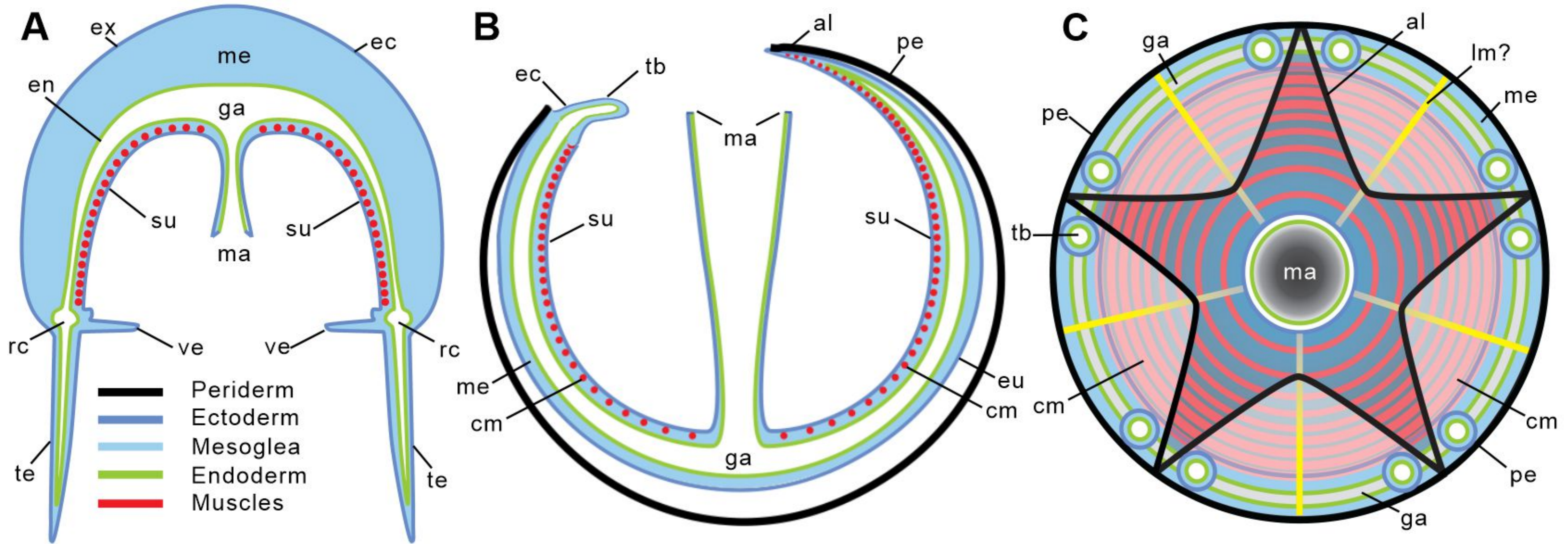
- 537 Han J, Li G-X, Kubota S, Ou Q, Toshino S, Wang X, Yang X-G, Uesugi K, Masato H, Sasaki O, Kano H,
538 Sato T, Komiya T (2016b) **Internal Microanatomy and Zoological Affinity of the Early Cambrian**
539 **Olivoooides** Acta Geologica Sinica - English Edition **90**:38–65.
540 <https://doi.org/10.1111/1755-6724.12641>
- 541 Hoyle G, Williams M (1980) **The musculature of Peripatus and its innervation** Philos. Trans. R. Soc.
542 Lond. B **288**:481–510. doi: 10.1098/rstb.1980.0024
- 543 Hyman LH (1940) **The invertebrates** 726 McGraw Hill.
- 544 Kesidis G, Slater BJ, Jensen S, Budd GE (2019) **Caught in the act: priapulid burrowers in early**
545 **Cambrian substrates** Proceedings of the Royal Society B: Biological Sciences **286**:20182505.
546 <https://doi.org/10.1098/rspb.2018.2505>
- 547 Lechable M, Jan A, Duchene A, Uveira J, Weissbourd B, Gissat L, Collet S, Gilletta L, Chevalier S, Leclère
548 L, Peron S, Barreau C, Lasbleiz R, Houliston E, Momose T (2020) **An improved whole life cycle culture**
549 **protocol for the hydrozoan genetic model *Clytia hemisphaerica*** Biol Open **9**:bio051268. doi:
550 10.1242/bio.051268
- 551 Leclère L, Röttinger E (2017) **Diversity of cnidarian muscles: function, anatomy, development and**
552 **regeneration** Frontiers in Cell and Developmental Biology **4**:157. doi: 10.3389/fcell.2016.00157
- 553 Liu AG, Matthews JJ, Menon LR, Mcllroy D, Brasier MD (2014) ***Haootia quadriformis* n. gen., n. sp.,**
554 **interpreted as a muscular cnidarian impression from the Late Ediacaran period (approx. 560 Ma)**
555 Proceedings of the Royal Society B: Biological Sciences **281**:20141202.
556 <https://doi.org/10.1098/rspb.2014.1202>
- 557 Liu AG, Matthews JJ, Menon LR, Mcllroy D, Brasier MD (2015) **The arrangement of possible muscle**
558 **fibres in the Ediacaran taxon *Haootia quadriformis*** Proceedings of the Royal Society B: Biological
559 Sciences **282**:20142949. <https://doi.org/10.1098/rspb.2014.2949>
- 560 Liu Y-H, Li Y, Shao T-Q, Zhang H-Q, Wang Q, Qiao J-P (2014a) ***Quadrapyrgites* from the lower**
561 **Cambrian of South China: growth pattern, post-embryonic development, and affinity** Chinese
562 Science Bulletin **59**:4086–4095. <https://doi.org/10.1007/s11434-014-0481-5>
- 563 Liu Y-H, Shao T-Q, Zhang H-Q, Wang Q, Zhang Y-N, Chen C, Liang Y-C, Xue J-Q (2017) **A new**
564 **scyphozoan from the Cambrian Fortunian Stage of South China** Palaeontology **60**:511–518.
565 <https://doi.org/10.1111/pala.12306>
- 566 Ortega-Hernández J (2015) **“Lobopodians”** Current Biology **25**:R873–5. doi: 10.1016/j.cub.2015.07.028
- 567 Pan B, Topper TP, Skovsted CB, Miao L-Y, Li G-X (2017) **Occurrence of Microdictyon from the lower**
568 **Cambrian Xinji Formation along the southern margin of the North China Platform** Journal of
569 Paleontology **92**(1):59–70. <https://doi.org/10.1017/jpa.2017.47>
- 570 Peng S-H, Babcock LE, Cooper RA (2012) **The Cambrian Period** Elsevier.
- 571 Qian Y (1977) **Hyalolitha and some problematica from the Lower Cambrian Meishucun Stage in**
572 **central and S. W. China** Acta Palaeontologica Sinica **16**:255–275.
- 573 Qian Y (1999) **Taxonomy and biostratigraphy of small shelly fossils in China (In Chinese)** Science
574 Press, Beijing.
- 575 Raikova EV (1988) **On systematic position of Polypodium hydriforme Ussov (Cnidaria)** Leningrad:
576 Zoological Institute of the Academy of Sciences of the USSR.

- 577 Ramondenc S, Ferrieux M, Collet S, Benedetti F, Guidi L, Ramondenc FL (2017) **From egg to maturity:**
578 **a closed system for complete life cycle studies of the holopelagic jellyfish *Pelagia noctiluca*** Journal
579 of Plankton Research **41**:207–217. <https://doi.org/10.1093/plankt/fbz013>
- 580 Sawaki Y, Nishizawa M, Suo T, Komiya T, Hirata T, Takahata N, Sano Y, Han J, Kon Y, Maruyama S
581 (2008) **Internal structures and U–Pb ages of zircons from a tuff layer in the Meishucunian formation,**
582 **Yunnan Province, South China** Gondwana Research **14**:148–158.
583 <https://doi.org/10.1016/j.gr.2007.12.003>
- 584 Schmidt-Rhaesa A (2007) **The Evolution of Organ Systems** Oxford University Press.
- 585 Sinigaglia C, Peron S, Eichelbrenner J, Chevalier S, Steger J, Barreau C, Houliston E, Leclère L
586 (2020) **Pattern regulation in a regenerating jellyfish** Elife **9**: e54868. doi: 10.7554/eLife.54868
- 587 Smith CL, Mayorova TD (2019) **Insights into the evolution of digestive systems from studies of**
588 ***Trichoplax adhaerens*** Cell and Tissue Research **377**:353–367.
589 <https://doi.org/10.1007/s00441-019-03057-z>
- 590 Smith M, Caron JB (2015) ***Hallucigenia*'s head and the pharyngeal armature of early ecdysozoans**
591 Nature **523**:75–78. <https://doi.org/10.1038/nature14573>
- 592 Smith M, Ortega-Hernández J (2014) ***Hallucigenia*'s onychophoran-like claws and the case for**
593 **Tactopoda** Nature **514**:363–366. <https://doi.org/10.1038/nature13576>
- 594 Steiner M, Qian Y, Li G-X, Hagadorn JW, Zhu M-Y (2014) **The developmental cycles of early Cambrian**
595 **Olivooidea fam. nov. (?Cycloneuralia) from the Yangtze Platform (China)** Palaeogeography
596 Palaeoclimatology Palaeoecology **398**:97–124. <https://doi.org/10.1016/j.palaeo.2013.08.016>
- 597 Sun W-G (1986) **Precambrian medusoids: The *Cyclomedusa* plexus and *Cyclomedusa*-like**
598 **pseudofossils** Precambrian Research **31**:325–360. [https://doi.org/10.1016/0301-9268\(86\)90039-2](https://doi.org/10.1016/0301-9268(86)90039-2)
- 599 Vannier J (2012) **Gut contents as direct indicators for trophic relationships in the Cambrian marine**
600 **ecosystem** PLoS One **7**:e52200. doi: 10.1371/journal.pone.0052200
- 601 Vannier J, Calandra I, Gaillard C, Żylińska A (2010) **Priapulid worms: Pioneer horizontal burrowers at**
602 **the Precambrian-Cambrian boundary** Geology **38**:711–714. <https://doi.org/10.1130/G30829.1>
- 603 Vannier J, Martin ELO (2017) **Worm-lobopodian assemblages from the Early Cambrian Chengjiang**
604 **biota: Insight into the “pre-arthropodan ecology”?** Palaeogeography Palaeoclimatology
605 Palaeoecology **468**:373–387. <https://doi.org/10.1016/j.palaeo.2016.12.002>
- 606 Wang X, Han J, Vannier J, Ou Q, Yang X-G, Uesugi K, Sasaki O, Komiya T (2017) **Anatomy and affinities**
607 **of a new 535-million-year-old medusozoan from the Kuanchuanpu Formation, South China**
608 Palaeontology **60**:853–867. <https://doi.org/10.1111/pala.12320>
- 609 Wang X, Vannier J, Yang X-G, Kubota S, Ou Q, Yao X-Y, Uesugi K, Sasaki O, Komiya T, Han J (2020) **An**
610 **intermediate type of medusa from the early Cambrian Kuanchuanpu Formation, South China**
611 Palaeontology **63**:775–789. <https://doi.org/10.1111/pala.12483>
- 612 Westfall JA, Yamataka S, Enos PD (1971) **Ultrastructural evidence of polarized synapses in the nerve**
613 **net of *Hydra*** Journal of Cell Biology **51**:318–323. doi: 10.1083/jcb.51.1.318
- 614 Young FJ, Vinther J (2017) **Onychophoran-like myoanatomy of the Cambrian gilled lobopodian**
615 ***Pambdelurion whittingtoni*** Palaeontology **60**(1):27–54. doi: 10.1111/pala.12269
- 616 Zaika-Novatskiy VS, Velikanov VA, Koval AP (1968) **First representative of the Ediacara fauna in the**
617 **Vendian of the Russian Platform (upper Precambrian)** PalZ. **2**: 269–270.

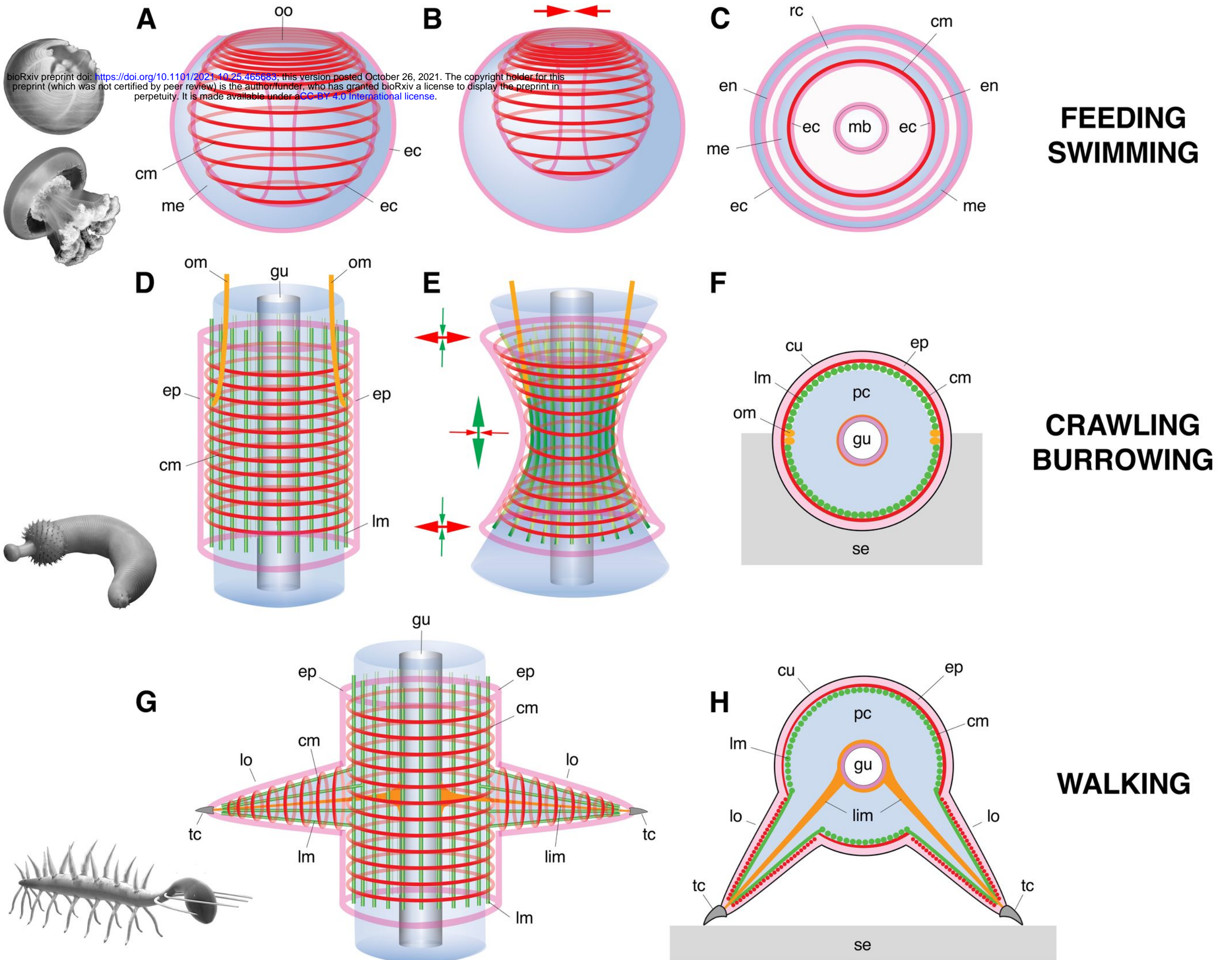
- 618 Zapata F, Goetz FE, Smith SA, Howison M, Siebert S, Church SH et al. (2015) **Phylogenomic Analyses**
619 **Support Traditional Relationships within Cnidaria** PLoS ONE **10**:e0139068.
620 <https://doi.org/10.1371/journal.pone.0139068>
621 Zhang X-G, Smith MR, Yang J, Hou J-B (2016) **Onychophoran-like musculature in a phosphatized**
622 **Cambrian lobopodian** Biology Letters **12**:20160492. <https://doi.org/10.1098/rsbl.2016.0492>

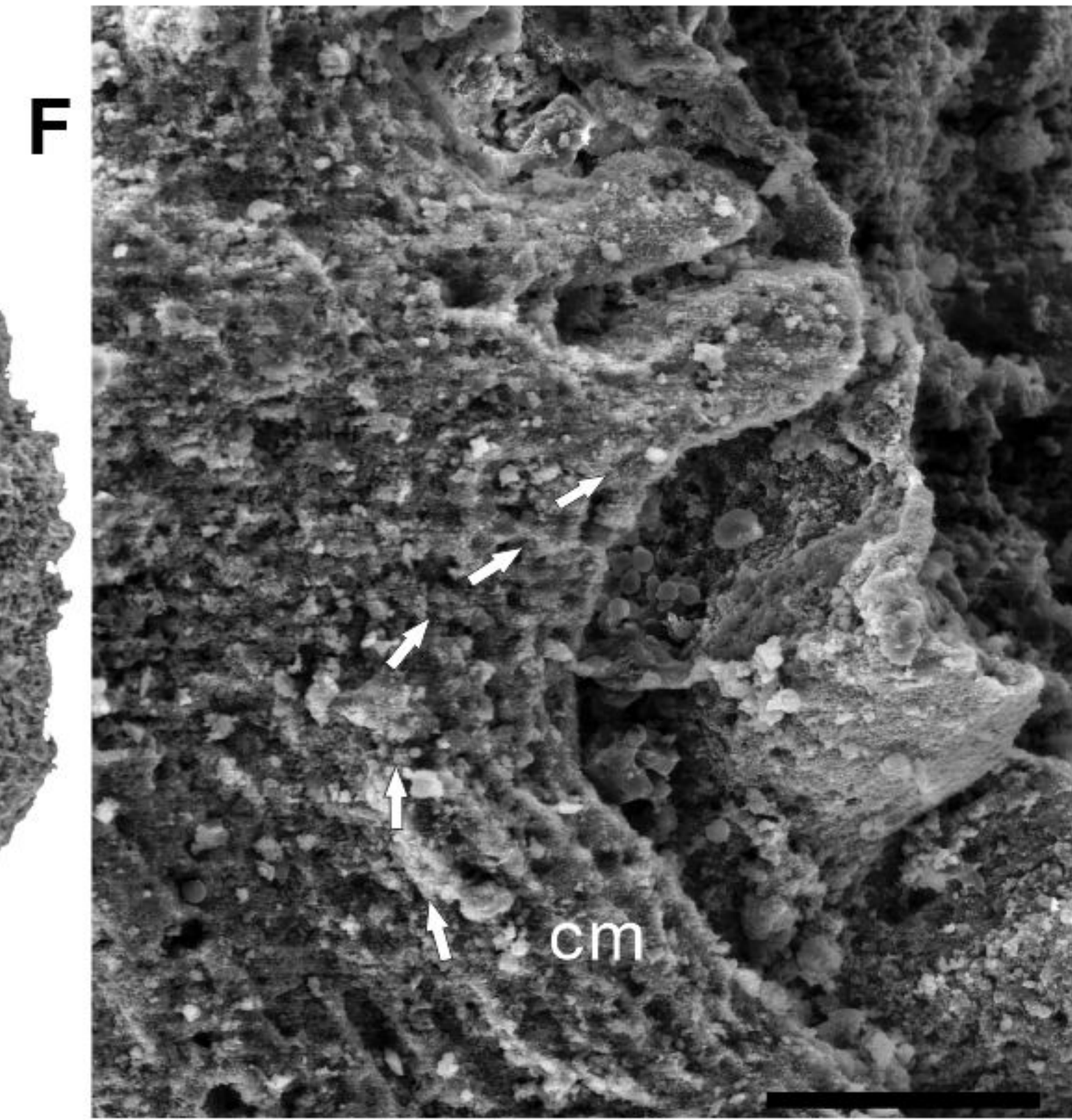
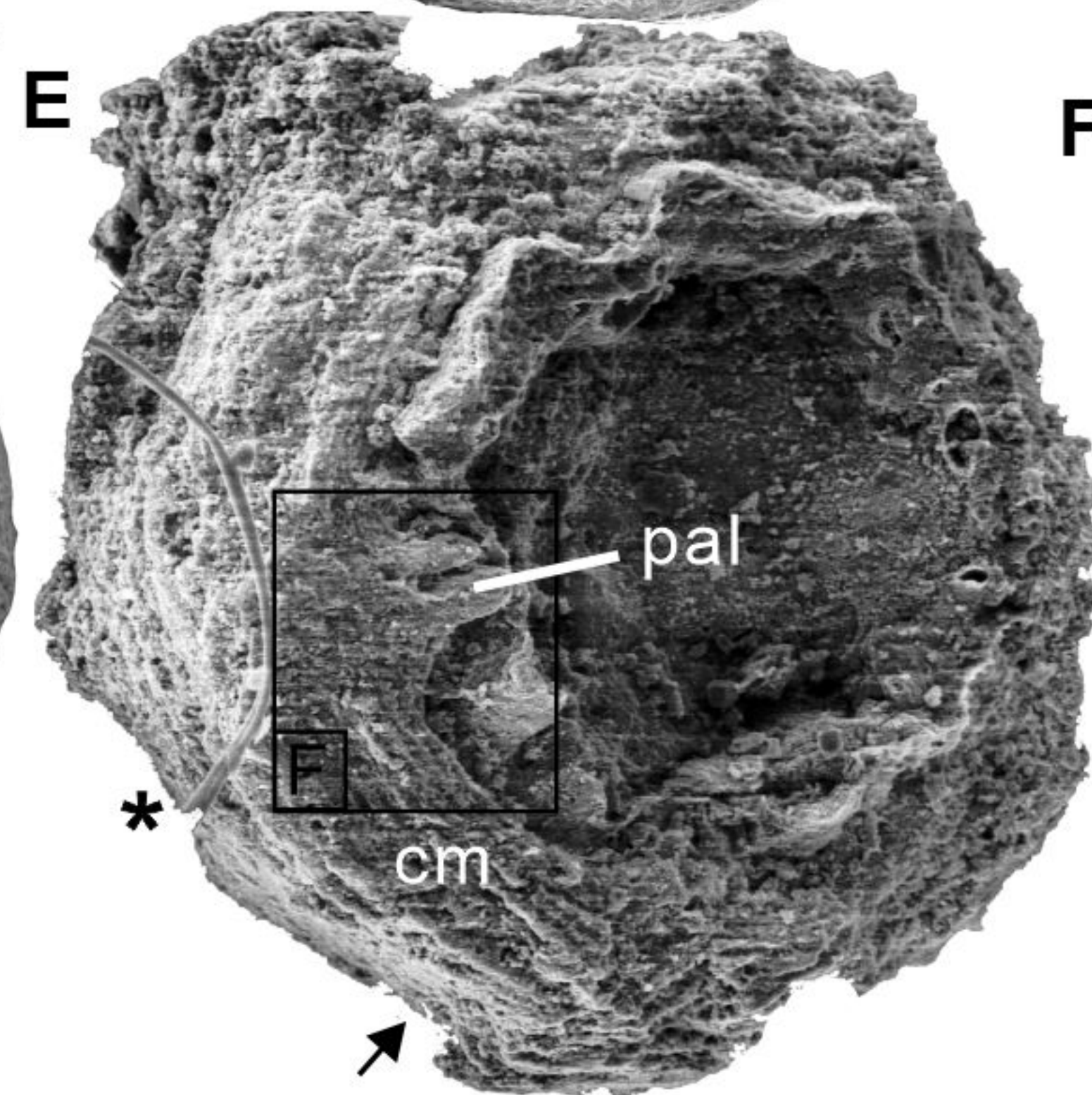
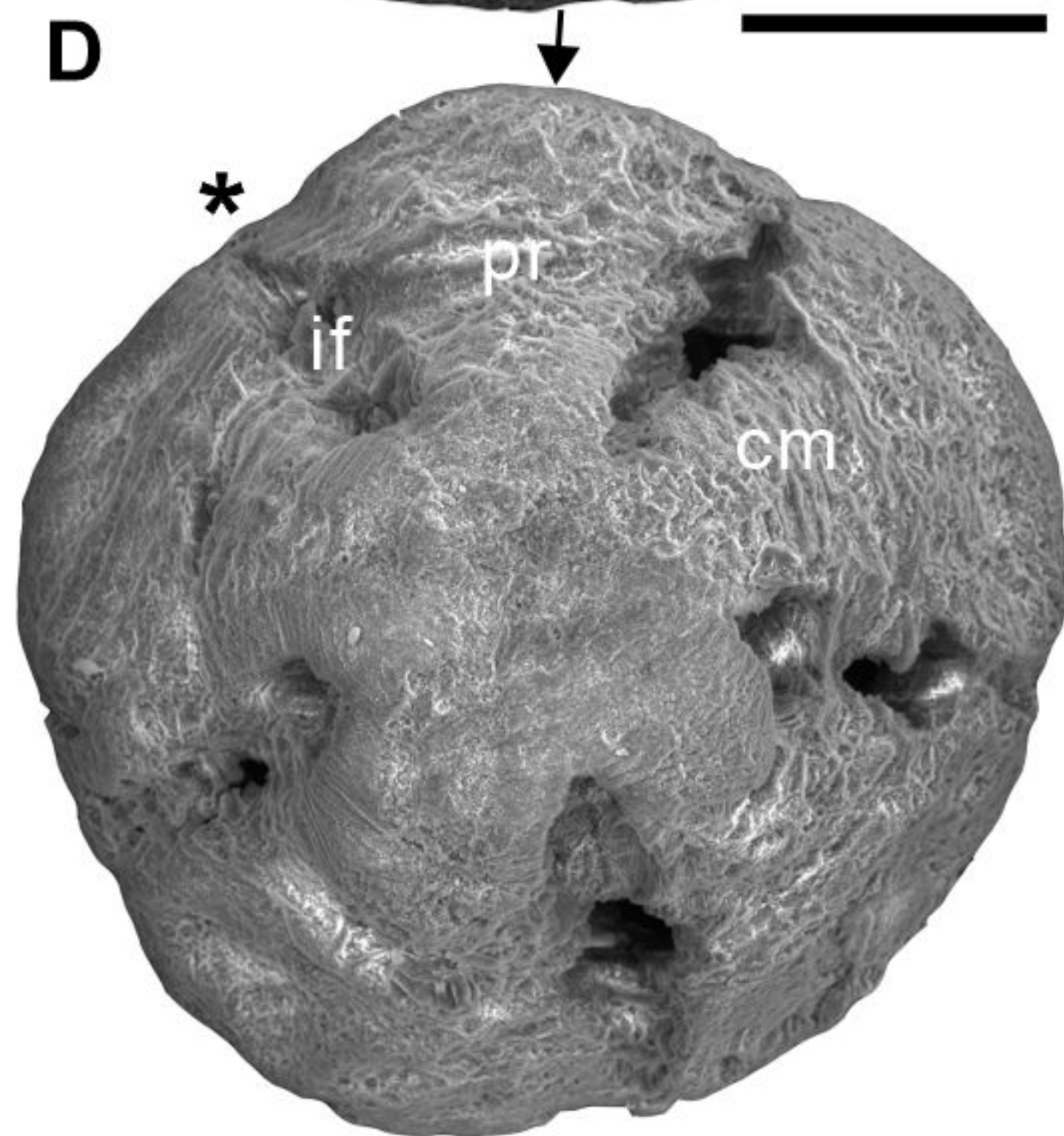
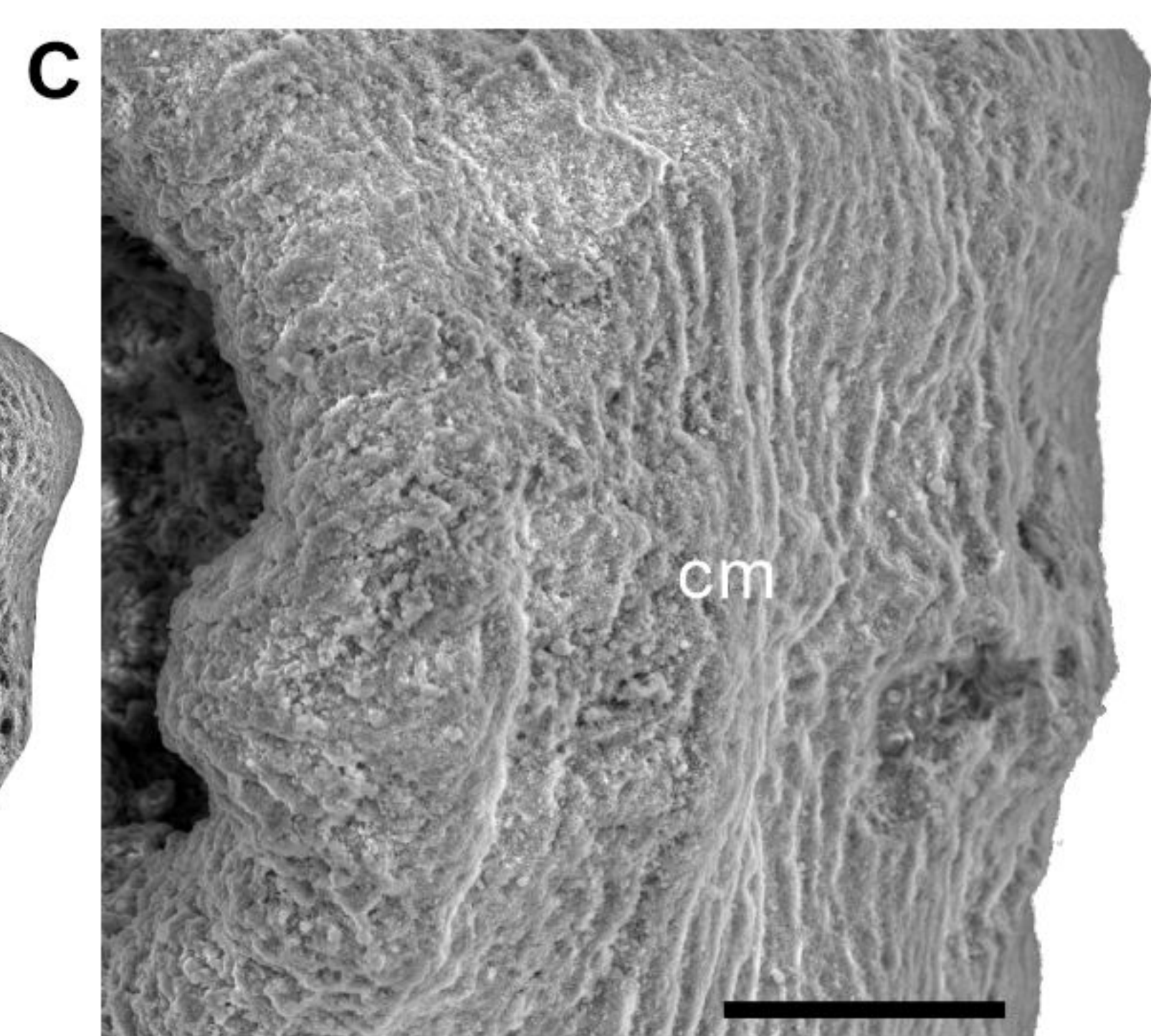
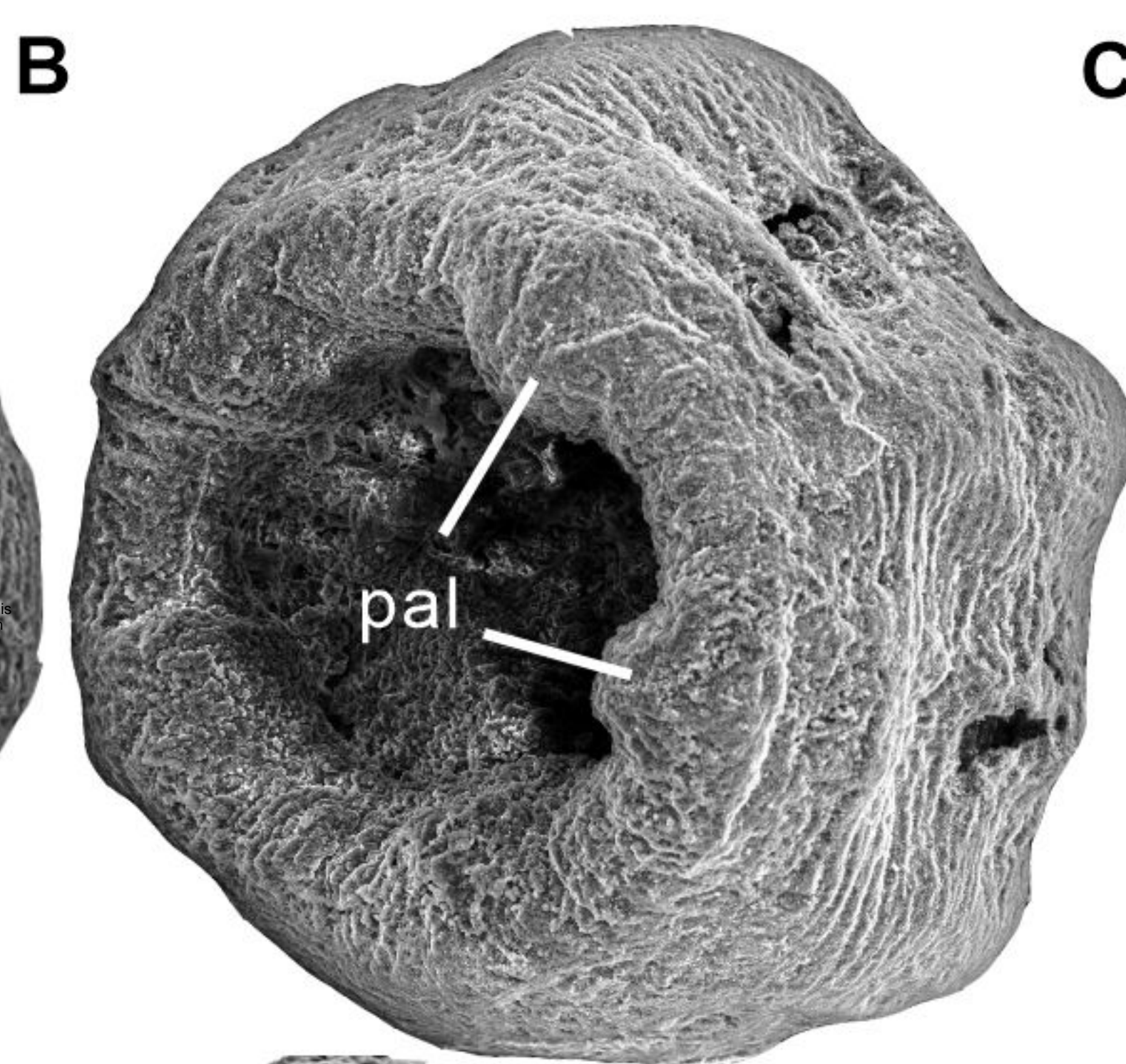
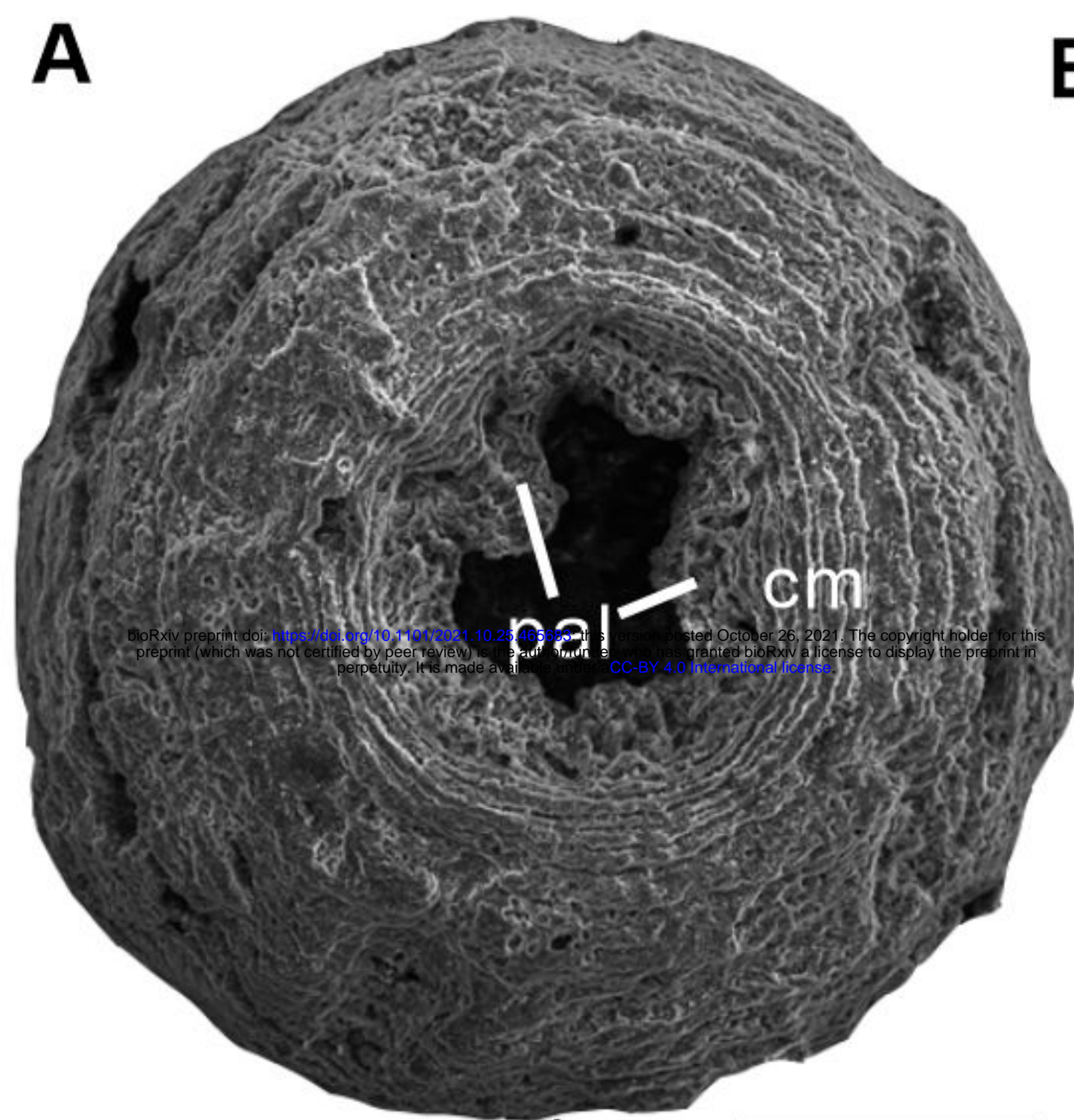


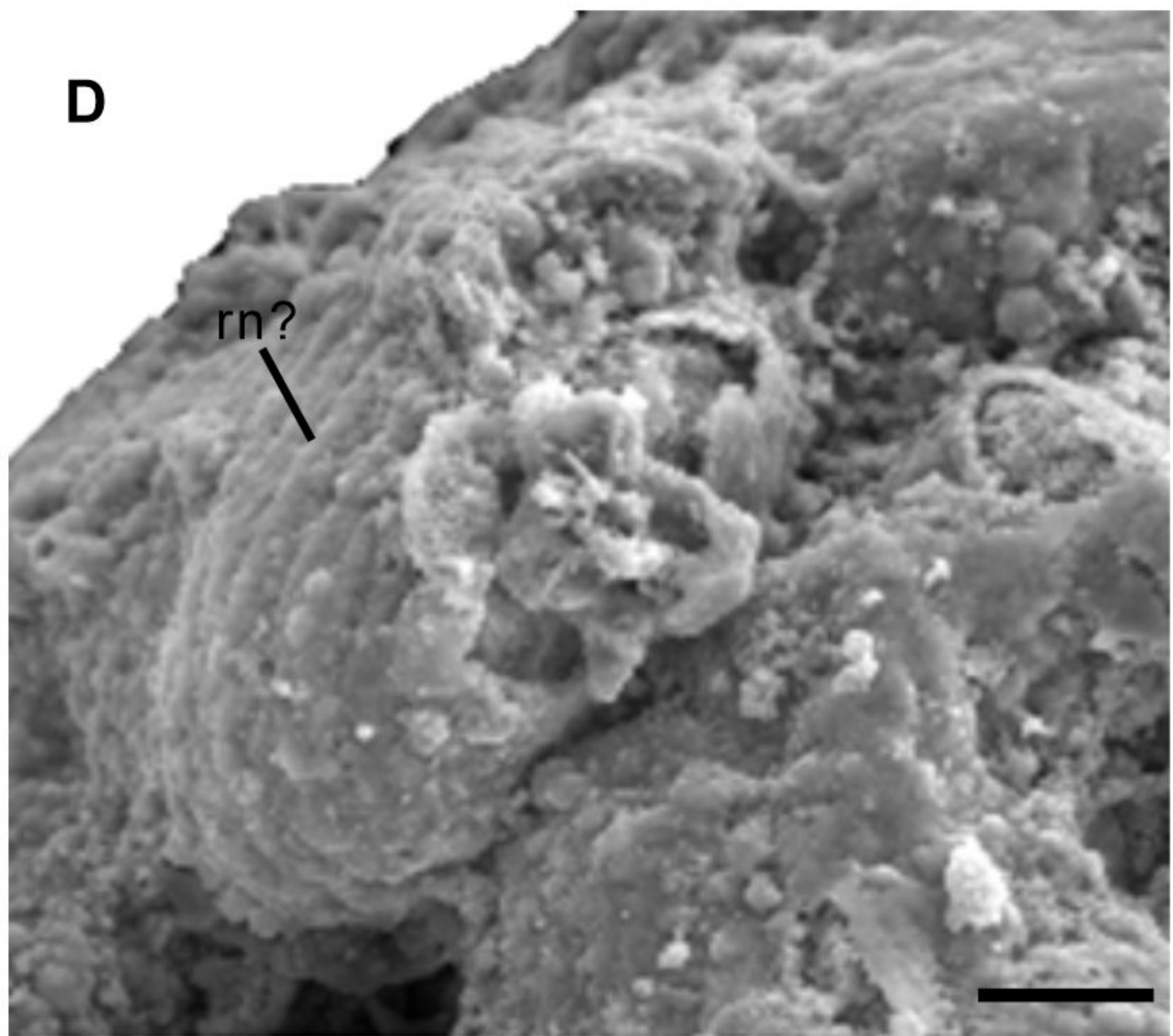
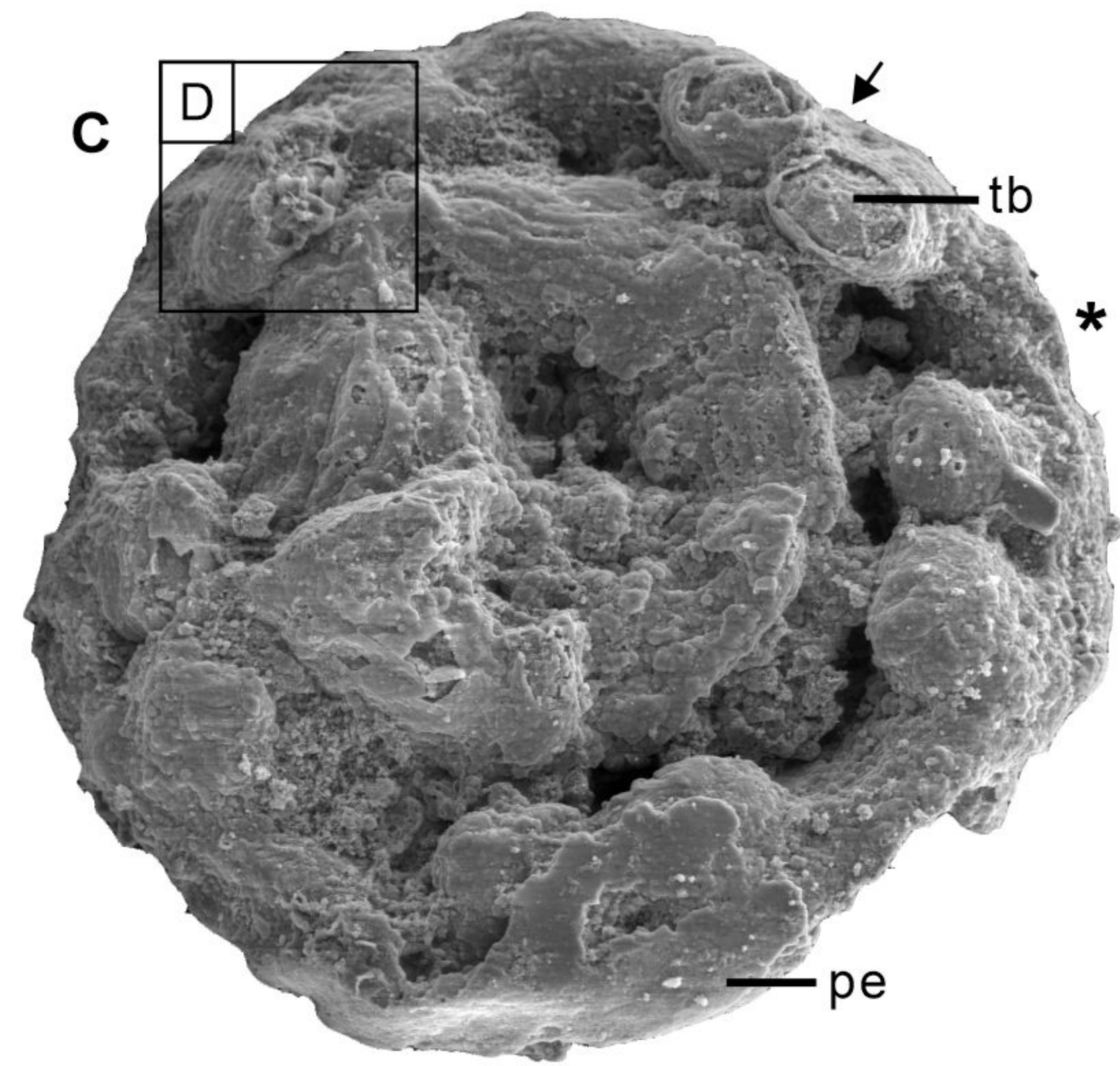
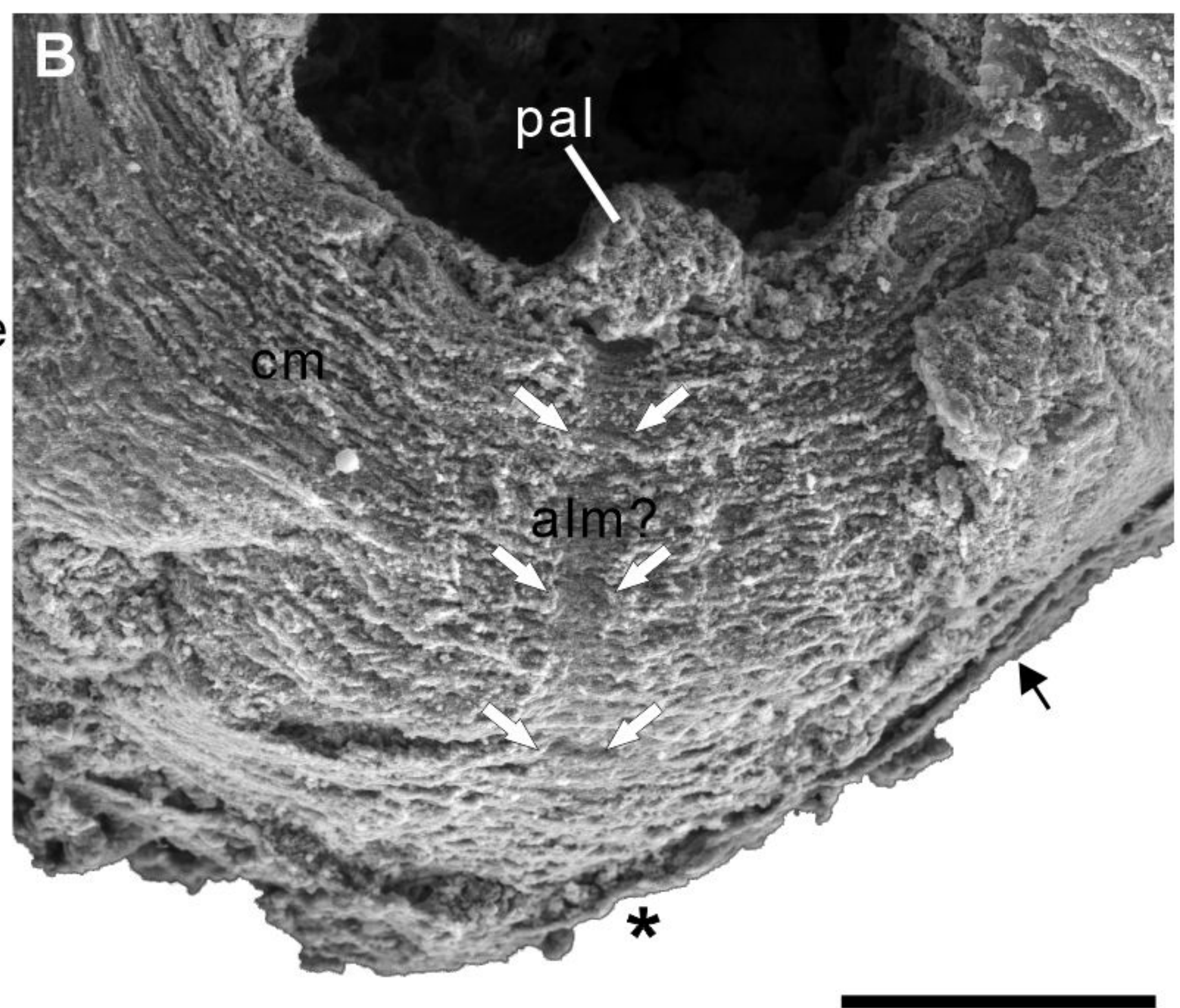
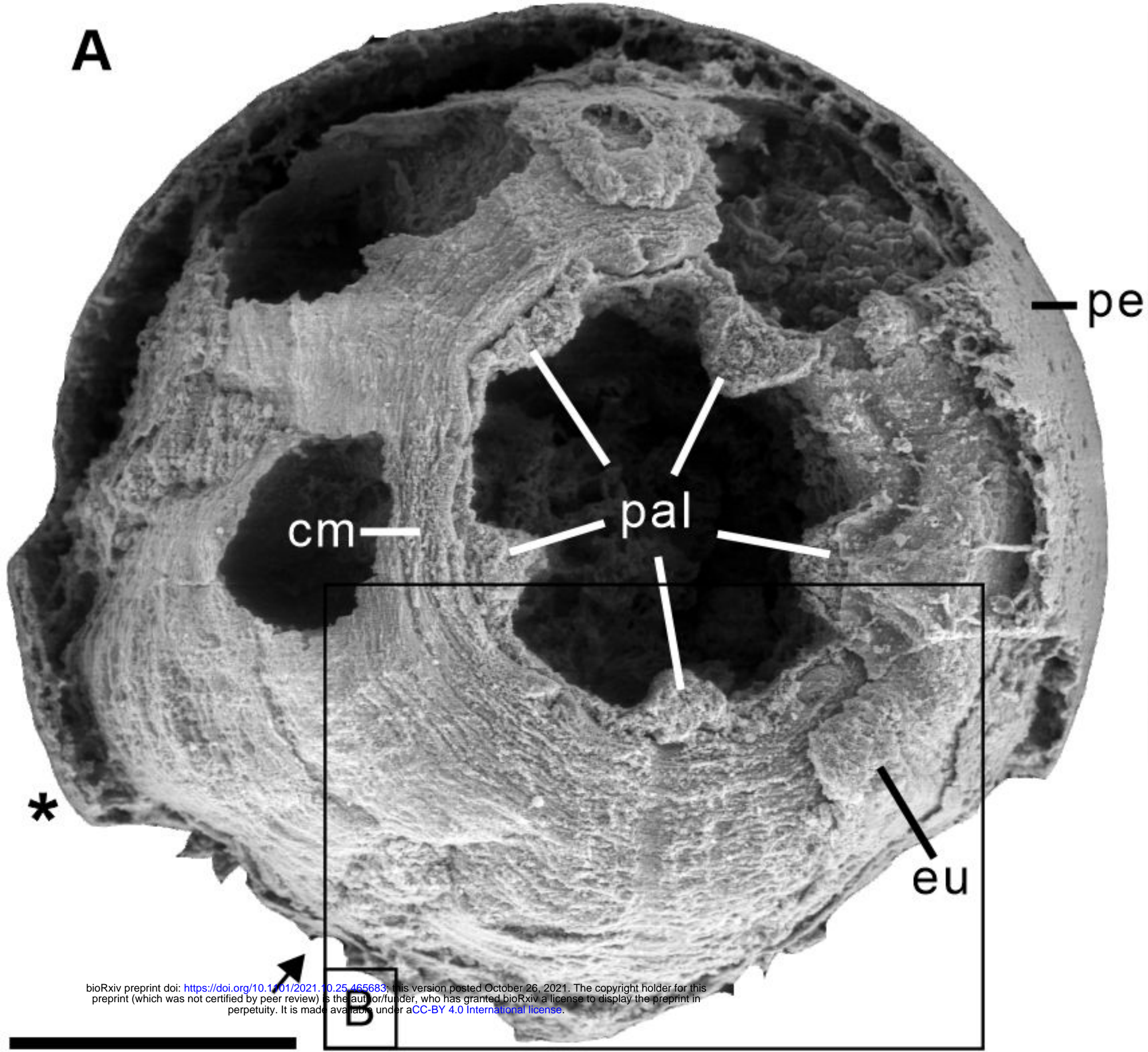


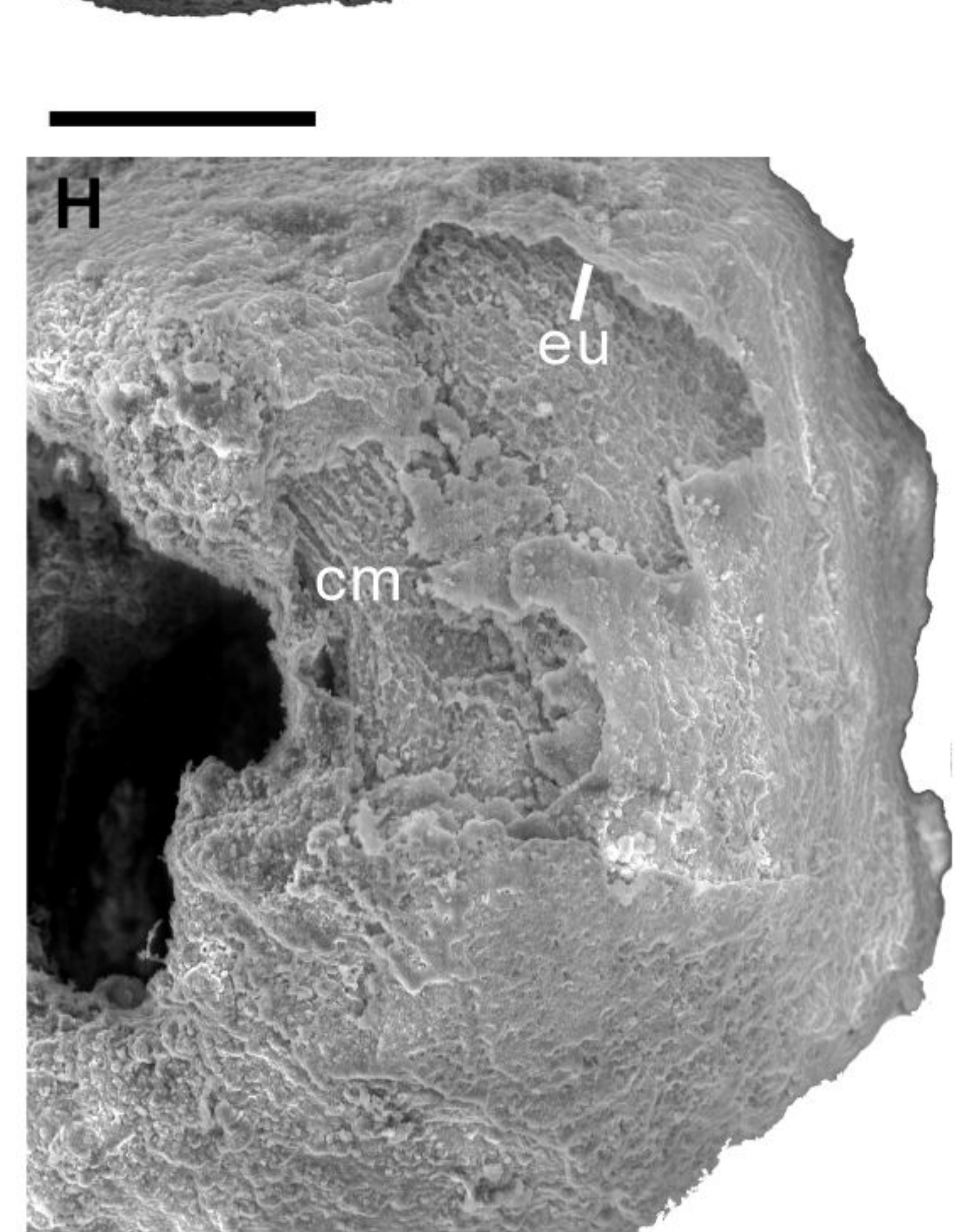
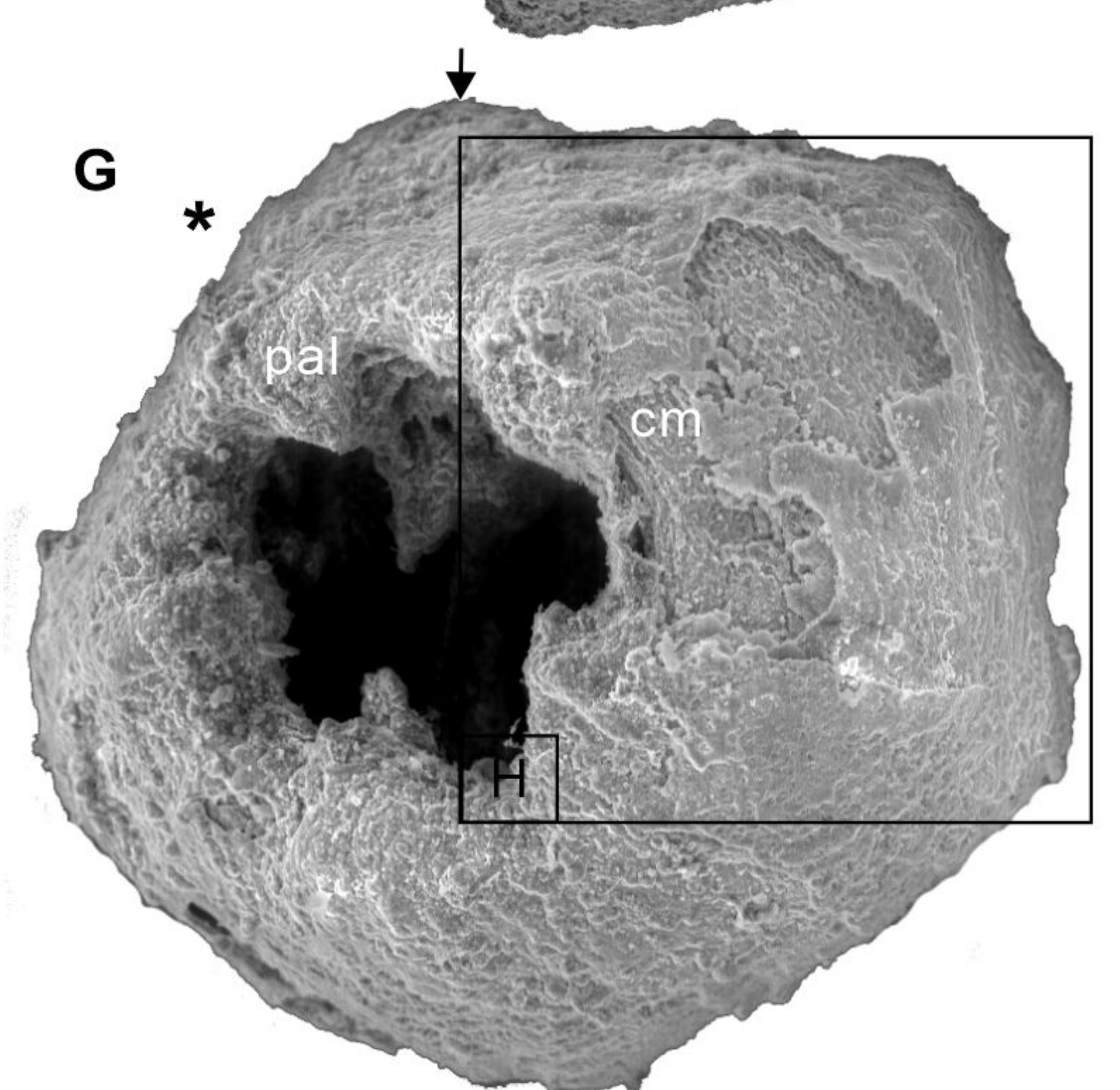
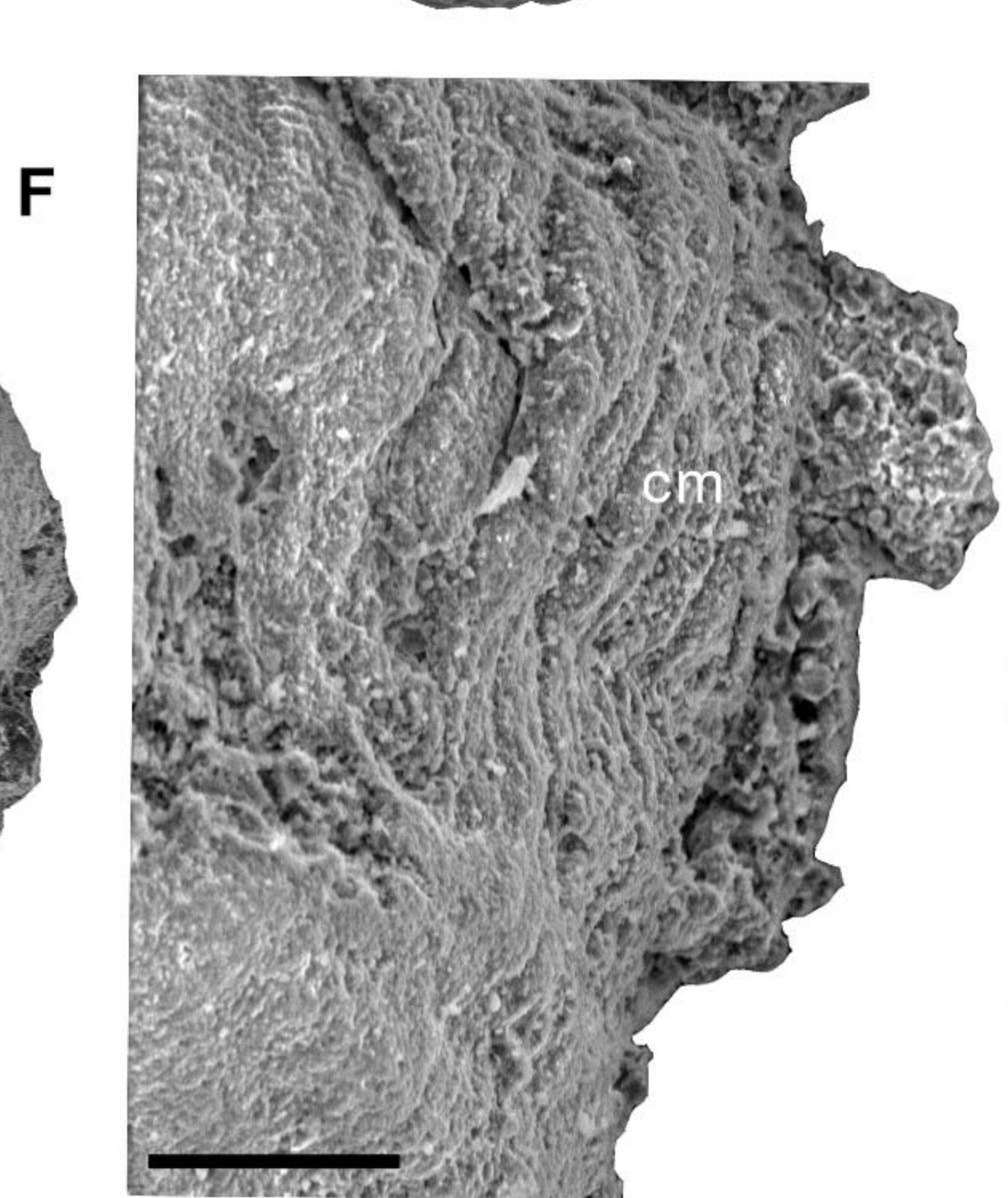
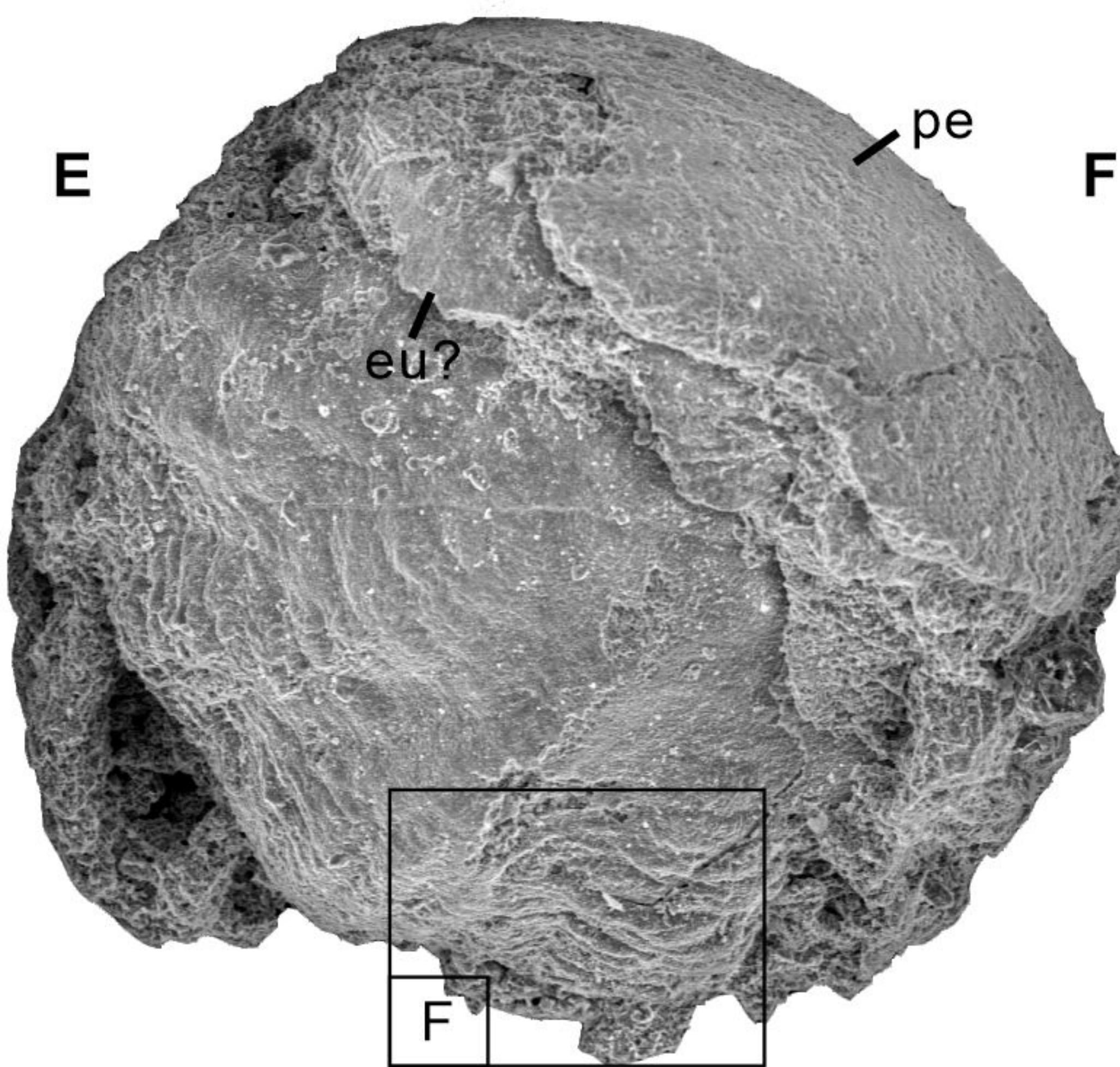
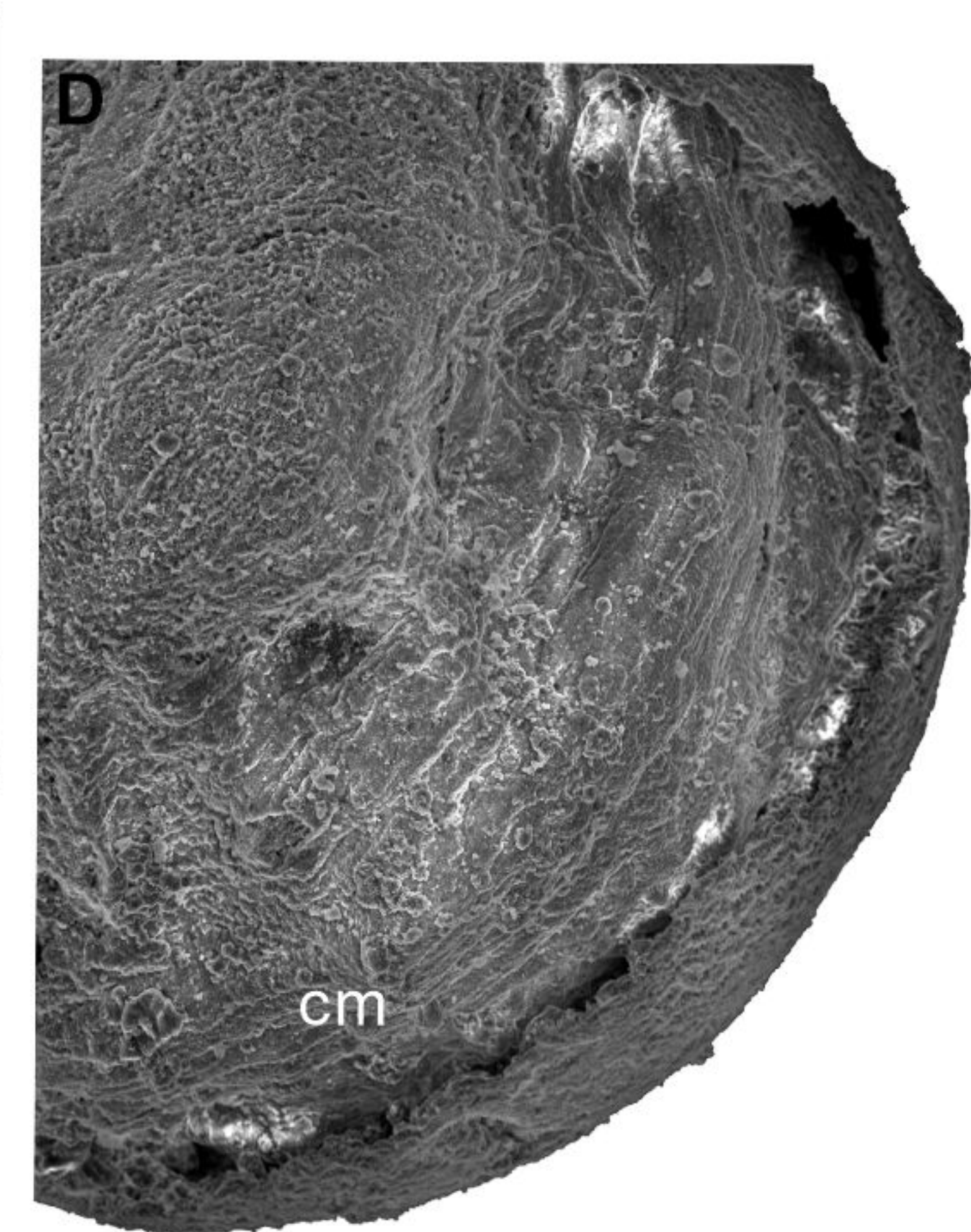
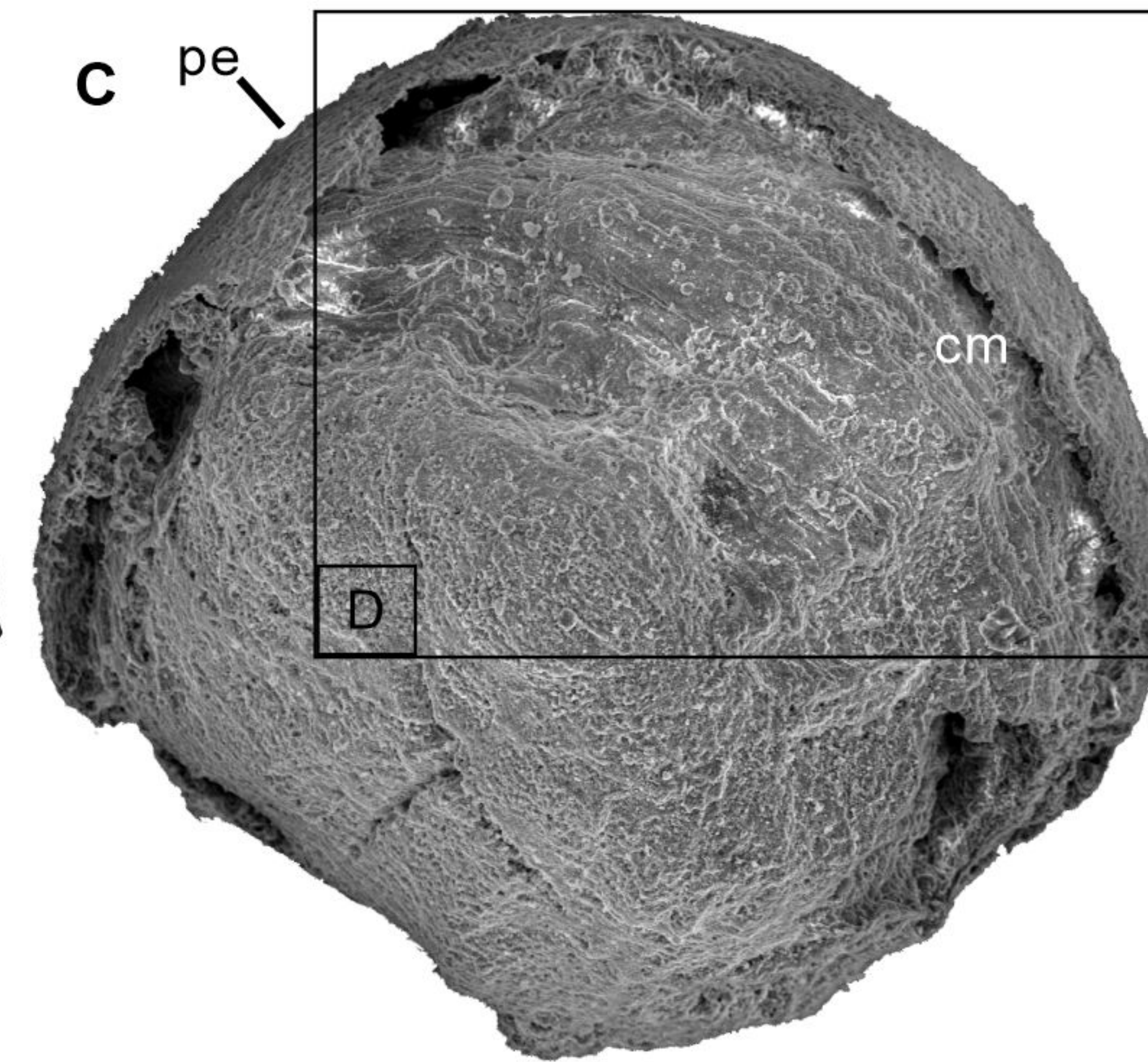
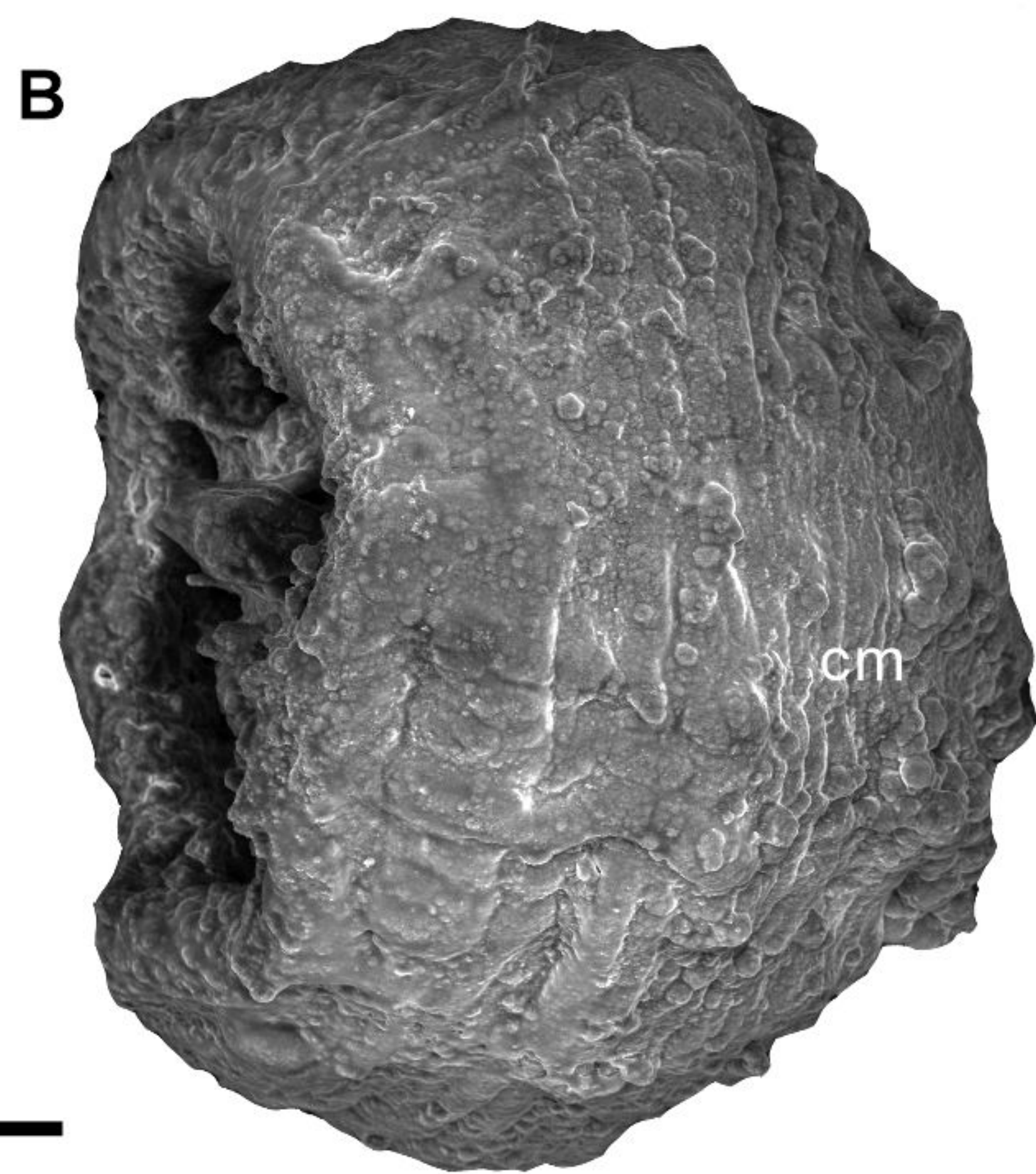
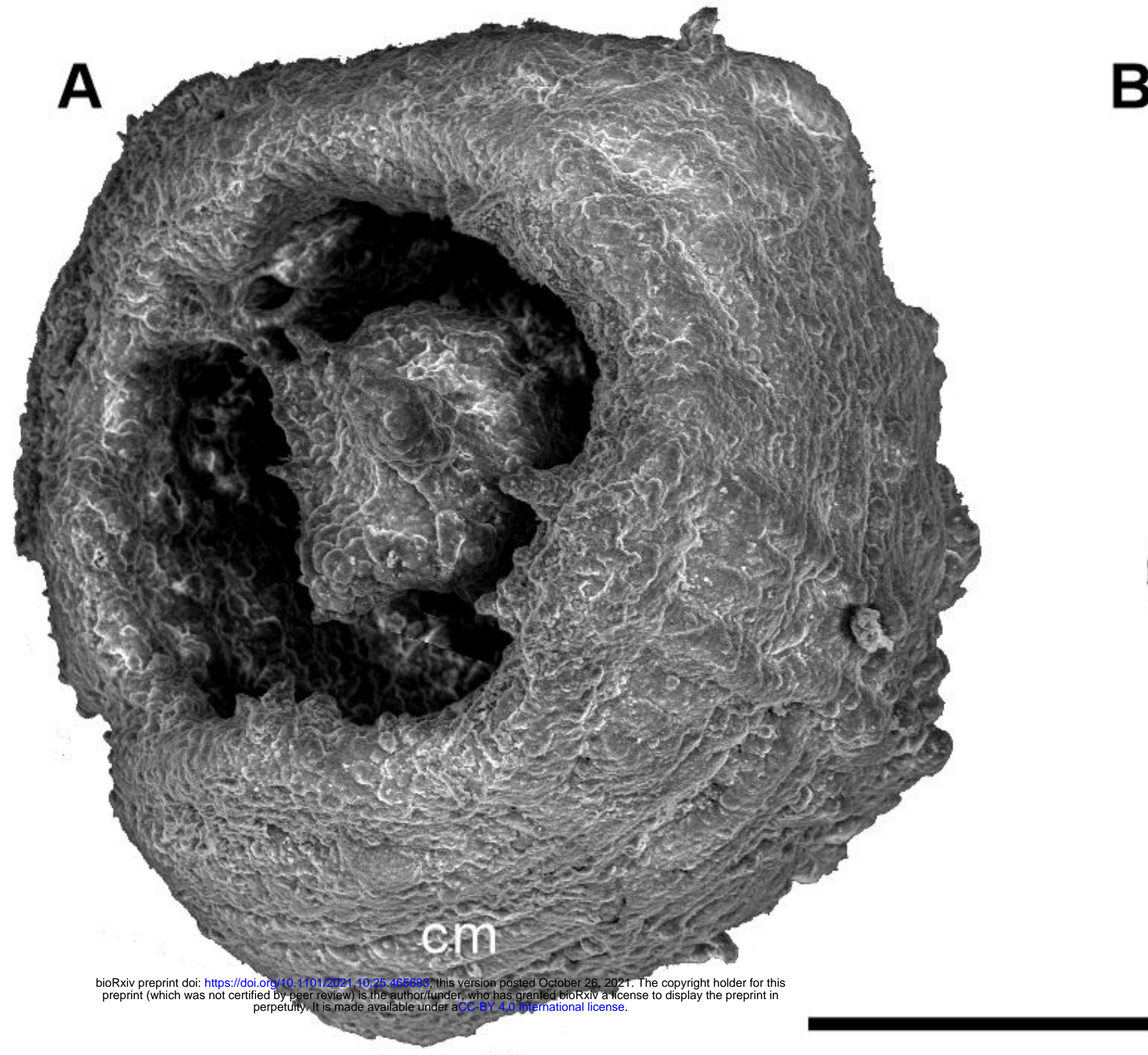


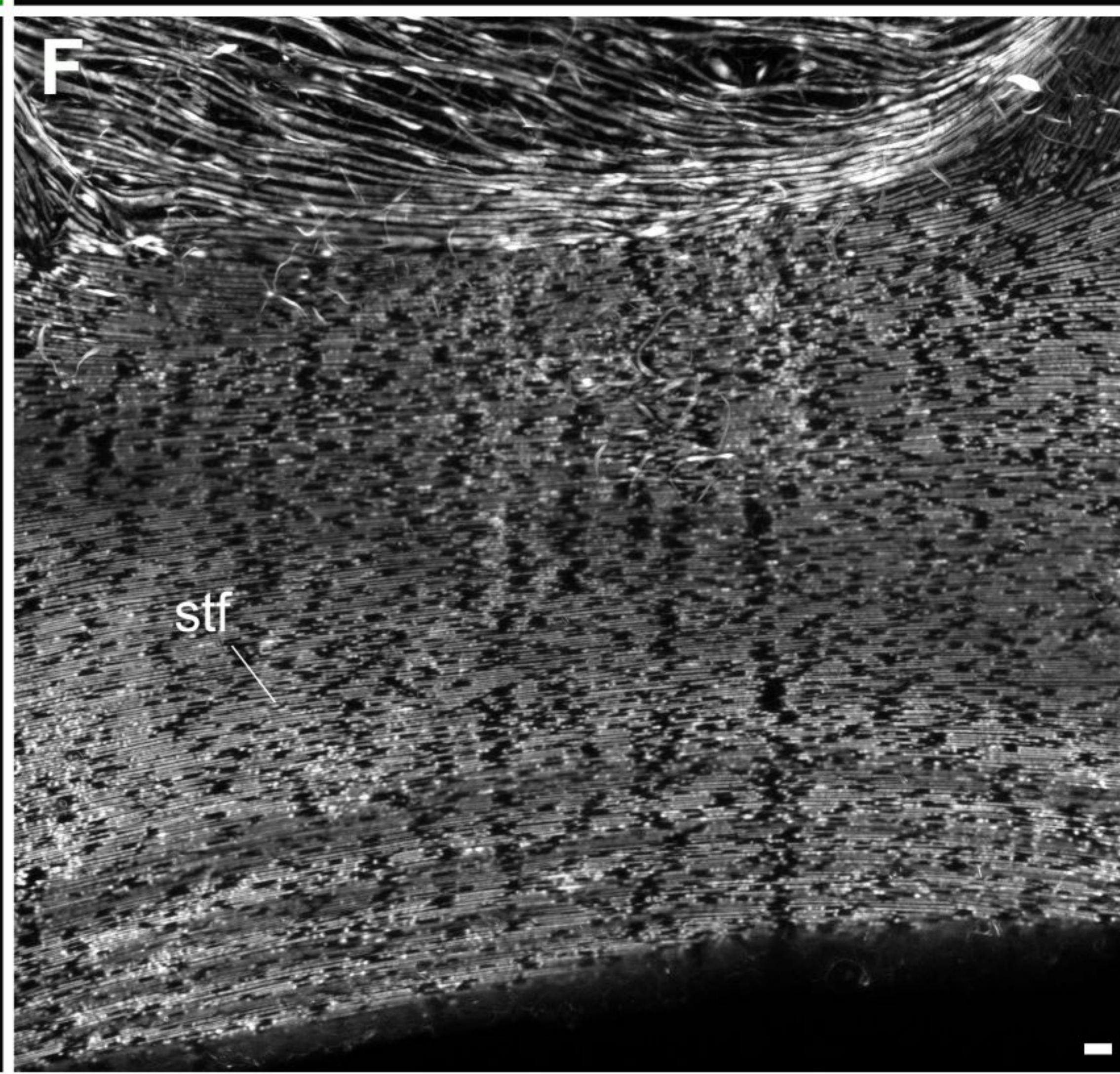
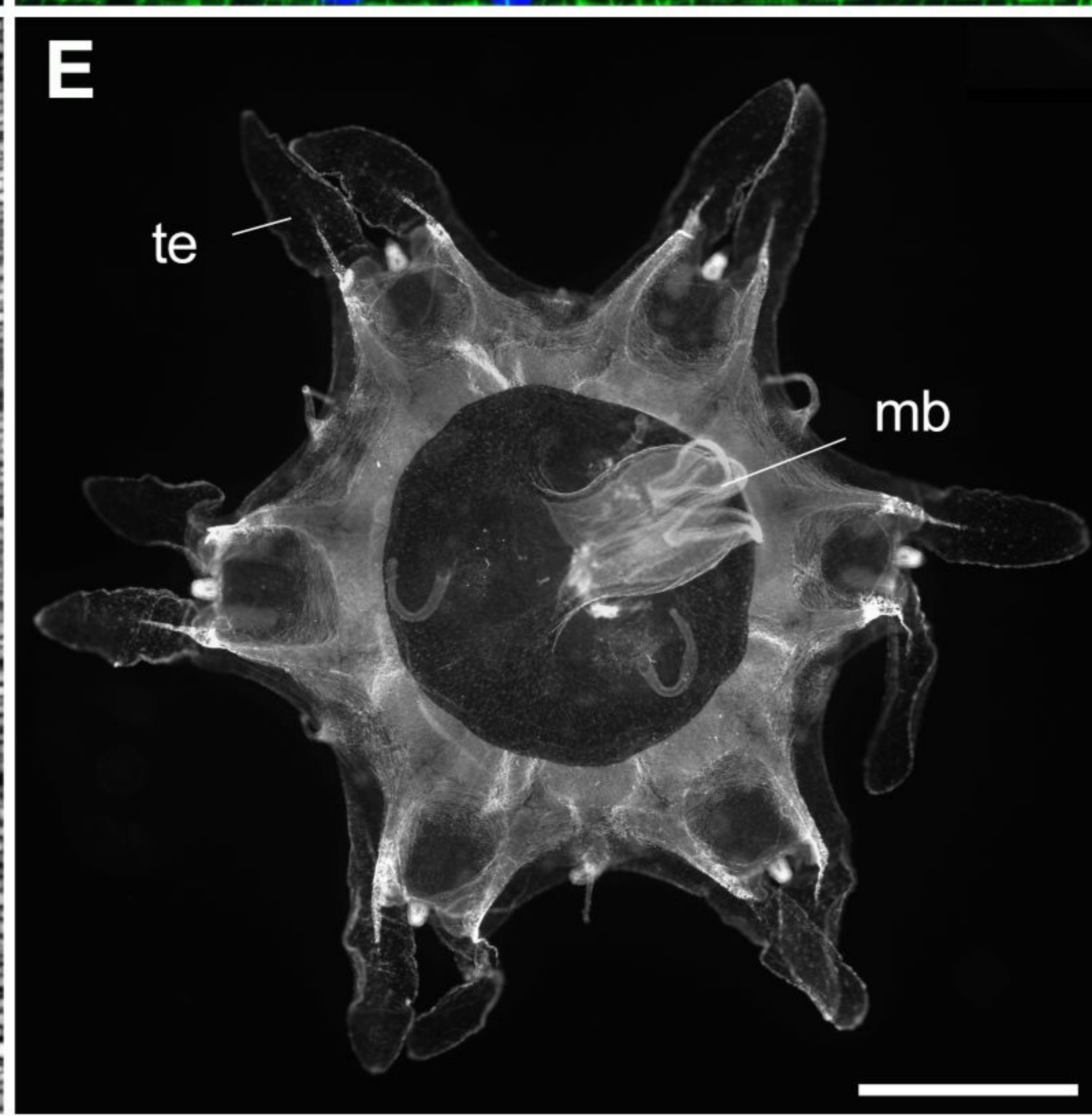
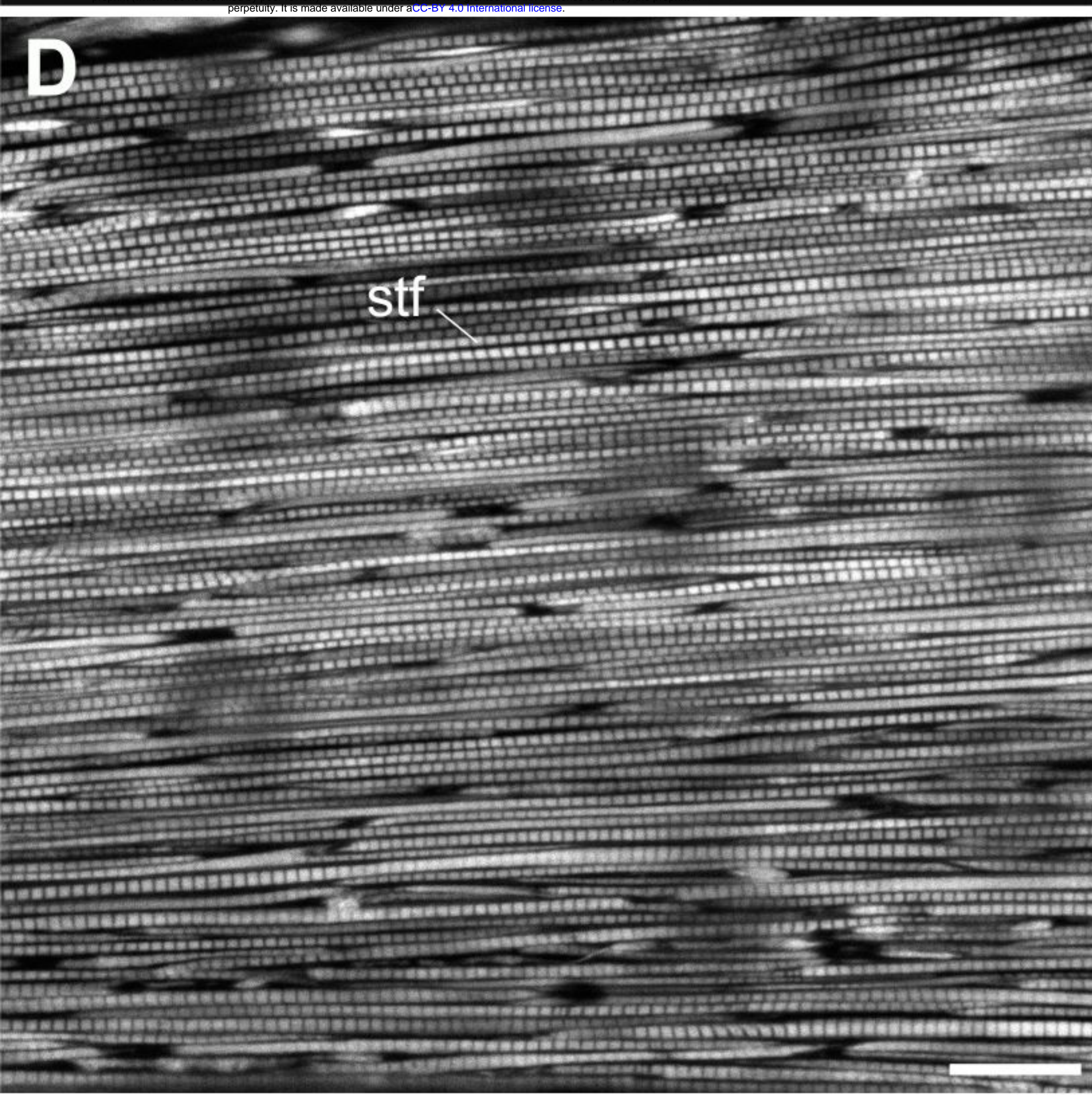
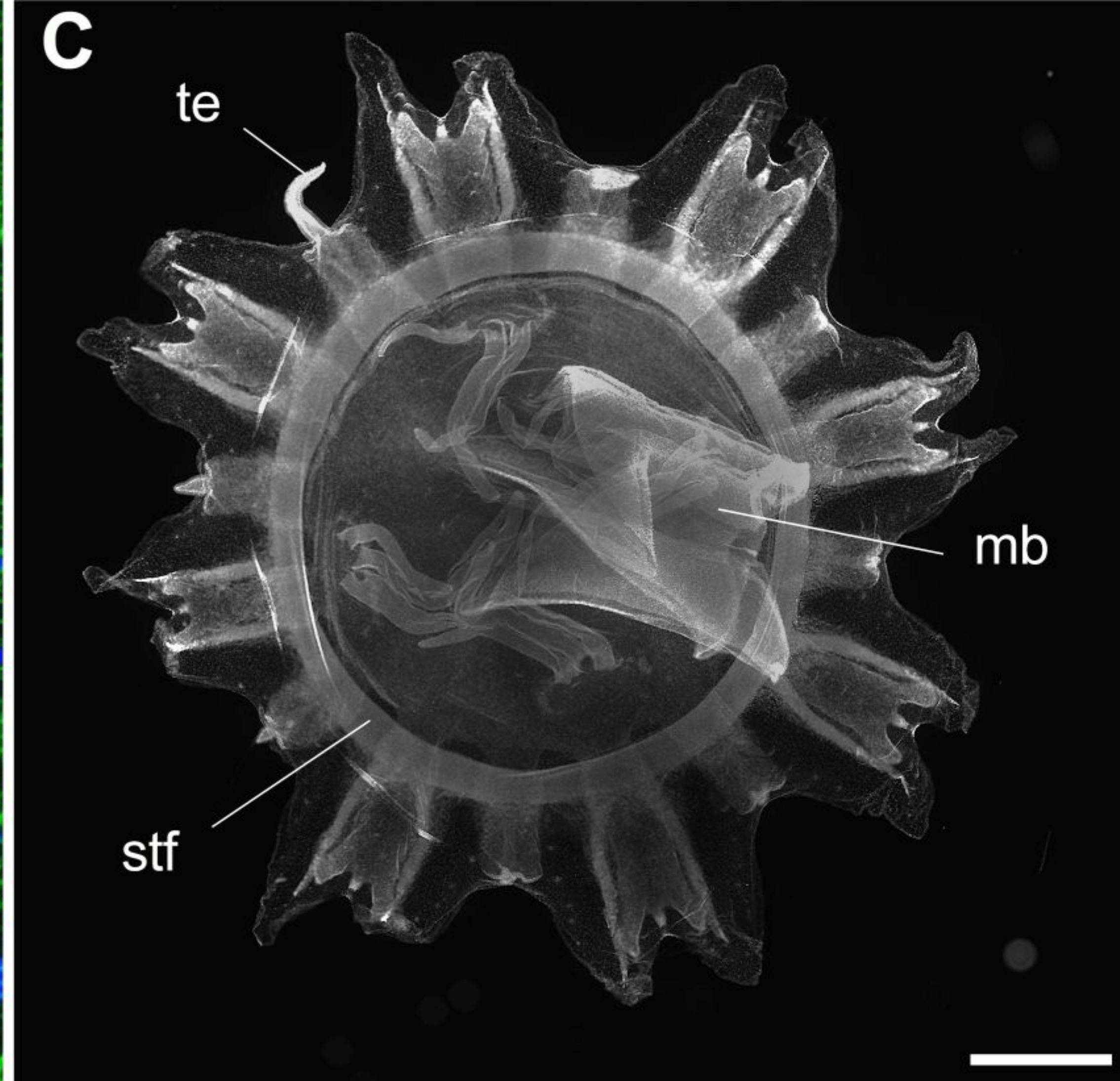
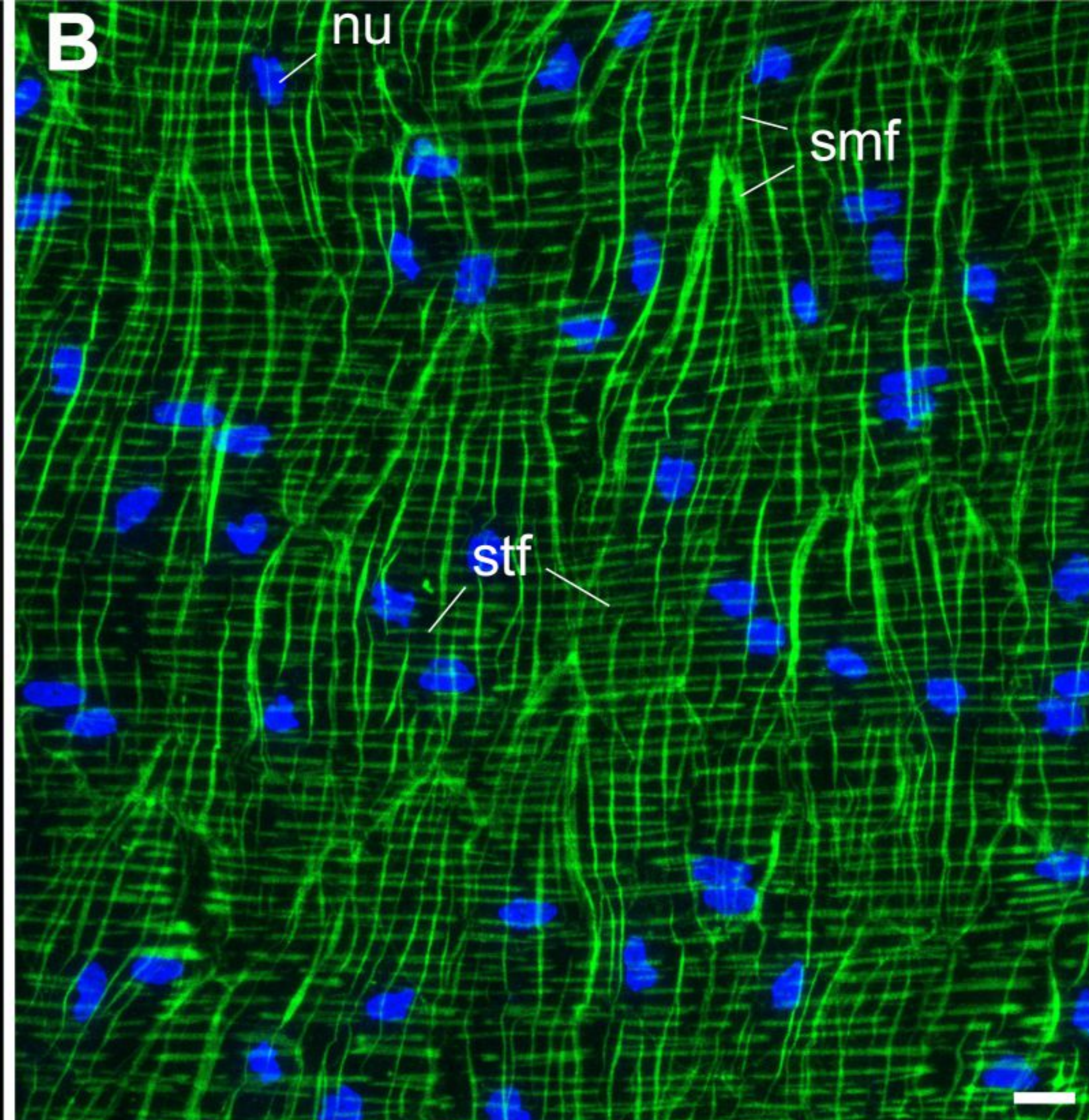
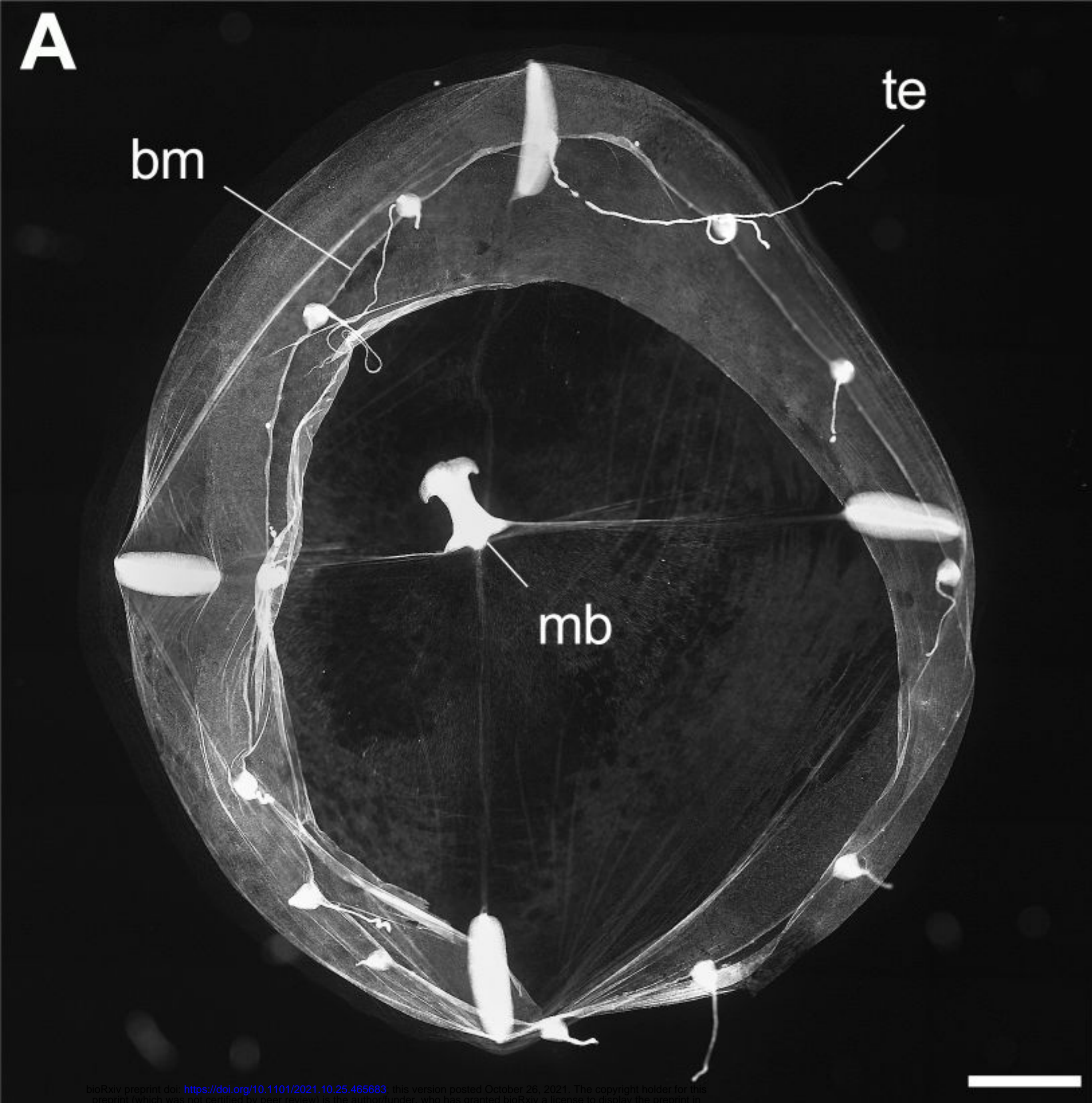
bioRxiv preprint doi: <https://doi.org/10.1101/2021.10.25.465663>; this version posted October 26, 2021. The copyright holder for this preprint (which was not certified by peer review) is the author/funder, who has granted bioRxiv a license to display the preprint in perpetuity. It is made available under aCC-BY 4.0 International license.

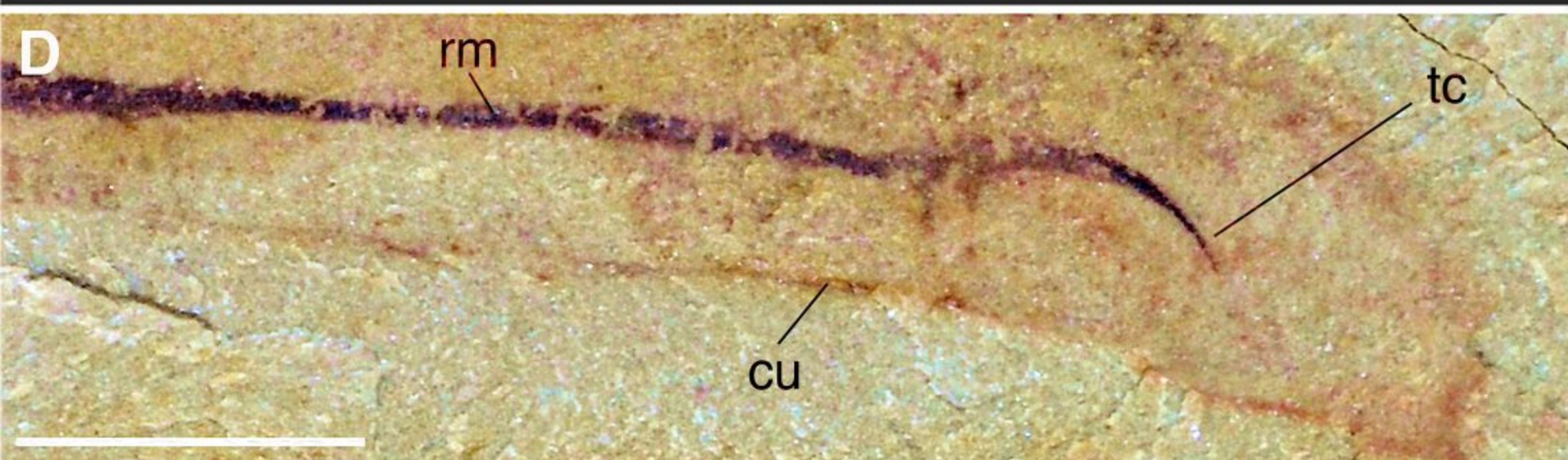
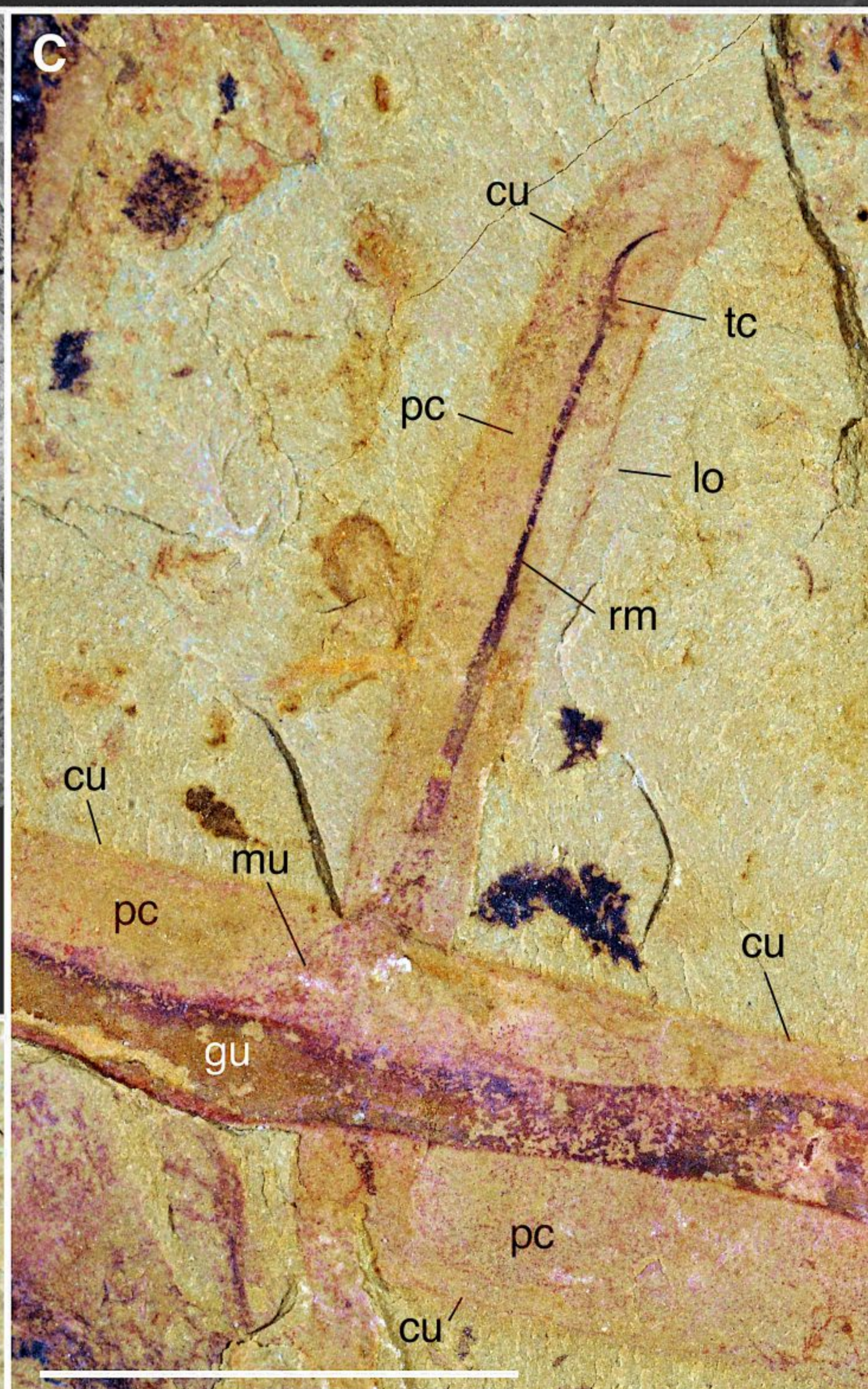
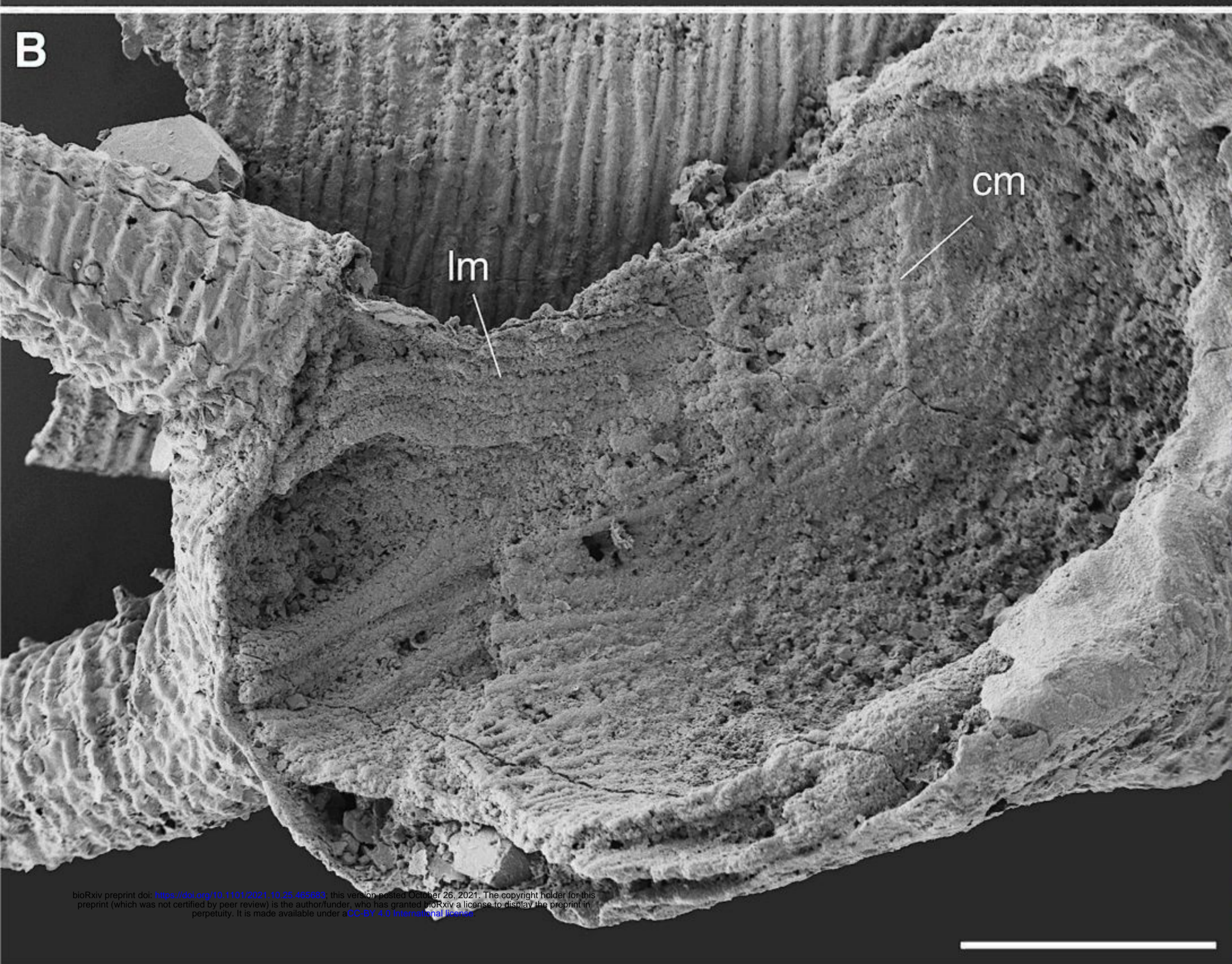
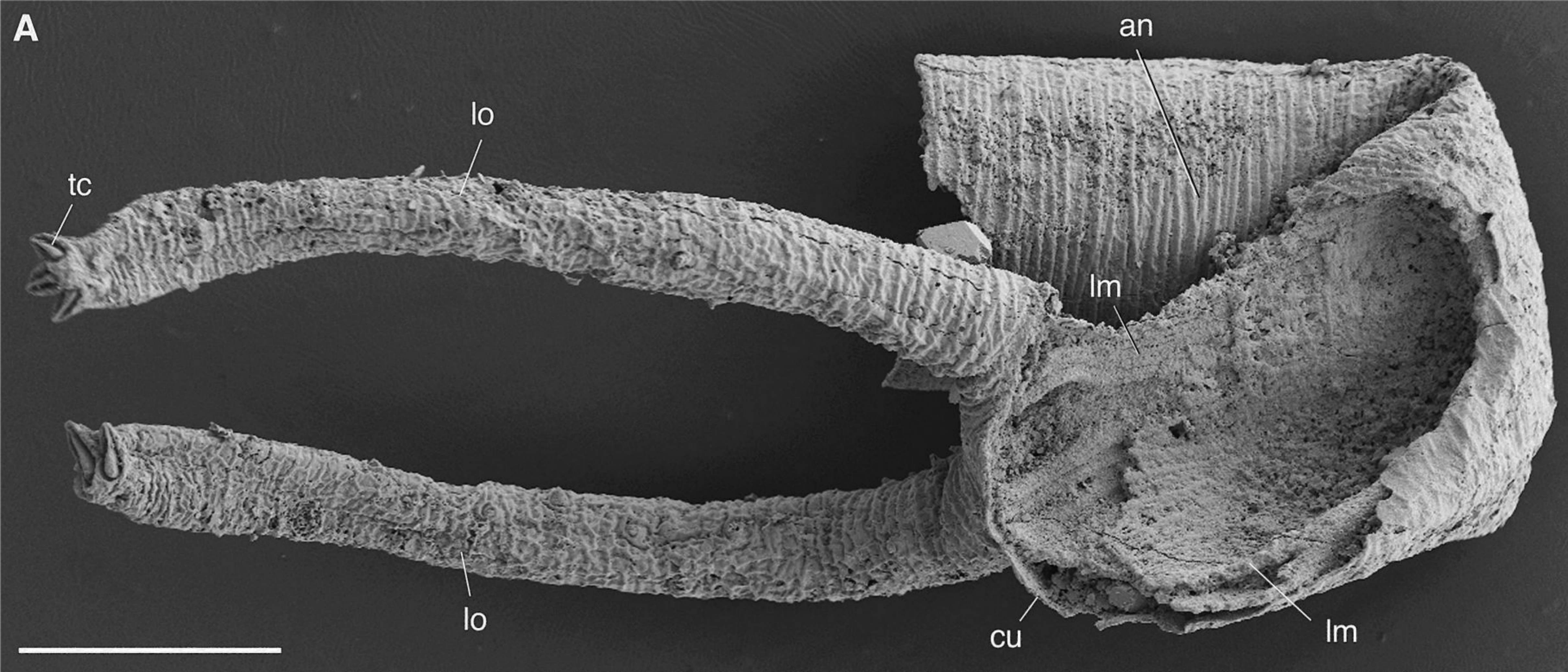


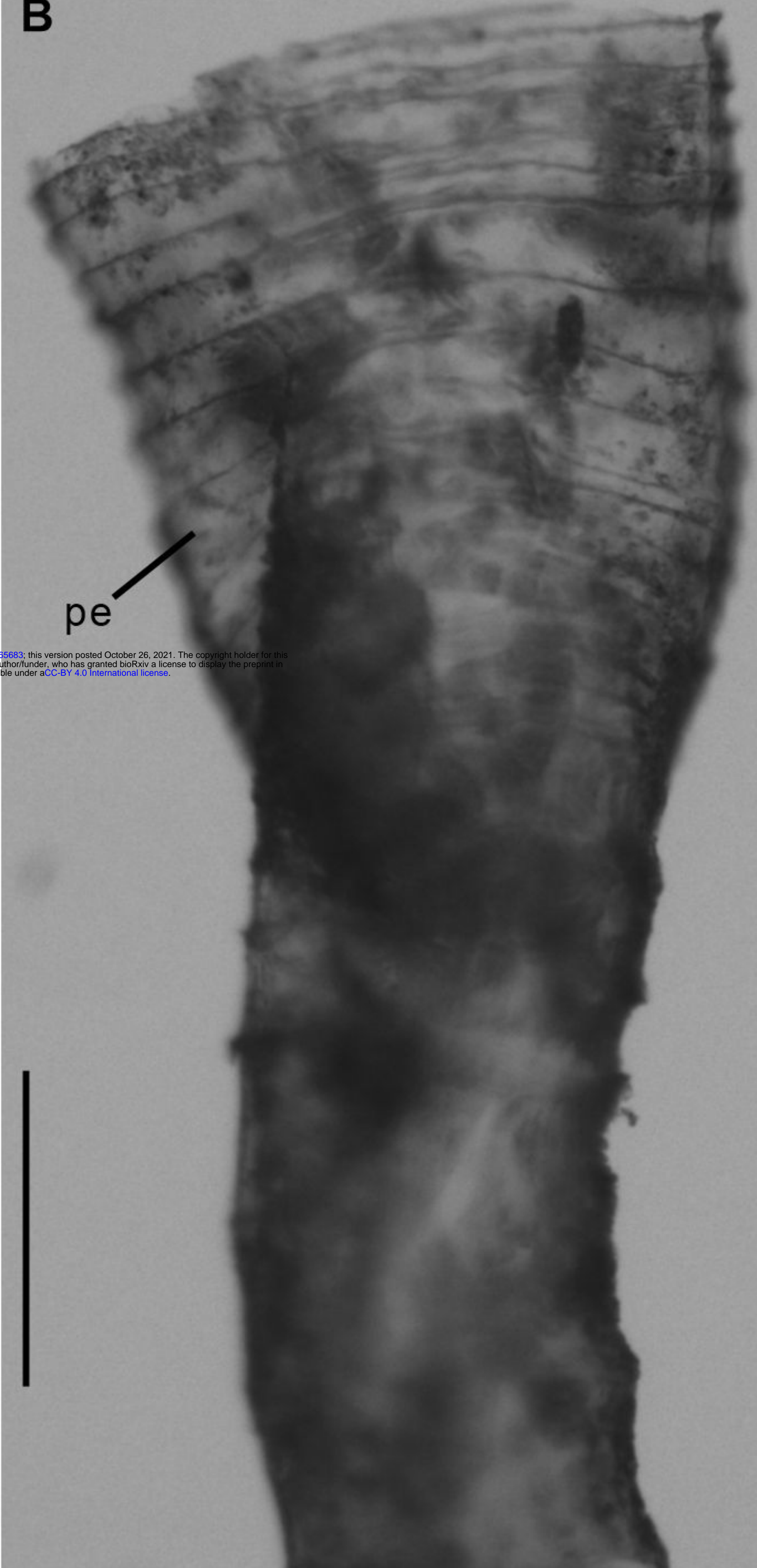
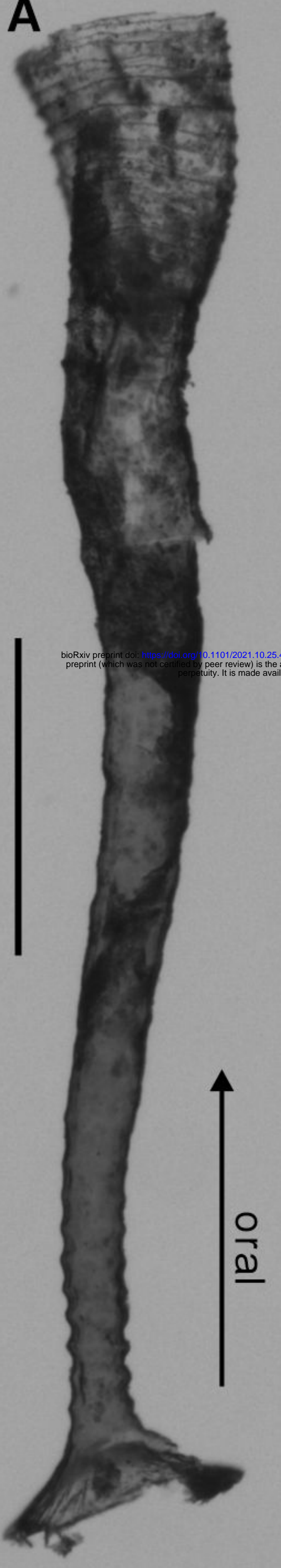












bioRxiv preprint doi: <https://doi.org/10.1101/2021.10.25.465683>; this version posted October 26, 2021. The copyright holder for this preprint (which was not certified by peer review) is the author/funder, who has granted bioRxiv a license to display the preprint in perpetuity. It is made available under aCC-BY 4.0 International license.

